Volume 22, Number 1, 2022 ISSN 1562-8353

NONLINEAR DYNAMICS AND SYSTEMS THEORY
An International Journal of Research and Surveys

Volume 22 Number 1 2022

CONTENTS

 ISSN 1562-8353 Printed in Ukraine
To receive contents and abstracts by e-mail, visit our Website at: **http://www.e-ndst.kiev.ua**

NONLINEAR DYNAMICS & SYSTEMS THEORY

Volume 22, No. 1, 2022

Nonlinear Dynamics and Systems Theory

An International Journal of Research and Surveys

InforMath Publishing Group
http://www.e-ndst.kiev.ua

Nonlinear Dynamics and Systems Theory

An International Journal of Research and Surveys

INSTRUCTIONS FOR CONTRIBUTORS

(1) General. Nonlinear Dynamics and Systems Theory (ND&ST) is an international journal devoted to publishing peer-refereed, high quality, original papers, brief notes and review articles focusing on nonlinear dynamics and systems theory and their practical applications in engineering, physical and life sciences. Submission of a manuscript is a representation that the submission has been approved by all of the authors and by the institution where the work was carried out. It also represents that the manuscript has not been previously published, has not been copyrighted, is not being submitted for publication elsewhere, and that the authors have agreed that the copyright in the article shall be assigned exclusively to InforMath Publishing Group by signing a transfer of copyright form. Before submission, the authors should visit the website:

http://www.e-ndst.kiev.ua

for information on the preparation of accepted manuscripts. Please download the archive Sample_NDST.zip containing example of article file (you can edit only the file Samplefilename.tex).

(2) Manuscript and Correspondence. Manuscripts should be in English and must meet common standards of usage and grammar. To submit a paper, send by e-mail a file in PDF format directly to

Professor A.A. Martynyuk, Institute of Mechanics,
Nesterov str.3, 03057, MSP 680, Kiev-57, Ukraine
e-mail: journalndst@gmail.com

or to one of the Regional Editors or to a member of the Editorial Board. Final version of the manuscript must typeset using LaTex program which is prepared in accordance with the style file of the Journal. Manuscript texts should contain the title of the article, name(s) of the author(s) and complete affiliations. Each article requires an abstract not exceeding 150 words. Formulas and citations should not be included in the abstract. AMS subject classifications and key words must be included in all accepted papers. Each article requires a running head (abbreviated form of the title) of no more than 30 characters. The sizes for regular papers, survey articles, brief notes, letters to editors and book reviews are: (i) 10-14 pages for regular papers, (ii) up to 24 pages for survey articles, and (iii) 2-3 pages for brief notes, letters to the editor and book reviews.

(3) Tables, Graphs and Illustrations. Each figure must be of a quality suitable for direct reproduction and must include a caption. Drawings should include all relevant details and should be drawn professionally in black ink on plain white drawing paper. In addition to a hard copy of the artwork, it is necessary to attach the electronic file of the artwork (preferably in PCX format).

(4) References. Each entry must be cited in the text by author(s) and number or by number alone. All references should be listed in their alphabetic order. Use please the following style:

Journal: [1] H. Poincare, Title of the article. *Title of the Journal* **volume** (issue) (year) pages. [Language]

Book: [2] A.M. Lyapunov, *Title of the Book.* Name of the Publishers, Town, year.

Proceeding: [3] R. Bellman, Title of the article. In: *Title of the Book.* (Eds.). Name of the Publishers, Town, year, pages. [Language]

(5) Proofs and Sample Copy. Proofs sent to authors should be returned to the Editorial Office with corrections within three days after receipt. The corresponding author will receive a sample copy of the issue of the Journal for which his/her paper is published.

(6) Editorial Policy. Every submission will undergo a stringent peer review process. An editor will be assigned to handle the review process of the paper. He/she will secure at least two reviewers' reports. The decision on acceptance, rejection or acceptance subject to revision will be made based on these reviewers' reports and the editor's own reading of the paper.

NONLINEAR DYNAMICS AND SYSTEMS THEORY
An International Journal of Research and Surveys
Published by InforMath Publishing Group since 2001

Volume 22 Number 1 2022

CONTENTS

Founded by A.A. Martynyuk in 2001.
Registered in Ukraine Number: KB No 5267 / 04.07.2001.

NONLINEAR DYNAMICS AND SYSTEMS THEORY
An International Journal of Research and Surveys

Impact Factor from SCOPUS for 2020: SJR – 0.360, SNIP – 1.040 and CiteScore – 1.4

Nonlinear Dynamics and Systems Theory (ISSN 1562–8353 (Print), ISSN 1813–7385 (Online)) is an international journal published under the auspices of the S.P. Timoshenko Institute of Mechanics of National Academy of Sciences of Ukraine and Curtin University of Technology (Perth, Australia). It aims to publish high quality original scientific papers and surveys in areas of nonlinear dynamics and systems theory and their real world applications.

AIMS AND SCOPE

Nonlinear Dynamics and Systems Theory is a multidisciplinary journal. It publishes papers focusing on proofs of important theorems as well as papers presenting new ideas and new theory, conjectures, numerical algorithms and physical experiments in areas related to nonlinear dynamics and systems theory. Papers that deal with theoretical aspects of nonlinear dynamics and/or systems theory should contain significant mathematical results with an indication of their possible applications. Papers that emphasize applications should contain new mathematical models of real world phenomena and/or description of engineering problems. They should include rigorous analysis of data used and results obtained. Papers that integrate and interrelate ideas and methods of nonlinear dynamics and systems theory will be particularly welcomed. This journal and the individual contributions published therein are protected under the copyright by International InforMath Publishing Group.

PUBLICATION AND SUBSCRIPTION INFORMATION

Nonlinear Dynamics and Systems Theory will have 5 issues in 2022, printed in hard copy (ISSN 1562–8353) and available online (ISSN 1813–7385), by InforMath Publishing Group, Nesterov str., 3, Institute of Mechanics, Kiev, MSP 680, Ukraine, 03057. Subscription prices are available upon request from the Publisher, EBSCO Information Services (`mailto:journals@ebsco.com`), or website of the Journal: `http://e-ndst.kiev.ua`. Subscriptions are accepted on a calendar year basis. Issues are sent by airmail to all countries of the world. Claims for missing issues should be made within six months of the date of dispatch.

ABSTRACTING AND INDEXING SERVICES

Papers published in this journal are indexed or abstracted in: Mathematical Reviews / MathSciNet, Zentralblatt MATH / Mathematics Abstracts, PASCAL database (INIST–CNRS) and SCOPUS.

Nonlinear Dynamics and Systems Theory, **22** (1) (2022) 1–12

Capacity and Anisotropic Sobolev Spaces with Zero Boundary Values

Y. Akdim [1], R. Elharch [2*], M. C. Hassib [2] and S. Lalaoui Rhali [2]

[1] *LAMA Laboratory, Department of Mathematics, Faculty of Sciences Dhar El Mahraz, Sidi Mohamed Ben Abdellah University , P.O. Box 1796 Atlas Fez, Morocco.*
[2] *Laboratory of Engineering Sciences (LSI), Polydisciplinary Faculty of Taza, Sidi Mohamed Ben Abdellah University, P.O. Box 1223 Taza , Morocco.*

Received: July 23, 2021; Revised: December 29, 2021

Abstract: The aim of this work is to study the capacity theory in anisotropic Sobolev spaces. In particular, we will give main properties of capacity, including monotonicity, countable subadditivity and several convergence results. Moreover, we will define the anisotropic Sobolev space with zero boundary values $B_0^{1,\vec{p}}(\Omega)$, where Ω is an open bounded set of $\mathbb{R}^N (N \geq 2)$, $\vec{p} = (p_0, p_1, ..., p_N)$ and $1 < p_0, p_1, ..., p_N < \infty$. This allows us to prove that the Dirichlet energy integral has a minimizer in the anisotropic Sobolev space with zero boundary values $B_0^{1,\vec{p}}(\Omega)$.

Keywords: *capacity; anisotropic Sobolev space with zero boundary values; Dirichlet energy.*

Mathematics Subject Classification (2010): 31B15, 31C15, 46E35, 70Kxx, 93XX.

1 Introduction

The notion of capacity is an essential tool in the study of nonlinear potential theory, which allows us to measure sets more precisely than the usual Lebesgue measure, to see that functions are better defined almost everywhere (quasi everywhere). Capacities play a key role in the study of solutions of partial differential equations, for example, Boccardo et al. studied in [6] the existence and non existence of solutions of the following problem:

$$(\mathcal{P}) \begin{cases} -\triangle u + u \mid \nabla u \mid^2 = \mu & in \ \Omega, \\ u = 0 & on \ \partial\Omega, \end{cases}$$

* Corresponding author: mailto:rachid.elharch@usmba.ac.ma

where Ω is a bounded open set in $\mathbb{R}^N, N \geq 2$, and μ is a Radon measure on Ω. More precisely, the authors proved the existence of a solution u in $H_0^1(\Omega)$ for the problem $(\mathcal{P})$ if and only if the measure μ does not charge the sets of capacity zero in Ω. Capacity is also a tool to understand the point-wise behavior of functions in Sobolev spaces.

The theory of nonlinear potential was studied by Maz'ya and Khalvin in [13] and by Meyers in [20] in the L^p space ($1 < p < +\infty$) by introducing the concept of capacity in those spaces which allowed very rich applications in functional analysis, harmonic analysis, theory of probabilities and partial differential equations. The Sobolev capacity for constant exponent spaces has found a great number of applications, see Maz'ya [19], Evans and Gariepy [8], and Heinonen et al. in [12]. Also, Kilpeläinen introduced in [14] the weighted Sobolev capacity and discussed the role of capacity in the point-wise definitions of functions in Sobolev spaces involving the weights of Muckenhoup's A_p-class. On the other hand, Harjulehto et al. [9] generalized the Sobolev capacity to the variable exponent case. Later, this notion was defined in Orlicz spaces in [4] by N. Aissaoui and A. Benkirane and in Musielak-Orlicz space by M. C. Hassib, Y. Akdim, A. Benkirane and N. Aissaoui in [2, 3].

In a recent work [5], we have defined the $C_{k,\vec{p}}$ capacity in anisotropic Sobolev spaces. Also, we proved that $C_{k,\vec{p}}$ is a Choquet capacity.

The Sobolev space with zero boundary values was classically defined as a completion of compactly supported smooth functions with respect to the Sobolev space [18]. Indeed, the Sobolev space with zero boundary is essential to specify or compare boundary values of Sobolev functions. This is particularly important in connection with boundary value problems in the calculus of variations and partial differential equations and with comparison principales in potential theory. Then, the variable exponent Sobolev space with zero boundary values has been defined in [10] following a method developed by Kilpeläinen, Kinnunen and Martio in [16] for metric measure spaces. On the other hand, this notion was generalized by M. C. Hassib and Y. Akdim [11] to weighted variable exponent Sobolev spaces on metric measure spaces. In [22], T. Ohno and T. Shimomura studied the Musielak-Orlicz-Sobolev space with zero boundary values on any metric space endowed with a Borel regular measure.

Our goal in this work is to study the anisotropic Sobolev space with zero boundary values using the concept of capacity.

The present paper is organized as follows. In the second section, we recall some preliminary results on anistropic Sobolev spaces and some properties of capacities. In Section 3, we develop a capacity theory in this space by including monotonicity, countable subadditivity and serval convergence results, we define the anisotropic Sobolev space with zero boundary values and we show some of its properties. As an application of our results, we consider, in Section 4, the Dirichlet energy and we prove that it has a minimizer in anisotropic Sobolev spaces with zero boundary values.

2 Preliminaries

2.1 Anisotropic Sobolev spaces

Let Ω be an open bounded domain in $\mathbb{R}^N (N \geq 2)$ with boundary $\partial\Omega$.
Let $1 < p_0, p_1, ..., p_N < \infty$ and denote

$$\vec{p} = (p_0, p_1, ..., p_N),\ D^0 u = u \text{ and } D^i u = \frac{\partial u}{\partial x_i} \quad \text{for } i = 1, ..., N.$$

Set

$$\underline{p} = \min\{p_0, p_1, ..., p_N\}, \text{ then } \ \underline{p} > 1.$$

The anisotropic Sobolev space $W^{1,\vec{p}}(\Omega)$ is defined as follows:

$$W^{1,\vec{p}}(\Omega) = \{u \in L^{p_0}(\Omega) \ \ and \ \ D^i u \in L^{p_i}(\Omega), i = 1, ..., N\}.$$

We recall that the $W^{1,\vec{p}}(\Omega)$ is a separable, reflexive Banach space (see [1]) with respect to the norm

$$\|u\|_{W^{1,\vec{p}}(\Omega)} = \sum_{i=0}^{N} \|D^i u\|_{L^{p_i}(\Omega)}.$$

We recall also the space $W_0^{1,\vec{p}}(\Omega)$ is the closure of $C_0^\infty(\Omega)$ with respect to this norm. The theory of such anisotropic spaces was developed in [25], [21], [23], [24]. It was shown that $C_0^\infty(\Omega)$ is dense in $W_0^{1,\vec{p}}(\Omega)$ and $W_0^{1,\vec{p}}(\Omega)$ is a reflexive Banach space. For any $\vec{p} = (p_0, p_1, ..., p_N)$, with $1 < p_i < \infty$, $i = 0, 1, ..., N$, the dual space of the anisotropic Sobolev space $W_0^{1,\vec{p}}(\Omega)$ is equivalent to $W^{-1,\vec{p'}}(\Omega)$, where $\vec{p'} = (p'_0, p'_1, ..., p'_N)$ and $p'_i = \dfrac{p_i}{p_i - 1}$ for all $i = 0, 1, ..., , N$.

Proposition 2.1 *Let $p \in [1, +\infty[$ and $(f_n)_n$ be a sequence in $(L^p(\mu), \|.\|_p)$ whose series of norms $\sum_n \|f_n\|_p$ converges. Then the series of functions $\sum_n f_n$ converges for the norm $\|.\|_p$ and we have $\|\sum_n f_n\|_p \leq \sum_n \|f_n\|_p$.*

Proof. For $n \in \mathbb{N}^*$ fixed, according to the Minkowski inequality, we have

$$\left\| \sum_{k=0}^{n} |f_k| \right\|_p \leq \sum_{k=0}^{n} \|f_k\|_p \leq \sum_{k=0}^{+\infty} \|f_k\|_p.$$

It follows from the monotone convergence theorem that

$$\left(\int_\Omega \left(\sum_{k=0}^{+\infty} |f_k| \right)^p d\mu \right)^{\frac{1}{p}} \leq \sum_{k=0}^{+\infty} \|f_k\|_p.$$

Thus,

$$\left\| \sum_{k=0}^{+\infty} f_k \right\|_p \leq \sum_{k=0}^{+\infty} \|f_k\|_p.$$

Proposition 2.2 *[[7]] Let E be a Banach space. If $(f_n)_n$ converges weakly to f in E, then $\|f_n\|$ is bounded and $\|f\| \leq \liminf \|f_n\|$.*

By the application of Proposition 2.1, we have the following result.

Lemma 2.1 *Let (f_n) be a sequence in $W^{1,\vec{p}}(\Omega)$ whose series of norms $\sum_n \|f_n\|_{W^{1,\vec{p}}(\Omega)}$ converges. Then we have*

$$\|\sum_n f_n\|_{W^{1,\vec{p}}(\Omega)} \leq \sum_n \|f_n\|_{W^{1,\vec{p}}(\Omega)}.$$

2.2 Capacity

Definition 2.1 Let E be a topological space and T be the class of Borel sets in E, and let $C : T \to [\ 0,+\infty\ ]$ be a function.
1) The function C is called a capacity if the following axioms are satisfied:
i) $C(\emptyset) = 0$.
ii) $X \subset Y \Rightarrow C(X) \leq C(Y)$ for all X and Y in T (*monotonicity*).
iii) For all sequences $(X_n) \subset T$

$$C(\bigcup_n X_n) \leq \sum_n C(X_n)\ (countable\, subadditivity).$$

2) The capacity C is called an outer capacity if, for all $X \in T$,

$$C(X) = \inf\{C(O) : O \supset X, O \text{ is open }\}.$$

3) The capacity C is called an interior capacity if, for all $X \in T$,

$$C(X) = \sup\{C(K) : K \subset X, K \text{ is compact}\}.$$

4) A property that holds true, except perhaps on a set of capacity zero, is said to be true C-quasi everywhere $(abbreviated\ C - q.e)$.

Definition 2.2 Let f be a real-valued function being finite C-q.e and (f_n) be a sequence of real-valued function being finite C-q.e.
1) We say that (f_n) converges to f in C-capacity if

$$\forall \varepsilon > 0, \lim_{n \to +\infty} C\left(\{x : |f_n(x) - f(x)| > \varepsilon\}\right) = 0.$$

2) We say that (f_n) converges to f C-quasi uniformly $(abbreviated\ \ C - q.u)$ if
$\forall \varepsilon > 0, \exists X \in T : C(X) < \varepsilon$ and (f_n) converges to f uniformly on X^c.

Using same arguments as in Remark 1.27 in [18], we obtain the following remark.

Remark 2.1 Let $\Omega \subset \mathbb{R}^N$ and u, $v \in W^{1,\vec{p}}(\Omega)$, then $\max(u,v) \in W^{1,\vec{p}}(\Omega)$ and $\min(u,v) \in W^{1,\vec{p}}(\Omega)$. Moreover, for $j = 1, ..., N$, we have

$$D^j \max(u,v) = \begin{cases} D^j u & almost\ everywhere\ in\ \ \{x \in \Omega,\ u(x) \geq v(x)\}, \\ D^j v & almost\ everywhere\ in\ \ \{x \in \Omega,\ v(x) \geq u(x)\}. \end{cases}$$

3 Anisotropic Sobolev $\vec{p}$ - Capacity

In the whole of this paper, we assume that Ω is an open bounded domain in $\mathbb{R}^N (N \geq 2)$ with boundary $\partial\Omega$ and μ is a measure of Lebesegue.

Definition 3.1 The anisotropic Sobolev $\vec{p}$ - capacity of the set $E \subset \Omega$ is defined by

$$C_{\vec{p}}(E) = \inf_{u \in A(E)} \left\{ \|u\|_{W^{1,\vec{p}}(\Omega)} \right\},$$

where

$$A(E) = \left\{ u \in W^{1,\vec{p}}(\Omega) : u \geq 1\ \ on\ \ an\ \ open\ \ set\ \ containing\ \ E\ \ and\ \ u \geq 0 \right\}.$$

If $A(E) = \phi$, we set $C_{\vec{p}}(E) = \infty$. Functions belonging to $A(E)$ are called admissible functions for E.

Lemma 3.1 *The anisotropic Sobolev $\vec{p}$ - capacity is a capacity.*

Proof.

i) It is obvious that $C_{\vec{p}}(\phi) = 0$.

ii) $A(E_2) \subset A(E_1)$ *implies* $C_{\vec{p}}(E_1) \leq C_{\vec{p}}(E_2)$ for every $E_1 \subset E_2$.

iii) Let $\varepsilon > 0$, we may assume that $\sum_{i=0}^{\infty} C_{\vec{p}}(E_i) < +\infty$.

Let (E_i) be a subset of Ω $\Big($ if $\sum_{i=0}^{\infty} C_{\vec{p}}(E_i) = +\infty$, there is nothing to show$\Big)$, then

$$\forall i \in \mathbb{N}, \;\; C_{\vec{p}}(E_i) < +\infty,$$

therefore, we choose $u_i \in A(E_i)$ so that

$$\|u_i\|_{W^{1,\vec{p}}(\Omega)} \leq C_{\vec{p}}(E_i) + \varepsilon \times 2^{-i-1}, \quad i = 0, 1, 2, ...$$

Let $v = \sup u_i$, we show that v is an admissible function for $\bigcup_{i=0}^{+\infty} E_i$.

Indeed, for all $i \in \mathbb{N}$, we have by Lemma 2.1 that

$$\|\sup u_i\|_{W^{1,\vec{p}}(\Omega)} \leq \|\sum_{i=0}^{+\infty} u_i\|_{W^{1,\vec{p}}(\Omega)} \leq \sum_{i=0}^{+\infty} \|u_i\|_{W^{1,\vec{p}}(\Omega)},$$

thus,

$$\|v\|_{W^{1,\vec{p}}(\Omega)} \leq \sum_{i=0}^{+\infty} \|u_i\|_{W^{1,\vec{p}}(\Omega)} \leq \sum_{i=0}^{+\infty} C_{\vec{p}}(E_i) + \varepsilon,$$

which implies that $v \in W^{1,\vec{p}}(\Omega)$. Since $u_i \in A(E_i)$, there exists an open set $O_i \supset E_i$ such that $u_i \geq 1$ on O_i for every i= 0,1,2,..., it follows that $v = \sup u_i \geq 1$ on $\bigcup_{i=1}^{+\infty} O_i$ which is an open set containing $\bigcup_{i=0}^{+\infty} E_i$.

Hence we conclude that $C_{\vec{p}}$ is a capacity.

Lemma 3.2 *Let $E \subset \Omega$. The anistropic Sobolev $\vec{p}$ - capacity of E is given by*

$$C_{\vec{p}}(E) = \inf_{u \in B(E)} \left\{ \|u\|_{W^{1,\vec{p}}(\Omega)} \right\},$$

where

$$B(E) = \Big\{ u \in A(E) : 0 \leq u \leq 1 \Big\}.$$

Proof. Clearly, we have

$$B(E) \subset A(E),$$

thus,

$$C_{\vec{p}}(E) \leq \inf_{u \in B(E)} \Big\{ \|u\|_{W^{1,\vec{p}}(\Omega)} \Big\}.$$

For the reverse inequality, let $\varepsilon > 0$ and let $u \in A(E)$ such that

$$\|u\|_{W^{1,\vec{p}}(\Omega)} \leq C_{\vec{p}}(E) + \varepsilon.$$

Then we have $v = \max(0, \min(u, 1)) \in B(E)$. Thus, $v \leq u$ and by Remark 2.1, we have

$$\left| \frac{\partial v}{\partial x_j} \right| \leq \left| \frac{\partial u}{\partial x_j} \right| \quad for\ j = 1, ..., N\ almost\ everywhere.$$

Thus,

$$\inf_{u \in B(E)} \left\{ \|u\|_{W^{1,\vec{p}}(\Omega)} \right\} \leq \|v\|_{W^{1,\vec{p}}(\Omega)} \leq \|u\|_{W^{1,\vec{p}}(\Omega)} \leq C_{\vec{p}}(E) + \varepsilon.$$

Letting $\varepsilon \to 0$, we obtain

$$\inf_{u \in B(E)} \left\{ \|u\|_{W^{1,\vec{p}}(\Omega)} \right\} \leq C_{\vec{p}}(E).$$

Theorem 3.1 *The anisotropic Sobolev $\vec{p}$ - capacity is an outer capacity.*

Proof. Indeed, by monotonicity, we have

$$C_{\vec{p}}(E) \leq \inf\{C_{\vec{p}}(O) : E \subset O \ \ is \ \ open\}.$$

To prove the other inequality, let $\varepsilon > 0$ and take $u \in A(E)$ such that

$$\|u\|_{W^{1,\vec{p}}(\Omega)} \leq C_{\vec{p}}(E) + \varepsilon.$$

Since $u \in A(E)$, there is an open set O containing E such that $u \geq 1$ on O.
This implies that

$$C_{\vec{p}}(O) \leq \|u\|_{W^{1,\vec{p}}(\Omega)} \leq C_{\vec{p}}(E) + \varepsilon.$$

The claim follows by letting $\varepsilon \to 0$.

Proposition 3.1 *Let μ be a Lebesegue measure on Ω and $E \subset \Omega$, then*

$$\mu(E) \leq \mu(\Omega) C_{\vec{p}}(E).$$

Proof. If $C_{\vec{p}}(E) = \infty$, there is nothing to prove. Thus we may assume that $C_{\vec{p}}(E) < \infty$. Let $\varepsilon > 0$ and take $u \in A(E)$ such that

$$\|u\|_{W^{1,\vec{p}}(\Omega)} \leq C_{\vec{p}}(E) + \varepsilon.$$

There is an open $O \supset E$ such that $u \geq 1$ in O and $u \geq 0$, thus

$$\mu(E) \leq \mu(O) \leq \int_O |u| d\mu \leq \int_\Omega |u| d\mu.$$

On the other hand, by Hölder's inequality, we have

$$\int_\Omega |u| d\mu \leq (\mu(\Omega))^{1 - \frac{1}{p_0}} \|u\|_{W^{1,\vec{p}}(\Omega)} \leq \mu(\Omega) \left(C_{\vec{p}}(E) + \varepsilon \right).$$

The claim follows by letting $\varepsilon \to 0$.

Theorem 3.2 *Let (k_n) be a decreasing sequence of compacts and $k = \bigcap_{n\in\mathbb{N}} k_n$, then*

$$\lim_{n\to\infty} C_{\vec{p}}(k_n) = C_{\vec{p}}(k).$$

Proof. First, we observe that $C_{\vec{p}}(k) \leq \lim_{n\to\infty} C_{\vec{p}}(k_n)$. On the other hand, let O be an open set such that $k \subset O$, thus

$$k \cap O^c = \phi.$$

The sequence $(k_n^{'})$ defined for all n by $k_n^{'} = k_n \cap O^c$ is a decreasing sequence of compacts that satisfies $\bigcap_{n\in\mathbb{N}} k_n^{'} = \emptyset$. Then, there exists n_0 such that $k_{n_0}^{'} = \emptyset$. Hence, for all $n \geq n_0$, $k_n^{'} = \emptyset$ and then $k_n \subset O$, for all $n \geq n_0$. Therefore,

$$\lim_{n\to\infty} C_{\vec{p}}(k_n) \leq C_{\vec{p}}(O).$$

And since $C_{\vec{p}}$ is an outer capacity, we obtain the claim by taking infimum over all open sets O containing k.

Proposition 3.2 *If there exists $u \in W^{1,\vec{p}}(\Omega)$ such that $u = +\infty$ on an open set containing E, then $C_{\vec{p}}(E) = 0$.*

Proof. Let $u \in W^{1,\vec{p}}(\Omega)$ be such that $u = +\infty$ on an open set O containing E, then $u \geq \alpha$, for all $\alpha > 0$. Therefore,

$$\forall\alpha > 0,\ C_{\vec{p}}(E) \leq \frac{1}{\alpha}\|u\|_{W^{1,\vec{p}}(\Omega)}.$$

Letting $\alpha \to +\infty$, we obtain $C_{\vec{p}}(E) = 0$.

Theorem 3.3 *Let u and $(u_n)_n$ be in $W^{1,\vec{p}}(\Omega)$ and consider the following propositions:*
i) $u_n \to u$ strongly in $W^{1,\vec{p}}(\Omega)$.
ii) $u_n \to u$ in $C_{\vec{p}}$-capacity .
iii) There is a subsequence (u_{n_j}) such that $u_{n_j} \to u$ in $C_{\vec{p}}$ - q.u.
iv) $(u_{n_j}) \to u$ in $C_{\vec{p}}$.- q.e.
Then we have

$$i) \Rightarrow ii) \Rightarrow iii) \Rightarrow iv).$$

Proof.

- We show that $i) \Rightarrow ii)$.

By Proposition 3.2, we have u and u_n are finite $C_{\vec{p}}$ -q.e, for all n.
Let $\varepsilon > 0$, then

$$C_{\vec{p}}\Big(\Big\{x : |u_n - u|(x) > \varepsilon\Big\}\Big) \leq \frac{\|u_n - u\|_{W^{1,\vec{p}}(\Omega)}}{\varepsilon}.$$

- We show that $ii) \Rightarrow iii)$.

Let $\varepsilon > 0$, then there exists u_{n_j} such that

$$C_{\vec{p}}\Big(\Big\{x : |u_{n_j} - u|(x) > 2^{-j}\Big\}\Big) \leq \varepsilon \cdot 2^{-j}.$$

We put

$$E_j = \Big\{x : |u_{n_j} - u|(x) > 2^{-j}\Big\} \ \textit{and} \ G_m = \bigcup_{j \geq m} E_j.$$

Then we have

$$C_{\vec{p}}(G_m) \leq \sum_{j \geq m} \varepsilon \cdot 2^{-j} < \varepsilon.$$

On the other hand,

$$\forall x \in (G_m)^c, \forall j \geq m \ \ |u_{n_j} - u|(x) \leq 2^{-j},$$

thus

$$u_{n_j} \to u \ \ in \ C_{\vec{p}} - q.u.$$

- We show that $iii) \Rightarrow iv)$.

We have

$$\forall j \in \mathbb{N}, \exists X_j : C_{\vec{p}}(X_j) \leq \frac{1}{j},$$

thus,

$$u_{n_j} \ \ converges \ uniformly \ to \ u \ on \ (X_j)^C.$$

We put $X = \bigcap_j X_j$, then $C_{\vec{p}}(X) = 0$ and $u_{n_j} \to u$ on X^C.

As an immediate consequence of Theorem 3.3 and Proposition 3.1, we have the following result.

Corollary 3.1 *If $(u_n)_n$ is a sequence which converges to u in $W^{1,\vec{p}}(\Omega)$, then there exists a subsequence of $(u_n)_n$ which converges to u, μ a.e.*

Definition 3.2 A function $u : \Omega \to [-\infty, +\infty]$ is called a $C_{\vec{p}}$ - quasicontinuous function in Ω if for every $\varepsilon > 0$, there is a set X such that $C_{\vec{p}}(X) < \varepsilon$ and $u_{|\Omega \setminus X}$ is continuous.

Theorem 3.4 *The anistropic Sobolev $\vec{p}$ - capacity $C_{\vec{p}}$ satisfies the following properties:*

1) If O is an open set of Ω and $E \subset \Omega$ is such that $\mu(E) = 0$, then

$$C_{\vec{p}}(O) = C_{\vec{p}}(O - E).$$

2) Let u and v be $C_{\vec{p}}-$ quasicontinuous functions in Ω, we have
i) if $u = v$ almost everywhere in an open $O \subset \Omega$, then

$$u = v \ \ C_{\vec{p}} - \ \ quasi \ everywhere \ in \ \ O,$$

ii) If $u \leq v$ almost everywhere in an open $O \subset \Omega$, then

$$u \leq v \ \ C_{\vec{p}} - \ \ quasi \ everywhere \ in \ \ O.$$

Proof.

1) By monotonicity of $C_{\vec{p}}$, we get $C_{\vec{p}}(O) \geq C_{\vec{p}}(O-E)$.
Let $\varepsilon > 0$ and let $u \in A(O-E)$ be such that

$$\|u\|_{W^{1,\vec{p}}(\Omega)} \leq C_{\vec{p}}(O-E) + \varepsilon.$$

Then there exists an open $G \subset \Omega$ with $(O-E) \subset G$ and $u \geq 1$ almost everywhere in G. Since $G \cup O$ is open, $O \subset G \cup O$ and $u \geq 1$ almost everywhere in $G \cup (O-E)$, and almost everywhere in $G \cup O$ since $\mu(E) = 0$, we have $u \in A(O)$

$$C_{\vec{p}}(O) \leq \|u\|_{W^{1,\vec{p}}(\Omega)} \leq C_{\vec{p}}(O-E) + \varepsilon$$

by letting $\varepsilon \to 0$, we deduce that $C_{\vec{p}}(O) \leq C_{\vec{p}}(O-E)$.

2) Since $C_{\vec{p}}$ is an outer capacity, we get the results by [15].

Lemma 3.3 *For any bounded open $O \subset \Omega$, we have*

$$\mu(O) = 0 \Longleftrightarrow C_{\vec{p}}(O) = 0.$$

Proof. If $\mu(O) = 0$, then, by applying Theorem 3.4, we get $C_{\vec{p}}(O) = C_{\vec{p}}(O \backslash O) = C_{\vec{p}}(\phi) = 0$. On the other hand, if $C_{\vec{p}}(O) = 0$, then, by Proposition 3.1, $\mu(O) \leq C_{\vec{p}}(O) = 0$.

Proposition 3.3 *Let $(u_n)_n$, $u \in W^{1,\vec{p}}(\Omega)$ be such that $u_n \rightharpoonup u$ weakly in $W^{1,\vec{p}}(\Omega)$, then* $\liminf(u_n) \leq u \leq \limsup(u_n)$ $\quad C_{\vec{p}}$*-q.e.*

Proof. Since $W^{1,\vec{p}}(\Omega)$ is a reflexive space, $u_n \rightharpoonup u$ weakly in $W^{1,\vec{p}}(\Omega)$. Then, by the Banach-Saks theorem, there is a subsequence denoted again by (u_n) such that the sequence (g_n) defined by $g_n = \frac{1}{n}\sum\limits_{i=1}^{n} u_i$ converges to u strongly in $W^{1,\vec{p}}(\Omega)$.
By Theorem 3.3, there is a subsequence of (g_n) denoted again by (g_n) such that

$$\lim_{n \to +\infty} g_n = u \qquad C_{\vec{p}} - q.e.$$

On the other hand,

$$\liminf u_n \leq \lim_{n \to +\infty} g_n.$$

Therefore,

$$\liminf(u_n) \leq u \qquad C_{\vec{p}} - q.e.$$

For the second inequality, it suffices to replace u_n by $(-u_n)$ in the first inequality.

3.1 Anisotropic Sobolev spaces with zero boundary values

Definition 3.3 We say that a function u belongs to the anisotropic Sobolev space with zero boundary values, and we denote $u \in B_0^{1,\vec{p}}(\Omega)$ if there is a $C_{\vec{p}}$-quasicontinuous function $\tilde{u} \in W^{1,\vec{p}}(\mathbb{R}^N)$ such that $\tilde{u} = u$ almost everywhere in Ω and $\tilde{u} = 0$ $C_{\vec{p}}$ -quasi everywhere in $\mathbb{R}^N \backslash \Omega$. The set $B_0^{1,\vec{p}}(\Omega)$ is endowed with the norm

$$||u||_{B_0^{1,\vec{p}}(\Omega)} = ||\tilde{u}||_{W^{1,\vec{p}}(\mathbb{R}^N)}.$$

Theorem 3.5 $B_0^{1,\vec{p}}(\Omega)$ *is a Banach space.*

Proof. Let $(u_n)_n$ be a Cauchy sequence in $B_0^{1,\vec{p}}(\Omega)$, for every n, there is a $C_{\vec{p}}$-quasicontinuous function $\tilde{u_n} \in W^{1,\vec{p}}(\mathbb{R}^N)$ such that $\tilde{u}_n = u_n$ almost everywhere in Ω and $\tilde{u_n} = 0 C_{\vec{p}}$-quasi everywhere in $\mathbb{R}^N \backslash \Omega$.

Since $W^{1,\vec{p}}(\mathbb{R}^N)$ is a Banach space, there is a function u such that $\tilde{u_n} \to u$ in $W^{1,\vec{p}}(\mathbb{R}^N)$ as $n \to +\infty$. By applying Theorem 3.3, we deduce that u is $C_{\vec{p}}-$ quasi-continuous and by Proposition 3.3, we have $u = 0 \;\; C_{\vec{p}}$-q.e in $\mathbb{R}^N \backslash \Omega$. Consequently, $u \in B_0^{1,\vec{p}}(\Omega)$ and we conclude that the spaces $B_0^{1,\vec{p}}(\Omega)$ are complete.

Corollary 3.2 *The space* $B_0^{1,\vec{p}}(\Omega)$ *is reflexive.*

Proof. The space $W^{1,\vec{p}}(\mathbb{R}^N)$ is a reflexive Banach space, by applying Theorem 3.5, we deduce the space $B_0^{1,\vec{p}}(\Omega)$ is closed in $W^{1,\vec{p}}(\mathbb{R}^N)$ and therefore $B_0^{1,\vec{p}}(\Omega)$ is reflexive.

Corollary 3.3 *We have* $W_0^{1,\vec{p}}(\Omega) \subset B_0^{1,\vec{p}}(\Omega) \subset W^{1,\vec{p}}(\Omega)$.

Proof. Since $D(\Omega) \subset B_0^{1,\vec{p}}(\Omega)$ and by applying Theorem 3.5, we obtain the first inclusion. The second inclusion follows directly from the definition of the space $B_0^{1,\vec{p}}(\Omega)$.

Proposition 3.4 *Let* $u \in B_0^{1,\vec{p}}(\Omega)$ *and* $v \in W^{1,\vec{p}}(\mathbb{R}^N)$ *be bounded functions. If* v *is* $C_{\vec{p}}$*- quasicontinuous, then* $uv \in B_0^{1,\vec{p}}(\Omega)$.

Proof. Let $\tilde{u} \in W^{1,\vec{p}}(\mathbb{R}^N)$ be a $C_{\vec{p}}$- quasicontinuous representative function of u. $\tilde{u}v$ is $C_{\vec{p}}$- quasicontinuous in $\mathbb{R}^N$. Let $D = \{x \in \mathbb{R}^N \backslash \Omega : \tilde{u}v \neq 0\}$, $D = G \cup H$, where $G = \{x \in \mathbb{R}^N \backslash \Omega : \tilde{u} \neq 0\}$ and $H = \{x \in \mathbb{R}^N \backslash \Omega : v = \infty\}$. It is obvious that $C_{\vec{p}}(G) = 0$ and by Proposition 3.2, we have $C_{\vec{p}}(H) = 0$, thus $C_{\vec{p}}(D) = 0$. Therefore, $\tilde{u}v = 0 \; C_{\vec{p}}$ -quasi everywhere in Ω. Since $\tilde{u}v = uv$ a.e in Ω, we get $uv \in B_0^{1,\vec{p}}(\Omega)$.

Theorem 3.6 *Let* $O \subset \Omega$ *be such that* $C_{\vec{p}}(O) = 0$*, we have*

$$B_0^{1,\vec{p}}(\Omega) = B_0^{1,\vec{p}}(\Omega \backslash O).$$

Proof. It is obvious that $B_0^{1,\vec{p}}(\Omega \backslash O) \subset B_0^{1,\vec{p}}(\Omega)$.

Let $u \in B_0^{1,\vec{p}}(\Omega)$, then there is a $C_{\vec{p}}$- quasicontinuous function $\tilde{u} \in W^{1,\vec{p}}(\mathbb{R}^N)$ such that $\tilde{u} = u$ a.e in Ω and $\tilde{u} = 0 \; C_{\vec{p}}$- quasi everywhere in $\mathbb{R}^N \backslash \Omega$. Since $C_{\vec{p}}(O) = 0$, we have $\tilde{u} = 0 \; C_{\vec{p}}$ - quasi everywhere in $\mathbb{R}^N \backslash (\Omega \backslash O)$. Thus $u \in B_0^{1,\vec{p}}(\Omega \backslash O)$.

Remark 3.1 *If* $C_{\vec{p}}(\partial\Omega) = 0$*, then* $B_0^{1,\vec{p}}(\mathring{\Omega}) = B_0^{1,\vec{p}}(\overline{\Omega})$.

4 Application

4.1 The Dirichlet energy integral minimisers

Definition 4.1 Let $w \in W^{1,\vec{p}}(\Omega)$. For all $u \in B_0^{1,\vec{p}}(\Omega)$, we define $I_{\Omega,w}^{\vec{p}}(u)$ by

$$I_{\Omega,w}^{\vec{p}}(u) = \int_\Omega \mid w \mid dx + \sum_{i=0}^{N} \int_\Omega \left(\mid \frac{\partial u}{\partial x_i} \mid^{p_i} + \mid \frac{\partial w}{\partial x_i} \mid^{p_i} \right) dx.$$

$I_{\Omega,w}^{\vec{p}}$ is called the energy operator corresponding to the boundary value function w.

Lemma 4.1 *[17] Let H be a reflexive Banach space. If $I : H \to \mathbb{R}$ is a convex, lower semi-continuous and coercive operator, then there is an element in H that minimizes I.*

Theorem 4.1 *Let $B_0^{1,\vec{p}}(\Omega)$ be the anisotropic Sobolev space with zero boundary values. Then there exists a function $u \in B_0^{1,\vec{p}}(\Omega)$ such that*

$$I_{\Omega,w}^{\vec{p}}(u) = \inf_{v \in B_0^{1,\vec{p}}(\Omega)} I_{\Omega,w}^{\vec{p}}(v).$$

Proof. It follows from Theorem 3.5 and Corollary 3.2 that $B_0^{1,\vec{p}}(\Omega)$ is a reflexive Banach space. Since the function $x \to x^p$ is convex for every fixed $1 < p < \infty$, we deduce that $I_{\Omega,w}^{\vec{p}}$ is convex. Moreover, $I_{\Omega,w}^{\vec{p}}$ is lower semi-continuous and coercive, hence all assumptions of Lemma 4.1 are satisfied.

4.2 Conclusion

In this work, we first show that the anisotropic Sobolev $\vec{p}$-capacity $C_{\vec{p}}$ is an outer capacity and we give sufficient conditions ensuring that $C_{\vec{p}}(E) = 0$ whenever E is a subset of Ω. Then, we discuss the convergence of a sequence in $C_{\vec{p}}$-capacity. This allows us to show that the anisotropic Sobolev space with zero boundary values $B_0^{1,\vec{p}}(\Omega)$ is a reflexive Banach space. We also prove that $B_0^{1,\vec{p}}(\Omega)$ coincides with $B_0^{1,\vec{p}}(\Omega \backslash E)$ for all $E \subset \Omega$ satisfying $C_{\vec{p}}(E) = 0$. Finaly, we apply our results to show that the Dirichlet energy has a minimizer in anisotropic Sobolev spaces with zero boundary values.

References

[1] R. Adams. *Sobolev Space.* New York, Academic Press, 1975.

[2] N. Aissaoui, Y. Akdim, A. Benkirane and M. C. Hassib. Capacity and Non-linear Potential in Musielak-Orlicz Spaces. *Nonlinear Dynamics and Systems Theory* **16** (3) (2016) 276–293.

[3] N. Aissaoui, Y. Akdim, A. Benkirane and M. C. Hassib. Capacity, Theorem of H. Brezis and F.E. Browder type in Musielak-Orlicz-Sobolev Spaces and Application. *Nonlinear Dynamics and Systems Theory* **17** (2) (2017) 175–192.

[4] N. Aissaoui and A. Benkirane. Capacités dans les epaces d'Orlicz. *Ann. Sci. Math. Quèbec.* **18** (1) (1994) 1–23.

[5] Y. Akdim, R. Elharch, M. C Hassib and S. Lalaoui Rhali. Capacity in anisotropic Sobolev spaces. *Nonlinear Dynamics and Systems Theory* **21** (2) (2021) 115–125.

[6] L. Boccardo, T.Gallouët and L. Orsina. Existence and non existence of solutions for some nonlinear elliptic equations. *Journal d'Analyse Mathématique* **73** (1) (1997) 203–223.

[7] H. Brezis. *Analyse Fonctionnelle; Théorie et Applications.* Masson, Paris, 1983.

[8] L. C. Evans and R. F. Gariepy. *Measure Theory and Fine Properties of Functions CRC Press.* Boca Raton, 1992.

[9] P. Harjulehto, P. Hästö, M. Koskenoja and S. Varonen. Sobolev capacity on the space $W^{1,p(.)}(\mathbb{R}^N)$. *Journal of Function Spaces and Applications* **1** (1) (2003) 17–33.

[10] P. Harjulehto, P. Hästö, M. Koskenoja, S. Varonen. The Dirichlet energy integral and variable exponent Sobolev spaces with zero boundary values. *Potential Analysis* **25** (3) (2006) 205–222.

[11] M. C. Hassib, Y. Akdim. Weighted Variable Exponent Sobolev spaces on metric measure spaces. *Moroccan Journal of Pure and Applied Analysis* **4** (2) (2018) 62–76.

[12] J. Heinonen, T. Kilpeläinen and O. Martio. *Nonlinear Potential Theory of Degenerate Elliptic Equations*. New York: Oxford University Press, 1993.

[13] V. P. Khavin and V. G. Maz'ya. Nonlinear potential theory. *Uspekhi Math. Nauk* **27** (1972) 71–148.

[14] T. Kilpeläinen. Weighted Sobolev spaces and capacity. *Annales Academi Scientiarium Fennic. Mathematica* **19** (1) (1994) 95–113.

[15] T. Kilpeläinen. A remark on the uniqueness of quasi continuous functions. *Ann.Acad. Sci. Fenn. Math.* **23** (1998) 261–262.

[16] T. Kilpeläinen, J. Kinnunen, and O. Martio. *Sobolev spaces with zero boundary values on metric spaces. Potential Analysis.* **12** (3) (2000) 233–247.

[17] D. Kinderlehrer and G. Stampacchia. *An Introduction to Variational Inequalities and Their Applications.* Academic Press, London, 1980.

[18] J. Kinnunen. *Sobolev spaces. Department of Mathematics and Systems Analysis.* Aalto University, 2017.

[19] V. G. Maz'ya. *Sobolev spaces.* Translated from the Russian by TO Shaposhnikova. Springer Ser. Soviet Math., Springer, 1985.

[20] N. G. Meyers. A theory of capacities for potentials of functions in Lebesgue classes. *Math., Scand.* **26** (2) (1970) 255–292.

[21] S. M. Nikolski. On imbedding, continuation and approximation theorems for differentialble functions of several variables. *Russian Math. Surveys* **16** (5) (1961) 55–104.

[22] T. Ohno and T. Shimomura. Musielak-Orlicz-Sobolev spaces with zero boundary values on metric measure spaces. *Czechoslovak Mathematical Journal* **66** (2) (2016) 371–394.

[23] J. Rakosnik. Some remarks to anisotropic Sobolev spaces I. *Beiträge zur Analysis.* **13** (1979) 55–68.

[24] J. Rakosnik. Some remarks to anisotropic Sobolev spaces II. *Beiträge zur Analysis.* **15** (1981) 127–140.

[25] M. Troisi. Teoremi di inclusione per spazi di Sobolev non isotropi. *Ricerche Mat.* **18** (1969) 3–24.

Nonlinear Dynamics and Systems Theory, **22** (1) (2022) 13–20

First Integral of a Class of Two Dimensional Kolmogorov Systems

R. Boukoucha *

Department of Technology, Faculty of Technology, University of Bejaia,06000 Bejaia, Algeria.

Received: August 28, 2019; Revised: December 10, 2021

Abstract: In this paper, we are interested in studying the existence of a first integral and the curves which are formed by the trajectories of the autonomous planar Kolmogorov systems. Concrete examples exhibiting the applicability of our result are introduced.

Keywords: *dynamical system; Kolmogorov system; first integral; periodic orbits; limit cycle.*

Mathematics Subject Classification (2010): 34C05, 34C07, 37C27, 37K10.

1 Introduction

By definition, an autonomous planar Kolmogorov system is a system of the form

$$\begin{cases} x' = \dfrac{dx}{dt} = xF\left(x,y\right), \\ y' = \dfrac{dy}{dt} = yG\left(x,y\right), \end{cases} \tag{1}$$

these equations are equivalent to the differential equation

$$\frac{dy}{dx} = \frac{yQ\left(x,y\right)}{xP\left(x,y\right)},$$

where F , G are two functions in the variables x and y and the derivatives are taken with respect to the time variable. The theory of differential equations is one of the basic tools of mathematical science [1–3, 20]. System (1) is frequently used to model the iteration of two species occupying the same ecological niche [14, 16]. There are many

* Corresponding author: mailto:rachid_boukecha@yahoo.fr

natural phenomena which can be modeled by the Kolmogorov systems, for example, in mathematical ecology and population dynamics [11,15,17,18], chemical reactions, plasma physics [13], hydrodynamics [7], etc. We remind that in the phase plane, a limit cycle of system (1) is an isolated periodic orbit in the set of all its periodic orbits. In the qualitative theory of planar dynamical systems [9, 19], one of the most important topics is related to the second part of the unsolved Hilbert 16th problem [12]. There is a huge literature about limit cycles, most of it deal essentially with their detection, their number and their stability and rare are papers concerned with giving them explicitly [4, 5].

System (1) is integrable on an open set Ω of $\mathbb{R}^2$ if there exists a non constant C^1 function $H : \Omega \to \mathbb{R}$, called a first integral of the system on Ω, which is constant on the trajectories of the system (1) contained in Ω, i.e., if

$$\frac{dH(x,y)}{dt} = \frac{\partial H(x,y)}{\partial x} xF(x,y) + \frac{\partial H(x,y)}{\partial y} yG(x,y) \equiv 0 \text{ in the points of } \Omega.$$

Moreover, $H = h$ is the general solution of this equation, where h is an arbitrary constant. It is well known that for differential systems defined on the plane $\mathbb{R}^2$, the existence of a first integral determines their phase portrait [8], and one of the classical tools in the classification of all trajectories of a dynamical system is to find first integrals, for more details about the first integral, see for instance [6, 10].

In this paper, we are interested in studying the existence of a first integral and the curves which are formed by the trajectories of the autonomous planar Kolmogorov systems of the form

$$\begin{cases} x' = x\left(B_1(x,y)\sin\left(\frac{A_3(x,y)}{A_4(x,y)}\right) + B_3(x,y)\sin\left(\frac{A_1(x,y)}{A_2(x,y)}\right)\right), \\ y' = y\left(B_2(x,y)\sin\left(\frac{A_5(x,y)}{A_6(x,y)}\right) + B_3(x,y)\sin\left(\frac{A_1(x,y)}{A_2(x,y)}\right)\right), \end{cases} \tag{2}$$

where $A_1(x,y)$, $A_2(x,y)$, $A_3(x,y)$, $A_4(x,y)$, $A_5(x,y)$, $A_6(x,y)$, $B_1(x,y)$, $B_2(x,y)$ and $B_3(x,y)$ are homogeneous polynomials of degree a, a, b, b, c, c, n, n, m, respectively.

We define the trigonometric functions

$$\begin{aligned} &f_1(\theta) = B_1(\cos\theta,\sin\theta)\left(\cos^2\theta\right)\sin\left(\tfrac{A_3(\cos\theta,\sin\theta)}{A_4(\cos\theta,\sin\theta)}\right) + \\ &B_2(\cos\theta,\sin\theta)\left(\sin^2\theta\right)\sin\left(\tfrac{A_5(\cos\theta,\sin\theta)}{A_6(\cos\theta,\sin\theta)}\right), \\ &f_2(\theta) = B_3(\cos\theta,\sin\theta)\sin\left(\tfrac{A_1(\cos\theta,\sin\theta)}{A_2(\cos\theta,\sin\theta)}\right), \\ &f_3(\theta) = (\cos\theta\sin\theta)\,B_2(\cos\theta,\sin\theta)\sin\left(\tfrac{A_5(\cos\theta,\sin\theta)}{A_6(\cos\theta,\sin\theta)}\right) - \\ &(\cos\theta\sin\theta)\,B_1(\cos\theta,\sin\theta)\sin\left(\tfrac{A_3(\cos\theta,\sin\theta)}{A_4(\cos\theta,\sin\theta)}\right). \end{aligned}$$

2 Main Result

Our main result on the integrability and the periodic orbits of the Kolmogorov system (2) is as follows.

Theorem 2.1 *Consider the Komogorov system* (2)*, then the following statements hold.*

(1) *If* $f_3(\theta) \neq 0,\ A_i(\cos\theta, \sin\theta) \neq 0$ *for* $i = 2,4,6$ *and* $n \neq m$, *then system* (2) *has the first integral*

$$H(x,y) = \left(x^2+y^2\right)^{\frac{n-m}{2}} \exp\left((m-n)\int_0^{\arctan\frac{y}{x}} M(s)\,ds\right) - (n-m)\,F\left(\arctan\tfrac{y}{x}\right),$$

where $M(\theta) = \frac{f_1(\theta)}{f_3(\theta)}$, $N(\theta) = \frac{f_2(\theta)}{f_3(\theta)}$ *and* $F(\theta) = \int_0^\theta \exp\left((m-n)\int_0^w M(s)\,ds\right) N(w)\,dw$.

The curves which are formed by the trajectories of the differential system (2), *in Cartesian coordinates are written as*

$$x^2+y^2 = \left[\left(h+(n-m)\,F\left(\arctan\frac{y}{x}\right)\right)\exp\left((n-m)\int_0^{\arctan\frac{y}{x}} M(s)\,ds\right)\right]^{\frac{2}{n-m}},$$

where $h \in \mathbb{R}$. *Moreover, the system* (2) *has no periodic orbits.*

(2) *If* $f_3(\theta) \neq 0,\ A_i(\cos\theta, \sin\theta) \neq 0$ *for* $i = 2,4,6$ *and* $n = m$, *then system* (2) *has the first integral*

$$H(x,y) = \left(x^2+y^2\right)^{\frac{1}{2}} \exp\left(-\int_0^{\arctan\frac{y}{x}} (M(s)+N(s))\,ds\right),$$

and the curves which are formed by the trajectories of the differential system (2), *in Cartesian coordinates are written as*

$$\left(x^2+y^2\right)^{\frac{1}{2}} - h\exp\left(\int_0^{\arctan\frac{y}{x}} (M(s)+N(s))\,ds\right) = 0,$$

where $h \in \mathbb{R}$. *Moreover, the system* (2) *has no periodic orbits.*

(3) *If* $f_3(\theta) = 0$ *for all* $\theta \in \mathbb{R}$, *then system* (2) *has the first integral* $H = \frac{y}{x}$, *and the curves which are formed by the trajectories of the differential system* (2), *in Cartesian coordinates are written as* $y - hx = 0$, *where* $h \in \mathbb{R}$. *Moreover, the system* (2) *has no periodic orbits.*

Proof. In order to prove our results, we write the differential system (2) in polar coordinates (r,θ), defined by $x = r\cos\theta$ and $y = r\sin\theta$, then system (2) becomes

$$\begin{cases} r' = f_1(\theta)\,r^{n+1} + f_2(\theta)\,r^{m+1}, \\ \theta' = f_3(\theta)\,r^n, \end{cases} \tag{3}$$

where the trigonometric functions $f_1(\theta)$, $f_2(\theta)$, $f_3(\theta)$ are given in the Introduction, $r' = \frac{dr}{dt}$ and $\theta' = \frac{d\theta}{dt}$.

If $f_3(\theta) \neq 0$, $A_i(\cos\theta, \sin\theta) \neq 0$ for $i = 2,4,6$ and $n \neq m$, we take as a new independent variable the coordinate θ, then the differential system (3) becomes the differential equation

$$\frac{dr}{d\theta} = M(\theta)\,r + N(\theta)\,r^{1+m-n}, \tag{4}$$

where $M(\theta) = \frac{f_1(\theta)}{f_3(\theta)}$ and $N(\theta) = \frac{f_2(\theta)}{f_3(\theta)}$, which is a Bernoulli equation. By introducing the standard change of variables $\rho = r^{n-m}$, we obtain the linear equation

$$\frac{d\rho}{d\theta} = (n-m)\left(M(\theta)\,\rho + N(\theta)\right). \tag{5}$$

The general solution of linear equation (5) is

$$\rho(\theta) = \exp\left((n-m)\int_0^{\theta} M(s)\,ds\right)(\mu + (n-m)F(\theta)),$$

where $\mu \in \mathbb{R}$.

From the expression of the constant μ, we deduce the first integral of system (2) as

$$H(x,y) = \left(x^2+y^2\right)^{\frac{n-m}{2}} \exp\left((m-n)\int_0^{\arctan\frac{y}{x}} M(s)\,ds\right) + (m-n)F\left(\arctan\tfrac{y}{x}\right).$$

Let Γ be a periodic orbit surrounding an equilibrium located in one of the open quadrants, and let $h_{\Gamma} = H(\Gamma)$.

The curves $H = h$ with $h \in \mathbb{R}$, which are formed by the trajectories of the differential system (2), in Cartesian coordinates are written as

$$x^2+y^2 = \left[\left(h + (n-m)F\left(\arctan\frac{y}{x}\right)\right)\exp\left((n-m)\int_0^{\arctan\frac{y}{x}} M(s)\,ds\right)\right]^{\frac{2}{n-m}},$$

where $h \in \mathbb{R}$.

Therefore the periodic orbit Γ is contained in the curve

$$x^2+y^2 = \left[\left(h_{\Gamma} + (n-m)F\left(\arctan\frac{y}{x}\right)\right)\exp\left((n-m)\int_0^{\arctan\frac{y}{x}} M(s)\,ds\right)\right]^{\frac{2}{n-m}}.$$

But this curve cannot contain the periodic orbit Γ in the realistic quadrant $(x > 0, y > 0)$, because this curve in the realistic quadrant has at most a unique point on every straight line $y = \eta x$ for all $\eta \in \left]0,+\infty\right[$.

To be convinced by this fact, one has to compute the abscissa points of the intersection of this curve with the straight line $y = \eta x$ for all $\eta \in \left]0,+\infty\right[$, the abscissa is given by

$$\begin{aligned} x &= \frac{1}{\sqrt{1+\eta^2}}\left[(h_{\Gamma} + (n-m)F(\arctan\eta))\exp\left((n-m)\int_0^{\arctan\eta} M(s)\,ds\right)\right]^{\frac{1}{n-m}} \\ &= f(\eta). \end{aligned}$$

Since f is a function (of η), there exists at most one value of x on the half-line OX^{+}. Consequently, at most one point in the realistic quadrant $(x > 0, y > 0)$ exists. So, this curve cannot contain the periodic orbit.

Hence statement (1) of Theorem 1 is proved.

Suppose now that $f_3(\theta) \neq 0$, $A_i(\cos\theta, \sin\theta) \neq 0$ for $i = 2,4,6$ and $n = m$.

Taking as the independent variable the coordinate θ, this differential system (3) is written as

$$\frac{dr}{d\theta} = (M(\theta) + N(\theta))\,r. \tag{6}$$

The general solution of equation (6) is

$$r(\theta) = \mu \exp\left(\int_0^{\theta}(M(s)+N(s))\,ds\right),$$

where $\mu \in \mathbb{R}$.

From the expression of the constant μ, we deduce the first integral of system (2) as

$$H(x,y) = \left(x^2+y^2\right)^{\frac{1}{2}} \exp\left(-\int_0^{\arctan\frac{y}{x}} (M(s)+N(s))\,ds\right).$$

Let Γ be a periodic orbit surrounding an equilibrium located in one of the realistic quadrants $(x>0, y>0)$, and let $h_\Gamma = H(\Gamma)$.

The curves $H = h$ with $h \in \mathbb{R}$, which are formed by the trajectories of the differential system (2), in Cartesian coordinates are written as

$$\left(x^2+y^2\right)^{\frac{1}{2}} - h\exp\left(\int_0^{\arctan\frac{y}{x}} (M(s)+N(s))\,ds\right) = 0,$$

where $h \in \mathbb{R}$.

Therefore the periodic orbit Γ is contained in the curve

$$\left(x^2+y^2\right)^{\frac{1}{2}} = h_\Gamma \exp\left(\int_0^{\arctan\frac{y}{x}} (M(s)+N(s))\,ds\right).$$

Again, this curve cannot contain the periodic orbit Γ in the realistic quadrant $(x>0, y>0)$, for the same reason as in the previous case.

To be convinced by this fact, one has to compute the abscissa points of the intersection of this curve with the straight line $y=\eta x$ for all $\eta \in \left]0,+\infty\right[$, the abscissa is given by

$$x = \frac{h_\Gamma}{\sqrt{(1+\eta^2)}} \exp\left(\int_0^{\arctan\eta} (M(s)+N(s))\,ds\right) = f(\eta).$$

Since f is a function (of η), there exists at most one value of x on the half-line OX^+. Consequently, at most one point in the realistic quadrant $(x>0, y>0)$ exists. So, this curve cannot contain the periodic orbit.

Hence statement (2) of Theorem 1 is proved.

Assume now that $f_3(\theta) = 0$ for all $\theta \in \mathbb{R}$. Then from system (3) it follows that $\theta' = 0$. So, the straight lines through the origin of coordinates of the differential system (2) are invariant by the flow of this system. Hence, $\frac{y}{x}$ is a first integral of the system, then curves which are formed by the trajectories of the differential system (2), in Cartesian coordinates are written as $y - hx = 0$, where $h \in \mathbb{R}$, since all straight lines through the origin are formed by the trajectories, clearly, the system has no periodic orbits.

This completes the proof of statement (3) of Theorem 1.

2.1 Examples

The following examples are given to illustrate our result.

Example 1 If we take $A_1(x,y) = 5x^2+4y^2$, $A_2(x,y) = x^2+y^2$, $A_3(x,y) = \frac{\pi}{2}A_4(x,y)$, $A_5(x,y) = \frac{\pi}{2}A_6(x,y)$, $B_1(x,y) = x^4+x^3y+2x^2y^2+xy^3+y^4$, $B_2(x,y) = x^4+2x^3y+2x^2y^2+2xy^3+y^4$ and $B_3(x,y) = 3x^2-xy+3y^2$, then system (2) reads

$$\begin{cases} x' = x\left(\left(x^4 + x^3y + 2x^2y^2 + xy^3 + y^4\right) + \left(3x^2 - xy + 3y^2\right)\sin\left(\frac{5x^2+4y^2}{x^2+y^2}\right)\right), \\ y' = y\left(\left(x^4 + 2x^3y + 2x^2y^2 + 2xy^3 + y^4\right) + \left(3x^2 - xy + 3y^2\right)\sin\left(\frac{5x^2+4y^2}{x^2+y^2}\right)\right). \end{cases} \tag{7}$$

The Kolmogorov system (7) in polar coordinates (r, θ) becomes

$$\begin{cases} r' = \left(1 + \frac{3}{4}\sin 2\theta - \frac{1}{8}\sin 4\theta\right) r^5 + (3 - \cos\theta\sin\theta)\sin\left(\frac{9}{2} + \frac{1}{2}\cos 2\theta\right) r^3, \\ \theta' = \left(\cos^2\theta\sin^2\theta\right) r^4, \end{cases}$$

here $f_1(\theta) = 1 + \frac{3}{4}\sin 2\theta - \frac{1}{8}\sin 4\theta$, $f_2(\theta) = (3 - \cos\theta\sin\theta)\sin\left(\frac{9}{2} + \frac{1}{2}\cos 2\theta\right)$ and $f_3(\theta) = \cos^2\theta\sin^2\theta$. In the realistic quadrant $(x > 0, y > 0)$ it is the case (1) of Theorem 1, then the Kolmogorov system (7) has the first integral

$$H(x,y) = \left(x^2 + y^2\right)\exp\left(-2\int_0^{\arctan\frac{y}{x}} M(s)\,ds\right) - 2\int_0^{\arctan\frac{y}{x}} \exp\left(-2\int_0^{w} M(s)\,ds\right) B(w)\,dw,$$

where $M(s) = \dfrac{1 + \frac{3}{4}\sin 2s - \frac{1}{8}\sin 4s}{\cos^2 s\sin^2 s}$, $N(w) = \dfrac{(3 - \cos w\sin w)\sin\left(\frac{9}{2} + \frac{1}{2}\cos 2w\right)}{\cos^2 w\sin^2 w}$.

The curves $H = h$ with $h \in \mathbb{R}$, which are formed by the trajectories of the differential system (7), in Cartesian coordinates are written as

$$x^2+y^2 = \left(h + 2\int_0^{\arctan\frac{y}{x}} \exp\left(-2\int_0^{w} N(s)\,ds\right) N(w)\,dw\right)\exp\left(2\int_0^{\arctan\frac{y}{x}} M(s)\,ds\right),$$

where $h \in \mathbb{R}$. Moreover, the system (7) has no periodic orbits**.**

Example 2 If we take $A_1(x,y) = \pi x^2 + \pi y^2$, $A_2(x,y) = 2x^2 + 2y^2$, $A_3(x,y) = A_5(x,y) = y$, $A_4(x,y) = A_6(x,y) = x$, $B_1(x,y) = -x^2+xy-y^2$, $B_2(x,y) = x^2+xy+y^2$ and $B_3(x,y) = x^2 + y^2$, then system (2) reads

$$\begin{cases} x' = x\left(\left(-x^2 + xy - y^2\right)\sin\left(\frac{y}{x}\right) + \left(x^2 + y^2\right)\sin\left(\frac{\pi x^2+\pi y^2}{2x^2+2y^2}\right)\right), \\ y' = y\left(\left(x^2 + xy + y^2\right)\sin\left(\frac{y}{x}\right) + \left(x^2 + y^2\right)\sin\left(\frac{\pi x^2+\pi y^2}{2x^2+2y^2}\right)\right). \end{cases} \tag{8}$$

The Kolmogorov system (8) in polar coordinates (r, θ) becomes

$$\begin{cases} r' = \left(1 + \left(\frac{1}{2}\sin 2\theta - \cos 2\theta\right)\sin(\tan\theta)\right) r^3, \\ \theta' = (\sin 2\theta)\sin(\tan\theta)\, r^2. \end{cases}$$

In the realistic quadrant $(x > 0, y > 0)$ it is the case (2) of Theorem 1, then the Kolmogorov system (8) has the first integral

$$H(x,y) = \left(x^2 + y^2\right)^{\frac{1}{2}}\exp\left(-\int_0^{\arctan\frac{y}{x}}\left(\frac{1 + \left(\frac{1}{2}\sin 2s - \cos 2s\right)\sin(\tan s)}{(\sin 2s)\sin(\tan s)}\right) ds\right).$$

The curves $H = h$ with $h \in \mathbb{R}$, which are formed by the trajectories of the differential system (8), in Cartesian coordinates are written as

$$\left(x^2+y^2\right)^{\frac{1}{2}} - h\exp\left(\int_0^{\arctan\frac{y}{x}}\left(\frac{1+\left(\frac{1}{2}\sin 2s-\cos 2s\right)\sin(\tan s)}{(\sin 2s)\sin(\tan s)}\right)ds\right)=0,$$

where $h \in \mathbb{R}$. Moreover, the system (8) has no periodic orbits.

3 Conclusion

The elementary method used in this paper seems to be fruitful to investigate more general planar differential systems of ODEs in order to obtain an explicit expression for a first integral which characterizes its trajectories. This is one of the classical tools in the classification of all trajectories of dynamical systems.

Acknowledgment

The authors would like to express their gratitude to the referee for pointing out some references to our attention and for his valuable remarks.

References

[1] S. A. Alharbi, A. S. Rambely and A. O. Almatroud. Dynamic modelling the immune system and its functions by vitamins intervention. *Nonlinear Dynamics and Systems Theory* **19** (2) (2019) 263–273.

[2] M. De Angelis. Mathematical contributions to the dynamics of the josephson functions: State of the art and open problems. *Nonlinear Dynamics and Systems Theory* **15** (3) (2015) 231–241.

[3] C. H. D. Alliera. Existence of solutions for a biological model using topological degree theory. *Nonlinear Dynamics and Systems Theory* **19** (1) (2019) 1–9.

[4] A. Bendjeddou and R. Boukoucha. Explicit limit cycles of a cubic polynomial differential systems. *Stud. Univ. Babes-Bolyai Math.* **61** (1) (2016) 77–85.

[5] R. Boukoucha. Explicit limit cycles of a family of polynomial differential systems. *Electronic Journal of Differential Equations.* **2017** (217) (2017) 1–7.

[6] R. Boukoucha and A. Bendjeddou. On the dynamics of a class of rational Kolmogorov systems. *Journal of Nonlinear Mathematical Physics.* **23** (1) (2016) 21–27.

[7] F. H. Busse. *Transition to Turbulence Via the Statistical Limit Cycle Route.* Synergetics, Springer-Verlag, berlin, 1978.

[8] L. Cairó and J. Llibre. Phase portraits of cubic polynomial vector fields of Lotka–Volterra type having a rational first integral of degree 2. *J. Phys.* A **40** (2007) 6329–6348.

[9] F. Dumortier, J. Llibre and J. Artés. Qualitative Theory of Planar Differential Systems. Berlin, Springer, 2006.

[10] P. Gao. Hamiltonian structure and first integrals for the Lotka-Volterra systems. *Phys. Lett. A* **273** (2000) 85–96.

[11] X. Huang. Limit cycles in a Kolmogorov-type model. *Internat. J. Math. Math. Sci.* **13** (3) (1990) 555–566.

[12] D. Hilbert. Mathematische probleme. *Lecture, Second Internat. Congr. Math.* (Paris, 1900), *Nachr. Ges. Wiss. Gttingen Math. Phys. Kl.* (1900) 253-297*, English transl, Bull. Amer. Math. Soc.* **8** (1902), 437-479.

[13] G. Lavel and R. Pellat. Plasma physics. In: *Proceedings of Summer School of Theoreal Physics*, Gordon and Breach. New York, 1975.

[14] C. Li and J. Llibre. The cyclicity of period annulus of a quadratic reversible Lotka–Volterra system. *Nonlinearity.* **22** (2009) 2971–2979.

[15] J. Llibre and T. Salhi. On the dynamics of class of Kolmogorov systems. *J. Appl. Math. Comput.* **225** (2013) 242–245.

[16] J. Llibre and C. Valls. Polynomial, rational and analytic first integrals for a family of 3-dimensional Lotka-Volterra systems. *Z. Angew. Math. Phys.* **62** (2011) 761–777.

[17] N. G. Llyod, J. M. Pearson, E. Saez and I. Szanto. Limit cycles of a cubic Kolmogorov system. *Appl. Math. Lett.* **9** (1) (1996) 15–18.

[18] R.M. May. *Stability and Complexity in Model Ecosystems*. Princeton, New Jersey, 1974.

[19] L. Perko. *Differential Equations and Dynamical Systems*. Third edition. Texts in Applied Mathematics. 7. Springer-Verlag, New York, 2001.

[20] R. V. Ruzich. Mathematical analysis in a model of primary succession. *Nonlinear Dynamics and Systems Theory* **15** (4) (2015) 418–427.

Nonlinear Dynamics and Systems Theory, **22** (1) (2022) 21–45

Comprehensive Description of Solutions to Semilinear Sectorial Equations: an Overview

Radoslaw Czaja* and Tomasz Dlotko

Institute of Mathematics, University of Silesia in Katowice, Bankowa 14, 40-007 Katowice, Poland

Received: July 12, 2021; Revised: December 19, 2021

Abstract: Description of all possible types of behavior, or evolution, of solutions to a semilinear sectorial equation is given. The phase space is divided into separate regions containing bounded solutions, grow-up solutions and those which blow up in a finite time. An overview of results concerning the typical situation when solutions of various types of behavior coexist is given and illustrated by chosen examples of reaction-diffusion equations.

Keywords: *parabolic equation; sectorial equation; Cauchy problem; global solutions; grow-up solutions; blow-up solutions; comprehensive description.*

Mathematics Subject Classification (2010): Primary 35B40; Secondary 35B60, 35K15, 70K05, 93D30.

1 Introduction

This paper is devoted to the fundamental question connected with solutions of semilinear sectorial equations (1) being generalizations of parabolic equations: *Provided that a local in time solution exists, what is the expected future for the rest of its existence?*

It is known from the classical references, such as [20, Chapter I], that, in general, there are three potential forms of the further evolution of such solutions:
– the local solution may *blow up*, which means that its phase space norm becomes unbounded in a finite time; in general, it can be a consequence of unboundedness of the values of the solution or the values of some of its derivatives, even though the solution itself may stay bounded in the $L^{\infty}-$norm,
– the local solution may *grow up*, that is, it will exist for all positive times, while some of its norms will become unbounded as $t \to \infty$,

* Corresponding author: mailto:radoslaw.czaja@us.edu.pl

– the local solution will be extended globally in time with the required norms being bounded for all $t \geq 0$. This is a particularly interesting form of behavior, including the possibility that the equation generates a dynamical system possessing a *global attractor*.

Throughout the last 70 years, plenty of results appeared in the literature concerning qualitative behavior of solutions and describing separately the blow-up phenomenon, less known case of grow-up solutions and, finally, well studied globally bounded in time solutions, the latter including the particular case of semigroups with global attractors. From the abundance of references, we distinguish [20] and [15] for the local solvability of parabolic and sectorial equations, [24] for the issues regarding the blow-up, and [4, 12, 19, 31] for the existence of the global attractors for dissipative semigroups.

Usually, the authors study the above types of behavior as if these types would exist apart. The reason is perhaps connected with the fact that even the description of one kind is complicated enough. However, the situation we face in practice is the coexistence of all these three types of behavior for a single evolution equation.

Our aim in this paper is thus to describe such a general typical situation for the Cauchy problem for the semilinear sectorial equation

$$u_t + Au = F(u),\ t > 0, \quad u(0) = u_0, \tag{1}$$

where A is a sectorial positive operator and F stands for the nonlinear term. It is well-known that many ordinary and partial differential equations or systems from the Applied Sciences can be investigated within the approach of (1). This includes the heat propagation equation, reaction-diffusion systems, Fitzhugh-Nagumo equation, pattern formation models like the Cahn-Hilliard equation or viscous Cahn-Hilliard equation, models of fluid flows like the Burgers equation or the celebrated Navier-Stokes system and many others (see e.g. [4, 31, 33]). Wherever possible, we illustrate the discussed type of behavior of solutions using particular examples, mostly of ordinary differential equations or parabolic second order equations, that allow a more detailed description. Of course, the questions studied in this paper are much more involved for real world systems. Nevertheless, our paper may serve as a guide for the future application to the above mentioned problems.

The contents of this paper are as follows. In Section 2, we formulate the basic Assumption 2.1 on A and F in (1) and recall in Corollary 2.1, following [4, 15], the local existence of X^α solutions of (1) under this assumption (X^α stands for the phase space). In Definition 2.2, we introduce the partition of X^α according to the above-mentioned three types of behavior, introducing the subsets X^α_D, X^α_G and X^α_B. Moreover, we briefly describe consequences of their coexistence and mention some previous results from works where asymptotics of equations with solutions of different behavior was investigated.

In Section 3, we present a simple introductory example of a scalar reaction-diffusion problem (7), (8) exhibiting the coexistence of all three ways solutions may evolve.

In Section 4, we show in Theorem 4.1 that the life time of an X^α solution of (1) is a lower semicontinuous function of the initial data u_0. As Example 4.1 shows, in general, this function is not continuous, which makes it hard to characterize the components of the partition of X^α from Definition 2.2. Nevertheless, the *subordination condition* (18) together with an appropriate a priori estimate (17) allows to estimate the life time from below (see Theorem 4.2).

In Section 5, we present a range of examples of parabolic equations which possess, among others, solutions which grow up. The first example (20) shows that a linear reaction term leads to the existence of grow-up solutions. However, for the Neumann problem of the form (19), this observation can be generalized to nonlinearities with the divergent integral (21). Of course, this property still holds if we perturb the linear reaction term by a bounded nonlinearity. In this case, except for the grow-up solutions, all other solutions are globally bounded. As the example of (19), (25) exhibits, not only sub-linear nonlinearities lead to grow-up solutions. Furthermore, as seen in problems (26) and (27), reaction-diffusion equations with gradient-dependent nonlinearities may also possess grow-up solutions. In certain cases, the asymptotics of equations with grow-up solutions can be described in terms of non-compact attractors (see [22, 23]).

In Section 6, we briefly explain the reasons of appearance of blow-up solutions for parabolic equations and provide further examples of equations with solutions which become unbounded in finite time.

If the problem under consideration manifests at least two different kinds of behavior of solutions, there cannot exist a global attractor in the whole phase space in the sense of Definition 2.4. Nevertheless, there may be determined *local attractors*, like stable stationary solutions, and their *basins of attraction* can be considered. In Section 7, we discuss these notions and relate them with the existence of a Lyapunov function. In particular, a Lyapunov function on X^α_D for the problem (1) with A having compact resolvent guarantees that solutions which stay bounded must approach the set of equilibria, although the other solutions may become unbounded in a finite or infinite time (see Corollary 7.1).

For completeness of the presentation, we gather in the Appendix results concerning the existence of sufficiently regular solutions and their global extendibility in time for the homogeneous Neumann boundary problem for a reaction-diffusion equation with a gradient-dependent nonlinearity.

2 Setting of the Problem

Our purpose is to examine the behavior of solutions of evolution equations, which can be treated as autonomous abstract parabolic equations. To this end, consider an abstract Cauchy problem (1) under the following assumptions.

Assumption 2.1 *(i)* $-A\colon X \supset D(A) \to X$ *generates a strongly continuous analytic linear semigroup* $\{e^{-At}\colon t \geq 0\}$ *in a Banach space* X *and* $\operatorname{Re}\sigma(A) > 0$,
(ii) $F\colon X^\alpha \to X$ *is Lipschitz continuous on the bounded subsets of* $X^\alpha = D(A^\alpha)$ *for some* $\alpha \in [0, 1)$.

Remark 2.1 Note that the generation of a strongly continuous analytic semigroup by $-A$ is equivalent to the sectoriality of the operator A (see e.g. [4, 15]). If A is merely sectorial, the condition $\operatorname{Re}\sigma(A) > 0$ of positivity of its spectrum can always be achieved by adding a term cu to both sides of the differential equation in (1) with a sufficiently large constant c. Then we define fractional power spaces X^β, $\beta \in \mathbb{R}$, connected with the domains of the operators A^β (see also [4, 15]) and the semigroup $\{e^{-At}\colon t \geq 0\}$ satisfies

$$\left\|e^{-At}x\right\|_X \leq C_0 e^{-at}\left\|x\right\|_X,\ t \geq 0,\ \left\|e^{-At}x\right\|_{X^\beta} \leq C_\beta t^{-\beta} e^{-at}\left\|x\right\|_X,\ t > 0,\ x \in X, \quad (2)$$

for any $\beta > 0$ with some $a > 0$ and $C_0, C_\beta \geq 1$.

Following the formalism of Dan Henry, we introduce a *local* X^α *solution* of (1).

Definition 2.1 Let $u_0 \in X^\alpha$. A function u is called a *local* X^α *solution* of (1) if, for some $\tau > 0$, u belongs to $C([0, \tau); X^\alpha) \cap C((0, \tau); X^1) \cap C^1((0, \tau); X)$, $u(0) = u_0$ and the first equation in (1) holds in X for all $t \in (0, \tau)$.

Below we quote a general theorem devoted to the local in time solvability of abstract Cauchy problems even for nonautonomous equations. This theorem is a straightforward generalization of the well-known results from [15] or [4].

Theorem 2.1 *Let $A\colon X \supset D(A) \to X$ satisfy (i) of Assumption 2.1. Assume also that $G\colon [t_0, T_0) \times X^\alpha \to X$, where $-\infty < t_0 < T_0 \leq \infty$, is a continuous function satisfying for compact sets $K_1 \subset [t_0, T_0)$, $K_2 \subset (t_0, T_0)$ and each bounded set $B \subset X^\alpha$*

$$\|G(s, w_1) - G(s, w_2)\|_X \leq M_{K_1,B} \|w_1 - w_2\|_{X^\alpha}, \ s \in K_1, \ w_1, w_2 \in B,$$

$$\|G(s_1, w_1) - G(s_2, w_2)\|_X \leq M_{K_2,B}\big(|s_1 - s_2|^\theta + \|w_1 - w_2\|_{X^\alpha}\big), \ s_1, s_2 \in K_2, \ w_1, w_2 \in B$$

with some positive $M_{K_1,B}$, $M_{K_2,B}$ and $0 < \theta \leq 1$. Then, for any $w_0 \in X^\alpha$, there exists a unique local X^α solution of the problem

$$w_t + Aw = G(t, w), \ t_0 < t < T_0, \quad w(t_0) = w_0, \tag{3}$$

i.e., $w \in C([t_0, \tau); X^\alpha) \cap C((t_0, \tau); X^1) \cap C^1((t_0, \tau); X)$ and satisfies (3) in X on $[t_0, \tau)$. Under the above assumptions, this X^α solution is equivalently a function $w \in C([t_0, \tau); X^\alpha)$ satisfying the variation of constants formula

$$w(t) = e^{-A(t-t_0)} w_0 + \int_{t_0}^{t} e^{-A(t-s)} G(s, w(s)) ds, \ t \in [t_0, \tau).$$

Moreover, the local X^α solution can be extended to the maximal interval of existence $[0, \tau_{w_0})$, which means that either $\tau_{w_0} = T_0$ or $\tau_{w_0} < T_0$ and $\limsup_{t \to \tau_{w_0}^-} \|w(t)\|_{X^\alpha} = \infty$.

Henceforth, we understand a solution as an X^α solution defined on the maximal interval of existence. If $T_0 = \infty$ and the life time $\tau_{w_0} = \infty$, then we call such a solution *global*.

For our problem (1), we thus have the following existence result.

Corollary 2.1 *Under Assumption 2.1, for each $u_0 \in X^\alpha$, there exists a unique X^α solution $u = u(t, u_0)$ of (1) defined on its maximal interval of existence $[0, \tau_{u_0})$, i.e.,*

$$\text{either } \tau_{u_0} = \infty, \quad \text{or if } \ \tau_{u_0} < \infty, \ \text{ then } \ \limsup_{t \to \tau_{u_0}^-} \|u(t, u_0)\|_{X^\alpha} = \infty. \tag{4}$$

According to the alternative (4), we define a partition of X^α into three disjoint parts, which distinguish the behavior of a particular solution of (1).

Definition 2.2 We have $X^\alpha = X^\alpha_D \cup X^\alpha_G \cup X^\alpha_B$, where

• X^α_D denotes the set of initial data u_0 in X^α corresponding to global in time and *globally bounded solutions* for $t \geq 0$, that is, $\tau_{u_0} = \infty$ and the norm $\|u(t, u_0)\|_{X^\alpha}$ stays bounded as $t \to \infty$,

• X^α_G denotes the set of initial data u_0 in X^α corresponding to *global solutions which are unbounded* as $t \to \infty$, that is, $\tau_{u_0} = \infty$ and $\limsup_{t \to \infty} \|u(t, u_0)\|_{X^\alpha} = \infty$,

• X^α_B denotes the set of initial data $u_0 \in X^\alpha$ corresponding to solutions that *blow up in a finite time*, that is, $u(t, u_0)$ exists for $t > 0$ near 0, but there exists $\tau_{u_0} > 0$ such that $\limsup_{t \to \tau_{u_0}^-} \|u(t, u_0)\|_{X^\alpha} = \infty$.

Thus, the solutions starting from $u_0 \in X^\alpha_D$ are the *global bounded solutions*, the solutions originating from $u_0 \in X^\alpha_G$ are the *grow-up solutions* and those starting from $u_0 \in X^\alpha_B$ are called the *blow-up solutions*.

Clearly, knowledge of interiors and boundaries of the above-introduced sets would be vital for understanding the global dynamics of the problem under consideration on the entire phase space. Unfortunately, for many models arising from the Applied Sciences, global in time solvability is limited only to small initial data (see e.g. [17]).

In the last decades, we observed among scientists a kind of specialization in a specific behavior of solutions. The group being focused on global bounded solutions treated the other admissible behavior as non-existent and considered only equations for which $X^\alpha = X^\alpha_D$. This approach concentrated on the theory of *dissipative semigroups* and the description of asymptotic behavior of solutions using the notion of a *global attractor* (see [4, 12, 15, 19, 25, 33] among many others). Let us recall these notions.

Definition 2.3 A *semigroup* $\{S(t)\colon t \geq 0\}$ on a metric space M is a continuous mapping $S\colon \mathbb{R}^+ \times M \to M$, which satisfies

$$S(0, u_0) = u_0, \quad S(t+s, u_0) = S(t, S(s, u_0)) \text{ for all } t, s \geq 0 \text{ and all } u_0 \in M.$$

Henceforth, we will write $S(t)u_0 = S(t, u_0)$.

Definition 2.4 Let $\{S(t)\colon t \geq 0\}$ be a semigroup on a metric space (M, d). We say that a set $A \subset M$ *attracts* a set $B \subset M$ if for any $\varepsilon > 0$, there exists $T > 0$ such that

$$\operatorname{dist}(S(t)B, A) := \sup_{u_0 \in B} \inf_{v \in A} d(S(t)u_0, v) < \varepsilon \text{ whenever } t \geq T.$$

A nonempty compact set $\mathcal{A} \subset M$ is said to be a *global attractor* for $\{S(t)\colon t \geq 0\}$ if it is invariant, i.e., $S(t)\mathcal{A} = \mathcal{A}$ for all $t \geq 0$, and it attracts each bounded subset of M.

Definition 2.5 A semigroup $\{S(t)\colon t \geq 0\}$ on a metric space M is called *asymptotically compact* if for arbitrary sequences $t_n \to \infty$ and $\{u_n\} \subset M$ bounded, the sequence $\{S(t_n)u_n\}$ has a convergent subsequence in M. We say that $\{S(t)\colon t \geq 0\}$ is *dissipative* if there exists a bounded set $B_0 \subset M$ which attracts each bounded subset of M.

In the case of $X^\alpha = X^\alpha_D$, the solutions of (1) form a semigroup $\{S(t)\colon t \geq 0\}$ on X^α,

$$S(t)u_0 = u(t, u_0), \ t \geq 0, \ u_0 \in X^\alpha.$$

If there exists a bounded absorbing set $B_0 \subset X^\alpha$ for this semigroup, that is, for any bounded subset B of X^α there exists $t_B > 0$ such that $S(t)B \subset B_0$ for $t \geq t_B$ and the semigroup is asymptotically compact (or asymptotically smooth in the sense of [12]), then the semigroup is dissipative and it possesses a global attractor in X^α. This compact maximal invariant set $\mathcal{A}$ attracting all bounded subsets of X^α determines then all possible long-time dynamics of solutions (cp. e.g. [25, Proposition 10.14]). The global attractor contains, in particular, all stationary solutions, all periodic solutions (if they exist) and all bounded invariant complete orbits connecting them. Recently, much effort is put to thoroughly describe the structure of a global attractor (see for instance [8, 9] and references therein) for particular classes of equations.

Observe that the notion of a semigroup for (1) can be defined just on a subset M of X^α such that solutions originating from M exist globally in time and do not leave M. Such a general approach was presented in the introductory part of the monograph [27, Sections 2.1-2.3]. For instance, one can take $M = X^\alpha_D \cup X^\alpha_G$ or $M = X^\alpha_D$. Note, however, that in general, we do not know in advance whether M is a closed subset of X^α.

The case of a semigroup on $M = X^\alpha_D$ in the admissible presence of other behavior of solutions was considered, e.g. in [6]. Besides Assumption 2.1, it was required there the following.

Assumption 2.2 *The resolvent of the operator A is compact.*

In this setting, it was shown in [6] that the semigroup on $M = X^\alpha_D \neq \emptyset$ is asymptotically smooth. Hence the point dissipativity of $\{S(t)\colon t \geq 0\}$ on M implies that for any $u_0 \in X^\alpha$ the solution $u(\cdot, u_0)$ of (1) either blows up in a finite time, or grows up, or approaches a nonempty compact invariant set. Moreover, if all bounded complete orbits of points are uniformly bounded in X^α, then the solutions that stay bounded approach a maximal compact invariant set, which plays the role of the global attractor in this setting.

Note that the presence of grow-up solutions forbids that they approach a maximal invariant set which is bounded in X^α. In [3], the authors introduced a concept of an unbounded attractor, where the boundedness of the attractor was substituted by the minimality property. The asymptotic behavior of grow-up solutions was studied, for example, in [1,22,23] for 'slowly non-dissipative reaction-diffusion equations' of the form

$$\begin{cases} u_t = u_{xx} + bu + g(x,u,u_x), \ x \in (0,\pi), \ t > 0, \\ u_x(t,0) = u_x(t,\pi) = 0, \ t > 0, \quad u(0,x) = u_0(x), \ x \in (0,\pi), \end{cases} \tag{5}$$

with $b > 0$ and g being a C^2 bounded function. Such a problem defines a semigroup on $X^\alpha = X^\alpha_D \cup X^\alpha_G$ with $\alpha \in (\frac{3}{4}, 1)$ and with nonempty X^α_G. Then any solution to (5) converges either to a bounded stationary solution or a certain object called an equilibrium at infinity. For a characterization of the structure of a non-compact global attractor, see [23].

As regards the blow-up solutions, there exists a vast literature investigating the rates and the profiles of blow-up solutions to particular differential equations, but the notion, which would encompass the dynamics of the problem and include blow-up solutions, has not been formulated yet.

The aim of this paper is to emphasize that a typical situation is the coexistence of various types of behavior of solutions, formulate common properties of solutions, characterize their three classes, and indicate open problems connected with that partition.

3 Introductory Example

It is easy to find examples of systems allowing only for a limited set of behavior of solutions. In particular, if there is a global attractor for the system in a phase space, then all solutions need to exist globally and be bounded in the phase space. Many examples of such systems coming from the Applied Sciences are available, see e.g. [4, 15, 19, 31].

It is also simple to find a system having only blow-up solutions. For instance, the ODE problem

$$y' = y^2 + 1, \quad y(0) = y_0, \tag{6}$$

has an explicit solution

$$y(t) = \tan(t + \arctan(y_0)) \text{ defined for } t \in \big(-\pi/2 - \arctan(y_0), \pi/2 - \arctan(y_0)\big),$$

which blows up at the finite life time $\tau_{y_0} = \pi/2 - \arctan(y_0)$ for each $y_0 \in \mathbb{R}$.

We will now present a fairly complete analysis of a 1-D scalar parabolic equation, which exhibits the coexistence of all the three types of behavior: the blow-up solutions, the grow-up solutions, the bounded solutions approaching a certain local attractor as well as the bounded solutions being unstable equilibria.

Consider a 1-D Neumann semilinear parabolic problem of the form

$$\begin{cases} u_t = u_{xx} + f(u), \ t > 0, \ x \in (0, \pi), \\ u_x(t, 0) = u_x(t, \pi) = 0, \ t > 0, \quad u(0, x) = u_0(x), \ x \in (0, \pi), \end{cases} \tag{7}$$

with the nonlinearity f given by

$$f(y) = \frac{\mu}{2}(y^3 - y) \text{ for } y < 1 \ \text{ and } \ f(y) = \mu(y - 1) \text{ for } y \geq 1, \tag{8}$$

with $\mu > 0$. The polynomial occurring in the nonlinear term f in $(-\infty, 1)$ is *opposite* to the well-known 'bi-stable nonlinearity' as in the Chafee-Infante problem.

The existence of X^α solutions u to (7) as well as the subordination condition follow from a more general Example 4.2 below.

Now we analyze an ordinary differential equation connected with the parabolic problem (7) satisfied by the x-independent solutions $y = y(t)$ of (7), that means

$$y' = f(y), \ t > 0, \quad y(0) = y_0. \tag{9}$$

The equation in (9) is of separable variables and can be explicitly solved. Except for three equilibria: the asymptotically stable $y_0 = 0$, unstable $y_0 = -1$ and $y_0 = 1$, we have other bounded globally defined solutions

$$y(t) = \operatorname{sgn}(y_0) \left(1 - \left(1 - y_0^{-2}\right) e^{\mu t}\right)^{-1/2}, \ t \in \mathbb{R} \ \text{ for } \ y_0 \in (-1, 0) \cup (0, 1).$$

For $y_0 > 1$, the solutions $y(t) = (y_0 - 1)e^{\mu t} + 1$ are also globally defined for $t \in \mathbb{R}$, but they are unbounded as $t \to \infty$. Finally, the solutions for $y_0 < -1$ are given by

$$y(t) = -\left(1 - \left(1 - y_0^{-2}\right) e^{\mu t}\right)^{-1/2}, \ t \in \left(-\infty, -\mu^{-1} \ln\left(1 - y_0^{-2}\right)\right),$$

and blow up in a finite time.

Using the explicit form of solutions of the ordinary differential equation (9), we are able to give a description of solutions to (7) based on the *Comparison Principle* (see [28, Theorem 10.1]). We recall that theorem for completeness.

Proposition 3.1 *Consider a uniformly parabolic linear operator in divergence form in a bounded domain $\Omega \subset \mathbb{R}^N$ with regular boundary $\partial\Omega$:*

$$\mathcal{P}u := u_t - Au = u_t - \sum_{i,j=1}^{N} \left(a_{ij}(t, x)u_{x_i}\right)_{x_j}, \quad (t, x) \in (0, T) \times \Omega,$$

where $\{a_{ij}\}$ is a symmetric matrix with bounded coefficients. Let $g = g(t, x, u)$ be C^1 in u and Hölder continuous in t and x. Assume that u and v are C^1 functions of t in $[0, T]$ and C^2 functions in x in Ω, which satisfy the following three inequalities:

$$\begin{aligned} &\mathcal{P}u - g(t, x, u) \geq \mathcal{P}v - g(t, x, v), \ (t, x) \in (0, T) \times \Omega, \\ &u(0, x) \geq v(0, x), \ x \in \Omega, \\ &\frac{\partial u}{\partial \nu} + \beta u \geq \frac{\partial v}{\partial \nu} + \beta v, \ (t, x) \in (0, T) \times \partial\Omega, \end{aligned}$$

where $\beta = \beta(t, x) \geq 0$ on $(0, T) \times \partial\Omega$. Then $u(t, x) \geq v(t, x)$ for all $(t, x) \in [0, T] \times \overline{\Omega}$. Moreover, if, in addition, $u(0, x) > v(0, x)$ for x in an open subset $\Omega_1 \subset \Omega$, then we have $u(t, x) > v(t, x)$ in $[0, T] \times \overline{\Omega_1}$.

Using Proposition 3.1, we will compare the solutions of (7) and (9), and knowing the behavior of solutions to (9), we get the corresponding information for certain solutions of the parabolic problem (7). More precisely, having solutions u of (7) and y of (9), we see that $u_t - u_{xx} - f(u) = 0 = y' - f(y)$ as long as both solutions exist and $x \in (0, \pi)$. Moreover, $u_x(t, 0) = u_x(t, \pi) = 0$ and the same is true for the x-independent solution $y(t)$. Thus we can compare u with the solution y starting from $y_0 = \min_{x\in[0,\pi]} u_0(x)$ or $y_0 = \max_{x\in[0,\pi]} u_0(x)$. We introduce *the range* of initial data

$$R_{u_0} = \big[\min_{x\in[0,\pi]} u_0(x), \max_{x\in[0,\pi]} u_0(x)\big].$$

The following characterization is then a consequence of Proposition 3.1 (compare Theorem 4.2 and Proposition 4.1 below to get the estimates of the life time of solution u).

(i) Whenever $R_{u_0} \subset (-\infty, -1)$, the corresponding to u_0 solution of (7) blows up in a finite time τ_{u_0}. Moreover, τ_{u_0} is estimated from above by the blow-up time of the solution to (9) with $y_0 = \max_{x\in[0,\pi]} u_0(x)$, and estimated from below by the blow-up time of the solution to (9) with initial data $y_0 = \min_{x\in[0,\pi]} u_0(x)$.

(ii) If $R_{u_0} \subset (-1, 1)$, then the solution $u(\cdot, u_0)$ of (7) tends to zero as $t \to \infty$.

(iii) Whenever $R_{u_0} \subset (1, \infty)$, the corresponding solution grows up as $t \to \infty$.

Evidently, there are many initial data u_0 outside of the above three classes; then the situation is more delicate and requires further studies using more sophisticated tools. Nevertheless, the three types of behavior of solutions are present among the solutions of (7).

4 Life Time of Solutions

We have seen in problem (6) possessing only blow-up solutions that the life time was a continuous function of the initial data. However, we show below that, in general, the life time of a solution to a sectorial equation need not be upper semicontinuous, but certainly is a lower semicontinuous function.

Theorem 4.1 *Under Assumption 2.1, consider the X^α solution $u(t, u_0)$ of*

$$u_t + Au = F(u),\ t > 0, \tag{10}$$

satisfying the initial condition $u(0) = u_0 \in X^\alpha$. Then the life time τ_{u_0} is a lower semicontinuous function *of u_0. More precisely, we have*

$$\forall_{0<T<\tau_{u_0}} \exists_{\delta>0} \forall_{v_0\in X^\alpha}\ \|v_0 - u_0\|_{X^\alpha} < \delta \Rightarrow \tau_{v_0} > T,$$

where τ_{v_0} is the life time of the X^α solution of (10) *starting from v_0.*

Moreover, the solutions depend continuously on the initial data; for $0 < T < \tau_{u_0}$, there exists $\delta > 0$ and $L \geq 1$ such that if $\|v_0 - u_0\|_{X^\alpha} < \delta$, then we have

$$\|u(t, v_0) - u(t, u_0)\|_{X^\alpha} \leq L\, \|v_0 - u_0\|_{X^\alpha}\,,\ t \in [0, T]. \tag{11}$$

Proof. Let $u(t)$ be the solution of (10) corresponding to the initial data u_0 and let $v(t)$ be its 'perturbation', that is, the solution of (10) corresponding to the initial data v_0 (eventually close to u_0). Setting $w(t) := v(t) - u(t)$, we see that w is a solution of

$$w_t + Aw = F(w + u(t)) - F(u(t)),\ 0 < t < \tau_{u_0}, \quad w(0) = w_0, \tag{12}$$

with $w_0 = v_0 - u_0 \in X^\alpha$. Observe that

$$G(t,w) = F(w+u(t)) - F(u(t)),\ (t,w) \in [0,\tau_{u_0}) \times X^\alpha,$$

satisfies Theorem 2.1 with $\theta = 1$ since $u_t \in C((0,\tau_{u_0}), X^\alpha)$ (see [4, Corollary 2.3.1]). Thus, for any $w_0 \in X^\alpha$, we have a unique solution of (12) with the life time τ_{w_0}.

Let $h\colon \mathbb{R} \to [0,1]$ be of class C^1 such that $h(s) = 1$ for $s \le 1$ and $h(s) = 0$ for $s \ge 2$. We fix an arbitrary $T \in (0,\tau_{u_0})$. We define a function $H(t,z) = G(t, zh(\|z\|_{X^\alpha}))$, $(t,z) \in [0,T] \times X^\alpha$. Note that H is continuous, $H(t,0) = G(t,0) = 0$ and there exists $L_H > 0$ depending on F, T and u_0 such that

$$\|H(t,z_1) - H(t,z_2)\|_X \le L_H \|z_1 - z_2\|_{X^\alpha},\ t \in [0,T],\ z_1,z_2 \in X^\alpha, \tag{13}$$

since $\|zh(\|z\|_{X^\alpha})\|_{X^\alpha} \le 2$ for any $z \in X^\alpha$.

Let $E = C([0,T], X^\alpha)$ be equipped with *equivalent Bielecki's norm*

$$\|z\|_E = \max\{\|z(s)\|_{X^\alpha} e^{-\xi s} \colon s \in [0,T]\},$$

where $\xi > 0$ is so large that $C_\alpha L_H \Gamma(1-\alpha)\frac{1}{(a+\xi)^{1-\alpha}} < 1$. Let $z_0 \in X^\alpha$ and define the transformation $\Phi\colon E \to E$ by

$$\Phi(z)(t) = e^{-At} z_0 + \int_0^t e^{-A(t-s)} H(s,z(s))ds,\ t \in [0,T],\ z \in E.$$

Note that for $z_1, z_2 \in E$ and $t \in [0,T]$, using estimates (2), we get

$$\|\Phi(z_1)(t) - \Phi(z_2)(t)\|_{X^\alpha} \le C_\alpha L_H \int_0^t \frac{e^{-a(t-s)}}{(t-s)^\alpha} \|z_1(s) - z_2(s)\|_{X^\alpha} ds$$

$$\le C_\alpha L_H \|z_1 - z_2\|_E \int_0^t \frac{e^{-a(t-s)}}{(t-s)^\alpha} e^{\xi s} ds = C_\alpha L_H \|z_1 - z_2\|_E \frac{e^{\xi t}}{(a+\xi)^{1-\alpha}} \int_0^{(a+\xi)t} r^{-\alpha} e^{-r} dr.$$

Thus we obtain

$$\|\Phi(z_1) - \Phi(z_2)\|_E \le C_\alpha L_H \Gamma(1-\alpha) \frac{1}{(a+\xi)^{1-\alpha}} \|z_1 - z_2\|_E,\ z_1,z_2 \in E,$$

and Φ is a contraction on E. By the Banach Fixed Point Theorem, for any $z_0 \in X^\alpha$, there exists a unique $z \in C([0,T], X^\alpha)$, which satisfies

$$z(t) = e^{-At} z_0 + \int_0^t e^{-A(t-s)} H(s,z(s))ds,\ t \in [0,T]. \tag{14}$$

Take $z_1, z_2 \in X^\alpha$ and let $z(t,z_1)$, $z(t,z_2)$ be the corresponding solutions of (14) starting from z_1 and z_2, respectively. Let $y(t) = \|z(t,z_1) - z(t,z_2)\|_{X^\alpha}$ for $t \in [0,T]$ and note that by (2) and (13)

$$y(t) \le C_0 e^{-at} \|z_1 - z_2\|_{X^\alpha} + C_\alpha L_H \int_0^t \frac{e^{-a(t-s)}}{(t-s)^\alpha} y(s) ds,\ t \in [0,T].$$

By the Volterra type inequality (see e.g. [4, Lemma 1.2.9]) there exists a constant $L \ge 1$ such that the following Lipschitz condition holds:

$$\|z(t,z_1) - z(t,z_2)\|_{X^\alpha} \le L \|z_1 - z_2\|_{X^\alpha},\ t \in [0,T]. \tag{15}$$

Since $H(t,0)=0$, $t\in[0,T]$, we also have $z(t,0)=0$, $t\in[0,T]$. Take any $w_0\in X^\alpha$ such that $\|w_0\|_{X^\alpha}\le \frac{1}{L}$. By (15) we obtain $\|z(t,w_0)\|\le 1$ for $t\in[0,T]$. Since $H(t,z)=G(t,z)$ for $t\in[0,T]$ and $z\in X^\alpha$ such that $\|z\|_{X^\alpha}\le 1$, we obtain from (14)

$$z(t,w_0)=e^{-At}w_0+\int_0^t e^{-A(t-s)}G(s,z(s,w_0))ds,\ t\in[0,T].$$

Thus $z(t,w_0)$ is an X^α solution of (12) on $[0,T]$. By the uniqueness of solutions of (12), we see that $\tau_{w_0}>T$ for $w_0\in X^\alpha$ such that $\|w_0\|_{X^\alpha}\le\frac{1}{L}$. Set $\delta=\frac{1}{L}$ and take $v_0\in X^\alpha$ such that $\|v_0-u_0\|_{X^\alpha}<\delta$. Then the solution $w(t,w_0)$ of (12) with $w_0=v_0-u_0$ exists at least on the interval $[0,T]$. Hence $w(t,w_0)+u(t,u_0)$, $t\in[0,T]$, is an X^α solution of (10) on $[0,T]$ starting from v_0, which shows that $\tau_{v_0}>T$. Moreover, we have (11), which ends the proof. □

In general, the life time τ_{u_0} need not be upper semicontinuous with respect to u_0 as the following example shows.

Example 4.1 Consider the planar system of ordinary differential equations

$$\begin{cases} x'=1,\\ y'=e^y\sin x, \end{cases}\tag{16}$$

with the initial condition $u(0)=(x(0),y(0))=u_0\in\mathbb{R}^2$. If $u_0=(0,-\ln 2)$, then the solution $u(t)=(x(t),y(t))$ of (16) is $u(t,u_0)=(t,-\ln(\cos t+1))$ for $t\in(-\pi,\pi)$, if $u_n=(0,-\ln 2-\frac{1}{n})$, $n\in\mathbb{N}$, then the solution of (16) is $u(t,u_n)=(t,-\ln(\cos t+2e^{\frac{1}{n}}-1))$ for $t\in\mathbb{R}$, whereas if $\hat u_n=(0,-\ln 2+\frac{1}{n})$, $n\in\mathbb{N}$, then the solution of (16) is

$$u(t,\hat u_n)=(t,-\ln(\cos t+2e^{-\frac{1}{n}}-1)),\ t\in(-\arccos(1-2e^{-\frac{1}{n}}),\arccos(1-2e^{-\frac{1}{n}})).$$

Observe that $u_n\to u_0$, $\hat u_n\to u_0$ in $\mathbb{R}^2$ and $\tau_{u_n}=\infty$, $\tau_{\hat u_n}=\arccos(1-2e^{-\frac{1}{n}})$ for $n\in\mathbb{N}$. Thus, using the lower semicontinuity of τ_{u_0}, we obtain in this case

$$\pi=\tau_{u_0}=\liminf_{v_0\to u_0}\tau_{v_0}<\limsup_{v_0\to u_0}\tau_{v_0}=\infty.$$

It is of interest to estimate the life time τ_{u_0} of a solution u to (10). Note that it is typical for mathematical models of phenomena in the Applied Sciences that certain natural a priori estimates of solutions are available, for example, energy decay, conservation of mass, etc. Below we present a technique to estimate τ_{u_0} based on such an appropriate a priori estimate combined with a *subordination condition* for the nonlinearity due to Wolf von Wahl (see [32]). This condition (see (18) below) allows to translate, or sharpen, that natural a priori estimate into a form suitable to control the nonlinear term.

Theorem 4.2 *Assume that the following a priori estimate for the solution $u(t)$ of (10) satisfying $u(0)=u_0\in X^\alpha$ holds in a normed space $Y\supset X^\alpha$, that is, there exists a function $c\colon[0,T)\to[0,\infty)$, $0<T\le\infty$, bounded on compact intervals and such that*

$$\|u(t)\|_Y\le c(t),\ t\in(0,\min\{\tau_{u_0},T\}),\tag{17}$$

where τ_{u_0} denotes the life time of the solution. Furthermore, assume that the following subordination condition holds for the nonlinearity, that is, there exist a nondecreasing function $g\colon[0,\infty)\to[0,\infty)$ and a constant $\theta\in[0,1)$ such that

$$\|F(u(t))\|_X\le g(\|u(t)\|_Y)\left(1+\|u(t)\|^\theta_{X^\alpha}\right),\ t\in(0,\tau_{u_0}).\tag{18}$$

Then we have $\tau_{u_0}\ge T$.

Proof. On the contrary, suppose that $\tau_{u_0} < T$. The variation of constants formula

$$u(t) = e^{-At}u_0 + \int_0^t e^{-A(t-s)}F(u(s))ds,\ t \in (0, \tau_{u_0}),$$

the subordination condition (18) and the estimates (2) yield

$$\|u(t)\|_{X^\alpha} \le C_0 e^{-at}\|u_0\|_{X^\alpha} + \int_0^t C_\alpha \frac{e^{-a(t-s)}}{(t-s)^\alpha} g(\|u(s)\|_Y)\big(1 + \|u(s)\|^\theta_{X^\alpha}\big)ds.$$

Applying the a priori estimate (17), we obtain

$$\|u(t)\|_{X^\alpha} \le C_0\|u_0\|_{X^\alpha} + C_\alpha g\big(\sup_{s\in[0,\tau_{u_0}]} c(s)\big)\Big(1 + \Big(\sup_{s\in[0,t]}\|u(s)\|_{X^\alpha}\Big)^\theta\Big)a^{\alpha-1}\Gamma(1-\alpha).$$

Thus, setting

$$b(u_0) = C_0\|u_0\|_{X^\alpha} + C_\alpha a^{\alpha-1}\Gamma(1-\alpha)g\big(\sup_{s\in[0,\tau_{u_0}]} c(s)\big),$$

we get

$$\sup_{\tau\in[0,t]}\|u(\tau)\|_{X^\alpha} \le b(u_0)\Big(1 + \Big(\sup_{\tau\in[0,t]}\|u(\tau)\|_{X^\alpha}\Big)^\theta\Big),\ t \in [0, \tau_{u_0}).$$

Therefore, $\sup_{\tau\in[0,t]}\|u(\tau)\|_{X^\alpha}$ is estimated above by the non-negative root $z_0(u_0)$ of the algebraic equation $b(u_0)(1 + z^\theta) - z = 0$. Hence we obtain

$$\|u(t)\|_{X^\alpha} \le z_0(u_0),\ t \in [0, \tau_{u_0}),$$

which contradicts the maximality of τ_{u_0}. □

Remark 4.1 If $T = \infty$ in the a priori estimate (17), then the solution of (10) exists globally in time. Moreover, the argument of the above proof shows that if $T = \infty$ in (17) and the function $c(t)$ is bounded on $[0, \infty)$ by some constant $\hat{c}$, then the solution of (10) exists globally in time and is bounded by the non-negative root $\hat{z}_0(u_0)$ of the algebraic equation $\hat{b}(u_0)(1 + z^\theta) - z = 0$ with

$$\hat{b}(u_0) = C_0\|u_0\|_{X^\alpha} + C_\alpha a^{\alpha-1}\Gamma(1-\alpha)g(\hat{c}).$$

We also state a simple observation to estimate the life time τ_{u_0} from above.

Proposition 4.1 *Let $u(t)$ be a solution of* (10) *satisfying $u(0) = u_0 \in X^\alpha$ with the life time τ_{u_0}. Assume there exists a normed space Y such that X^α is continuously embedded into Y, and a function $\bar{c}$: $[0, T) \to [0, \infty)$, $0 < T < \infty$, such that* $\limsup_{t\to T^-}\bar{c}(t) = \infty$ *and $\|u(t)\|_Y \ge \bar{c}(t)$ for $t \in (0, \min\{\tau_{u_0}, T\})$. Then we have $\tau_{u_0} \le T$.*

For other results based on this technique, including the existence of a semigroup of global solutions of (10) with bounded orbits of bounded sets, dissipativity of this semigroup and the existence of its global attractor, we refer the reader to [4, Chapters 3 and 4].

Example 4.2 In a bounded domain $\Omega \subset \mathbb{R}^N$ of class C^2 (if $N \geq 2$) consider the Neumann boundary value problem

$$\begin{cases} u_t = \Delta u + f(u), \ t > 0, \ x \in \Omega, \\ \frac{\partial u}{\partial \nu} = 0, \ x \in \partial\Omega, \quad u(0,x) = u_0(x), \ x \in \Omega, \end{cases} \tag{19}$$

together with the corresponding to it ODE Cauchy problem (9). For $f\colon \mathbb{R} \to \mathbb{R}$ locally Lipschitz continuous, working in a base space $X = L^p(\Omega), p > N$, we consider the sectorial operator $A = -\Delta + I$ with the domain $D(A) = \{\phi \in W^{2,p}(\Omega)\colon \frac{\partial \phi}{\partial \nu} = 0 \text{ at } \partial\Omega\}$ (compare [33, Chapter 16]). Then, for a bounded subset B of $W^{1,p}(\Omega)$, we have

$$\|f(u) - f(v)\|_{L^p(\Omega)} \leq c\|f(u) - f(v)\|_{L^\infty(\Omega)} \leq c(B)\|u - v\|_{W^{1,p}(\Omega)}, \ u, v \in B.$$

By Corollary 2.1 local X^α solutions to (19) exist for any $\alpha \in [\frac{1}{2}, 1)$ since $X^{\frac{1}{2}} = D(A^{\frac{1}{2}}) = W^{1,p}(\Omega)$ (see [33, Theorem 16.10]) and $W^{1,p}(\Omega)$ is continuously embedded into $L^\infty(\Omega)$.

Furthermore, we have

$$\|f(u)\|_{L^p(\Omega)} \leq c\|f(u)\|_{L^\infty(\Omega)} \leq g(\|u\|_{L^\infty(\Omega)})(1 + \|u\|_{W^{1,p}(\Omega)})$$

with some nondecreasing function $g\colon [0,\infty) \to [0,\infty)$. For $\alpha \in (\frac{1}{2}, 1)$ the moments inequality

$$\|u\|_{X^{\frac{1}{2}}} \leq c\,\|u\|_X^{1-\frac{1}{2\alpha}}\,\|u\|_{X^\alpha}^{\frac{1}{2\alpha}}, \ u \in X^\alpha,$$

and the embedding $L^\infty(\Omega) \subset L^p(\Omega) = X$ imply the subordination condition (18).

This, together with an a priori estimate in $L^\infty(\Omega)$, allows to estimate the life time τ_{u_0} of solutions or extend the local solution globally in time (see Theorem 4.2 and Remark 4.1).

5 Grow-up Solutions

An interesting class of solutions that are global in time consists of the so-called *grow-up solutions*. Although these solutions exist globally, they have unbounded norms (usually the $L^\infty-$norm) when time t tends to infinity. As a prototype example of this type of behavior, consider the following 1-D problem:

$$\begin{cases} u_t = u_{xx} + \gamma u, \ t > 0, \ x \in (0,\pi), \\ u(t,0) = u(t,\pi) = 0, \ t > 0, \quad u(0,x) = u_0(x), \ x \in [0,\pi], \end{cases} \tag{20}$$

with $\gamma > 1$. For $u_0(x) = \sin x$, the problem (20) has an explicit solution of the form

$$u(t,x) = \sin x e^{(\gamma-1)t}, \ (t,x) \in [0,\infty) \times [0,\pi],$$

which grows up. We extend the analysis of the problem (20). The key point is the relation between the coefficient γ and the squares of natural numbers. Assume that $\gamma \in ((n-1)^2, n^2)$ for some $n \in \mathbb{N}$ and consider explicit solutions of the above problem corresponding to the initial data $u_0(x) = \sin(kx), k \in \mathbb{N}$, having the form $u(t,x) = \sin(kx)e^{(\gamma-k^2)t}$. When $k \leq n-1$, these are the grow-up solutions. Conversely, if $k \geq n$, then these solutions will decay to zero as $t \to \infty$. Therefore, for the problem (20) with a large positive number γ, we have simultaneous existence of grow-up solutions and solutions decaying to zero.

Moreover, if we let $\gamma = n^2, n \in \mathbb{N}$, we have also a stationary solution $u(t,x) = \sin(nx)$.

The solutions which grow up seem not to form a very large subclass of all the solutions. Anyway, generalizing the latter example, we return to the semilinear Neumann problem (19) under the assumptions of Example 4.2 having local in time solutions corresponding to the initial data $u_0 \in X^\alpha \subset W^{1,p}(\Omega)$ with $\alpha > \frac{1}{2}$, $p > N$. Following the idea known from the Hartman-Wintner theorem (see e.g. [11,14,16]), we are able to verify the global existence of a solution of (19) due to the corresponding properties of solutions to (9). The main assumption is the divergence of an integral

$$\int_a^\infty \frac{ds}{f(s)} = \infty. \tag{21}$$

Lemma 5.1 *Let $f\colon \mathbb{R} \to \mathbb{R}$ be a locally Lipschitz function and assume that $f([a,\infty)) \subset (0,\infty)$ and condition (21) hold for some $a \in \mathbb{R}$. Then all the local solutions to (19), as described above, corresponding to the initial data u_0 having values in the interval $[\inf u_0, \sup u_0] \subset [a,\infty)$, possess an a priori estimate in $L^\infty(\Omega)$ by the corresponding solutions of (9). Moreover, each such solution $u(t,u_0)$ can be extended globally in time and is a grow-up solution.*

Proof. First, note that due to the assumption (21), solutions $y(t) = y(t,y_0)$ to the ODE Cauchy problem (9) with $y_0 \geq a$ exist for all $t \geq 0$. Indeed, we have

$$t = \int_{y_0}^{y(t)} \frac{ds}{f(s)} \quad \text{as long as} \quad y(t) \quad \text{exists.} \tag{22}$$

Suppose contrary to the claim that y does not exist for all $t \geq 0$. Thus there must be a finite $\tau > 0$ and a sequence $t_n \to \tau$ such that $y(t_n) \to \infty$ as $n \to \infty$. From (21) and (22), we get $\tau = \infty$, which gives a contradiction. For u_0 such that $[\inf u_0, \sup u_0] \subset [a,\infty)$, a simple comparison argument of Proposition 3.1 and global existence of y yield

$$y(t, \inf_{x\in\Omega} u_0(x)) \leq u(t,x) \leq y(t, \sup_{x\in\Omega} u_0(x)), \ t \in [0,\tau_{u_0}), \ x \in \Omega. \tag{23}$$

Since the left-hand side of (23) is increasing to ∞ and is greater than or equal to $\inf_{x\in\Omega} u_0(x) \geq a$ and both sides are globally defined in time, it yields the $L^\infty(\Omega)$ a priori estimate for the solution of (19). Hence u is global in time by Theorem 4.2 via the subordination condition. □

Remark 5.1 A result similar to Lemma 5.1 holds if $f((-\infty,a]) \subset (-\infty,0)$ and

$$\int_{-\infty}^a \frac{ds}{f(s)} = -\infty$$

hold for some $a \in \mathbb{R}$. Then all solutions $u(t,u_0)$ to (19) with the initial data u_0 having values in $[\inf u_0, \sup u_0] \subset (-\infty,a]$ can be extended globally in time and are grow-up solutions.

Remaining inside the framework of (19), following [1], consider the Neumann problem

$$\begin{cases} u_t = \Delta u + bu + g(u), \ t > 0, \ x \in \Omega, \\ \frac{\partial u}{\partial \nu} = 0 \text{ on } \partial\Omega, \quad u(0,x) = u_0(x), \end{cases} \tag{24}$$

with $b > 0$ and g being a bounded C^1 function ($|g| \leq M$). As a consequence of the considerations of Example 4.2, local solutions to (24) exist in the phase space $D((-\Delta_{\mathcal{N},p})^\alpha)$ with $\alpha > \frac{1}{2}$, $p > N$ and $p \geq 2$. Moreover, for the nonlinearity $f(s) := bs+g(s)$, $s \in \mathbb{R}$, the condition (21) is satisfied with $a = \frac{M+\varepsilon}{b}$, $\varepsilon > 0$ and, consequently, *all solutions* fulfilling the condition $\inf_{x\in\Omega} u_0(x) \geq \frac{M+\varepsilon}{b}$ are extended globally in time and are grow-up solutions. Moreover, none of the solutions of (24) blows up.

We further observe that a faster than linear growth of nonlinearity does not exclude the existence of the grow-up solutions. Consider, namely, problem (19) with the nonlinearity

$$f(s) = s \ln s \text{ for } s > 1 \quad \text{and} \quad f(s) = 0 \text{ for } s \leq 1. \tag{25}$$

Evidently, condition (21) is now satisfied with $a = e$, the base of the natural logarithm. Hence, whenever $\inf_{x\in\Omega} u_0(x) \geq e$, the corresponding solution of (19), (25) exists globally in time and grows up. The phenomenon of grow-up is thus not limited to the equations in which nonlinear terms are sub-linear.

It is easy to find more complicated parabolic equations (with gradient-dependent nonlinearity) having grow-up solutions. Consider, for example, the 1-D Neumann problem

$$\begin{cases} u_t = u_{xx} + u_x^3 + 1 \equiv (u_{xx} - u) + u + u_x^3 + 1, \ t > 0, \ x \in (0,1), \\ u_x = 0 \text{ for } x = 0,1, \quad u(0,x) = u_0(x), \ x \in [0,1], \end{cases} \tag{26}$$

admitting, in particular, the x-independent solutions of the ODE $z'(t) = 1$.

We will consider problem (26) in the phase space $H_{\mathcal{N}}^{\frac{3}{2}+\varepsilon}(0,1)$ with $\varepsilon \in (0, \frac{1}{4})$. Indeed, when noting the embeddings $H^{\frac{3}{2}}(0,1) \subset W^{1,6}(0,1)$ and $H^{\frac{3}{2}+\varepsilon}(0,1) \subset W^{1,\infty}(0,1)$, the main component of the nonlinearity will satisfy

$$\begin{aligned} &\|(\phi_x)^3\|_{L^2(0,1)} = \|\phi_x\|^3_{L^6(0,1)} \leq c\|\phi\|^3_{W^{1,6}(0,1)} \leq c'\|\phi\|^3_{H^{\frac{3}{2}+\varepsilon}(0,1)}, \\ &\|(\phi_x)^3 - (\psi_x)^3\|_{L^2(0,1)} \leq \|((\phi_x) - (\psi_x))(\phi_x^2 + \phi_x\psi_x + \psi_x^2)\|_{L^2(0,1)} \\ &\leq c'(\|\phi\|_{H^{\frac{3}{2}+\varepsilon}(0,1)}, \|\psi\|_{H^{\frac{3}{2}+\varepsilon}(0,1)})\|\phi - \psi\|_{H^{\frac{3}{2}+\varepsilon}(0,1)}, \end{aligned}$$

and, consequently, the whole nonlinearity $f(u) = (u+u_x^3+1)$ defines a Lipschitz continuous on bounded sets Nemytskii operator acting from $H_{\mathcal{N}}^{\frac{3}{2}+\varepsilon}(0,1)$ into $L^2(0,1)$. Moreover, note that the operator $(-u_{xx} + u)$ with a Neumann boundary condition is *sectorial and positive* in $L^2(0,1)$. Thus, Corollary 2.1 establishes the local existence of solutions.

Note also that after changing the unknown function to $\overline{u}(t,x) = u(t,x) - t$, the new unknown will satisfy the problem

$$\begin{cases} \overline{u}_t = \overline{u}_{xx} + \overline{u}_x^3, \ t > 0, \ x \in (0,1), \\ \overline{u}_x = 0 \text{ for } x = 0,1, \quad \overline{u}(0,x) = u_0(x), \ x \in [0,1]. \end{cases} \tag{27}$$

Despite the violation of the *sub-quadratic growth condition* (see the Appendix) in (26), the derivative $v := u_x$ is bounded and fulfills the maximum principle since it solves

$$\begin{cases} v_t = v_{xx} + 3v^2 v_x, \ t > 0, \ x \in (0,1) \\ v = 0 \text{ for } x = 0,1, \quad v(0,x) = u_{0x}(x), \ x \in [0,1]. \end{cases} \tag{28}$$

We will justify shortly the last claim. Multiplying the first equation in (28) by $v^{2k-1}, k = 1, 2, \ldots$, and integrating, we obtain

$$\frac{1}{2k}\frac{d}{dt}\int_0^1 v^{2k}dx = -\frac{2k-1}{k^2}\int_0^1 [(v^k)_x]^2 dx \leq -\pi^2\frac{2k-1}{k^2}\int_0^1 v^{2k}dx,$$

where we used the fact that the function $v^k = (u_x)^k$, vanishing at $x = 0, 1$, fulfills the Poincaré inequality. Solving the differential inequality and taking the $2k$-roots, we get

$$\|u_x(t,\cdot)\|_{L^{2k}(0,1)} \leq \|u_{0x}\|_{L^{2k}(0,1)} \exp\Big(-\pi^2\frac{2k-1}{k^2}t\Big).$$

Letting $k \to \infty$, we obtain

$$\|u_x(t,\cdot)\|_{L^\infty(0,1)} \leq \|u_{0x}\|_{L^\infty(0,1)}. \tag{29}$$

Note that the *sub-quadratic growth condition* (cp. (41)) is not violated in the case of equation (28) for the derivative u_x. Having already the last estimate, we return to (26) and multiply the first equation by u, obtaining

$$\frac{1}{2}\frac{d}{dt}\int_0^1 u^2 dx = -\int_0^1 u_x^2 dx + \int_0^1 (u_x^3+1)u dx \leq (\|u_x\|^3_{L^\infty(0,1)} + 1)\|u\|_{L^2(0,1)},$$

and, consequently,

$$\|u(t,\cdot)\|_{L^2(0,1)} \leq \|u_0\|_{L^2(0,1)} + (\|u_{0x}\|^3_{L^\infty(0,1)} + 1)t. \tag{30}$$

As a result of the a priori estimates (29) and (30), the local solutions to (26) will be extended globally in time due to the following subordination condition:

$$\|u + u_x^3 + 1\|_{L^2(0,1)} \leq \|u_0\|_{L^2(0,1)} + (\|u_{0x}\|^3_{L^\infty(0,1)} + 1)(t+1).$$

As a consequence of the above considerations, we get the existence of grow-up solutions for *at least one* of the problems (26) or (27). Indeed, for the arbitrary initial data $u_0 \in H^{\frac{3}{2}+\varepsilon}(0,1)$ with $\varepsilon > 0$, there exist global in time solutions to both these problems. But the difference of their global solutions, $u(t, u_0)$ and $\bar{u}(t, u_0)$, corresponding to the initial data u_0, is equal to t. Consequently, at least one of them must grow up as $t \to \infty$.

The phenomenon of solutions that grow up can be also viewed in another way. Unboundedness of a norm, as $t \to \infty$, will be seen as a convergence 'to an equilibrium at infinity' (see e.g. [3]). The authors introduce there a modification of the notion of a global attractor replacing it with their *maximal attractor* for a semigroup $\{S(t)\colon t \geq 0\}$ generated by the equation (10) on a Banach space E (cp. [3, Definition 1.2]).

Definition 5.1 A closed set $\mathcal{U} \subset E$ is called a *maximal attractor* if $S(t)\mathcal{U} = \mathcal{U}$ for all $t \geq 0$, $\mathrm{dist}(S(t)K, \mathcal{U}) \to 0$ as $t \to \infty$, for any bounded set $K \subset E$, and there is no proper closed subset $\mathcal{U}' \subset \mathcal{U}$ having the above two properties.

Such maximal attractor can, however, be unbounded and not unique. Moreover, the existence of the semigroup excludes the blow-up of solutions starting from E. Also, the growth condition of the nonlinearity imposed there (in the case of the Hilbert space H) is rather restrictive (see [3, Property IV, p. 89]): $\|F(u)\|_H \leq \varepsilon\|u\|_H + C$ for some $\varepsilon, C > 0$.

The non-compact global attractors for slowly non-dissipative scalar reaction-diffusion equations of the form

$$\begin{cases} u_t = u_{xx} + bu + g(x, u, u_x),\ t > 0,\ x \in (0, \pi), \\ u_x = 0 \text{ for } x = 0, \pi, \quad u(0, x) = u_0(x), \end{cases} \tag{31}$$

were also investigated in [1, 22]. It turns out that a noncompact global attractor $\mathcal{U}$ can be decomposed as

$$\mathcal{U} = \mathcal{E}^c \cup \mathcal{E}^\infty \cup \mathcal{H},$$

where $\mathcal{E}^c$ denotes the set of bounded hyperbolic equilibria of (31), $\mathcal{E}^\infty$ is the set of 'equilibria at infinity' and $\mathcal{H}$ consists of heteroclinic connections between equilibria. A thorough study of this structure, using the zero number properties of solutions, was carried out in [23], where we refer the reader for details.

6 Blow-up Solutions

The blow-up of solutions in a finite time is a frequent form of behavior for evolution equations, taking its origins from the simple problem

$$y'(t) = y^2(t), \quad y(0) = y_0,$$

with a stationary zero solution and other solutions of the explicit form $y(t) = \frac{1}{y_0^{-1} - t}$ for $y_0 \neq 0$. Evidently, this fraction becomes unbounded in a finite time $\tau_{y_0} = y_0^{-1}$ provided that $y_0 > 0$. Thus, when using the notation of Section 2, the phase space $X^\alpha = \mathbb{R}$ decomposes into open $X_B^\alpha = (0, \infty)$, closed $X_D^\alpha = (-\infty, 0]$ and empty X_G^α. Detecting the blow-up solutions of more complicated equations and characterizing the decomposition of the phase space is, in general, much harder. Without explicit formulas for solutions, the best available tools are the comparison techniques, which eventually provide us sufficient conditions for justifying the occurrence of blow-up. However, the assumptions on nonlinear terms allowing to use the comparison techniques are limited to particular equations only and cannot be applied to most cases.

A similar type of behavior is observed for semilinear parabolic equations of the form

$$u_t = \Delta u + f(u, \nabla u), \tag{32}$$

though in that case there are more reasons for the finite life time of solutions. A simpler possibility is that the $L^\infty(\Omega)-$norm of the solution grows to infinity in a finite time (cp. Proposition 4.1). We can also face the phenomenon of the *gradient blow-up*. Recall that a gradient blow-up occurs when the solution u stays L^∞ bounded but it does not exist globally in time because some of the derivatives of u blow-up in a finite time. Let us shed some more light on the background of this case.

It is not easy to formulate a sufficient condition for the blow-up of the gradient of a solution; see, however, [7, 24, 29] and Proposition 6.1. Easier is to find hypotheses allowing to limit its growth. In a bounded domain $\Omega \subset \mathbb{R}^N$ with $\partial\Omega \in C^2$, consider the homogeneous Dirichlet boundary value problem for (32), assuming that $f(0, \nabla u) = 0$ and $\left|\frac{\partial f}{\partial u}\right| \leq L_1$, $\left|\frac{\partial f}{\partial u_{x_i}}\right| \leq L_\nabla$, with certain positive constants L_1, L_∇.

Multiplying equation (32) by Δu and integrating over Ω, we obtain

$$-\frac{1}{2}\frac{d}{dt}\int_\Omega |\nabla u|^2 dx = \int_\Omega (\Delta u)^2 dx + \int_\Omega f(u, \nabla u)\Delta u dx, \tag{33}$$

and further

$$\int_\Omega f(u,\nabla u)\Delta u dx = \int_{\partial\Omega} f(u,\nabla u)\frac{\partial u}{\partial\nu}dS - \int_\Omega \sum_i \Big(\frac{\partial f}{\partial u}u_{x_i} + \sum_j \frac{\partial f}{\partial u_{x_j}} u_{x_i x_j}\Big) u_{x_i} dx,$$

where the boundary integral vanishes due to the assumption $f(0,\nabla u) = 0$. Then the boundedness of the derivatives of f and the Cauchy inequality imply that

$$\left|\int_\Omega f(u,\nabla u)\Delta u dx\right| \le L_1 \int_\Omega |\nabla u|^2 dx + L_\nabla \int_\Omega \sum_{i,j} (\varepsilon |u_{x_i x_j}|^2 + \frac{1}{4\varepsilon}|u_{x_i}|^2) dx \qquad (34)$$

with an arbitrary $\varepsilon > 0$. Note that $\sum_{i,j} \|\phi_{x_i x_j}\|^2_{L^2(\Omega)} = \|\Delta\phi\|^2_{L^2(\Omega)}$ for $\phi \in H^2_0(\Omega)$ (see e.g. [10, (9.34)]). Combining (33) and (34), we choose a sufficiently small $\varepsilon > 0$ to obtain

$$\frac{d}{dt}\int_\Omega |\nabla u|^2 dx \le C(L_1, L_\nabla)\int_\Omega |\nabla u|^2 dx$$

and, consequently, an exponential bound for the spatial gradient of the solution.

As we discuss in the Appendix, for L^∞ bounded solutions, even the *sub-quadratic growth* of $f(u,\nabla u)$ with respect to the gradient is allowed, not leading to their blow-up. But a higher than quadratic growth of $f(u,\nabla u)$ with respect to ∇u leads, in general, to the blow-up of the spatial derivatives of the solution. Using the technique of sub-solutions, such form of behavior was studied in [7], where several examples of equations allowing the gradient blow-up were constructed. Different methods were used in [29] to formulate a sufficient condition for the gradient blow-up for a model Dirichlet problem

$$\begin{cases} u_t = \Delta u + |\nabla u|^p, \ t > 0, \ x \in \Omega, \\ u(t,x) = g(t,x), \ t > 0, \ x \in \partial\Omega, \quad u(0,x) = u_0(x), \ x \in \Omega, \end{cases} \qquad (35)$$

with $g \in C([0,T] \times \partial\Omega)$ for all $T > 0$, and $u_0 \in C^1(\overline{\Omega})$ fulfilling the compatibility condition $u_0(x) = g(0,x)$ on $\partial\Omega$.

Denoting by $\lambda_1 > 0$ the first positive eigenvalue of $-\Delta$ in $H^1_0(\Omega)$, with the corresponding normalized eigenfunction $\phi_1 > 0$, we recall (see [29, Theorem 2.1]) the following result.

Proposition 6.1 *When $p > 2$, then there exists a positive $k_0 = k_0(\Omega, p, g)$ such that if $\int_\Omega u_0(x)\phi_1(x)dx > k_0$, then the gradient blow-up for solution of (35) occurs.*

Certain generalizations of the above-mentioned result can be found in [29, Theorem 2.2].

There exists quite a large literature devoted to the occurrence of *blow-up* (see e.g. [24], [26] for more references). Several properties including *blow-up sets, blow-up rates* and *profiles* characterizing closer this phenomenon have already been investigated, at least for the basic model problem

$$\begin{cases} u_t - \Delta u = \lambda u + u|u|^{p-1}, \ t > 0, \ x \in \Omega, \\ u = 0 \ \text{ on } \ \partial\Omega, \quad u(0,x) = u_0(x), \ x \in \Omega, \end{cases}$$

with $p > 1$ and $\lambda \in \mathbb{R}$, in a bounded regular domain $\Omega \subset \mathbb{R}^N$. Popular are also the studies of a more general problem (see [30])

$$\begin{cases} u_t - \Delta u = u^p + g(t,x,u,\nabla u), \ t > 0, \ x \in \Omega \subset \mathbb{R}^N, \\ u = 0 \text{ on } \partial\Omega, \quad u(0,x) = u_0(x), \ x \in \Omega, \end{cases} \qquad (36)$$

with C^1 nonlinearity g satisfying $g(t,x,0,0) \geq 0$, the latter requirement being connected with the non-negativity of solutions. The solutions of (36) are searched in the set

$$X := \{0 \leq \phi \in C^1(\overline{\Omega})\colon \phi, \nabla\phi \in L^\infty(\Omega), \phi = 0 \text{ on } \partial\Omega\}$$

subject to the norm $\|\phi\|_X = \|\phi\|_{L^\infty(\Omega)} + \|\nabla\phi\|_{L^\infty(\Omega)}$. Further developments concerning the blow-up of solutions can be found in the recent monograph [24].

7 Local Attractors and Lyapunov Functions

As regards the solutions which exist globally in time, it is interesting to investigate their long-time behavior. For solutions which stay bounded, one may try to find out sets they approach. Conversely, having a given subset of the phase space, one may look for solutions which are attracted by this set. This inspires the introduction of the following notion.

Definition 7.1 Let $\{S(t)\colon t \geq 0\}$ be a semigroup on a metric space (M,d). The *basin of attraction* of a set $A \subset M$ is defined as

$$\Omega(A) = \{u_0 \in M\colon \lim_{t\to\infty} \operatorname{dist}(S(t)u_0, A) = 0\},$$

where $\operatorname{dist}(S(t)u_0, A) = \inf_{v\in A} d(S(t)u_0, v)$.

Remark 7.1 It is easy to see that the basins of attraction of the two disjoint compact sets need to be disjoint. In particular, the basins of attraction of two separate stationary points are disjoint. Indeed, let A_1 and A_2, $A_1 \cap A_2 = \emptyset$, be two disjoint compact sets with their basins of attraction $\Omega(A_1)$ and $\Omega(A_2)$, respectively, and suppose that $u_0 \in \Omega(A_1)\cap\Omega(A_2)$. Then, taking successive subsequences, we find $v \in A_1$, $w \in A_2$, and a sequence $t_n \to \infty$ such that $S(t_n)u_0 \to v$ and $S(t_n)u_0 \to w$. Consequently, $v = w$ by the uniqueness of the limit, which is not possible.

A special role in dynamical systems is played by compact invariant subsets of the phase space. The simplest ones are stationary points or periodic orbits. Some of them may attract their neighborhoods.

Definition 7.2 A compact set $\mathcal{A} \subset M$ is said to be an *attractor* (or a *local attractor*) for a semigroup $\{S(t)\colon t \geq 0\}$ on M if it is invariant and attracts an open neighborhood U of itself.

Note that if $\mathcal{A}$ is an attractor, then $\Omega(\mathcal{A}) \supset U$ and $\mathcal{A}$ becomes a global attractor provided that it attracts each bounded subset of M. Moreover, if $\mathcal{A}$ is an attractor, then its basin of attraction $\Omega(\mathcal{A})$ is an open subset of M. We recall next a sufficient condition for the existence of an attractor, the result being taken from [27, Section 2.3.5].

Proposition 7.1 *Let $\{S(t)\colon t \geq 0\}$ be a semigroup on $M \subset X$, where X is a complete metric space. Assume there are a compact set $K \subset M$ and a neighborhood U of K in M having the property that K attracts all bounded sets in U. Then the semigroup $\{S(t)\colon t \geq 0\}$ has an attractor $\mathcal{A} = \omega(K) \subset K$, where $\omega(K)$ is the $\omega-$limit set of K.*

The following result justifies the existence of an attractor for asymptotically compact semigroups (cp. Definition 2.5).

Proposition 7.2 *Assume that there exists a bounded closed set $A \subset M$ that attracts a neighborhood of itself. If the semigroup $\{S(t)\colon t \geq 0\}$ on M is asymptotically compact, then there exists an attractor $\mathcal{A} \subset A$.*

Remark 7.2 It is easy to observe that a finite sum of attractors is an attractor itself. Indeed, if $\mathcal{A}_1, \mathcal{A}_2$ are two attractors, then their sum is evidently compact and invariant. Moreover, the sum of the neighborhoods of $\mathcal{A}_1$ and $\mathcal{A}_2$ will be attracted by $\mathcal{A}_1 \cup \mathcal{A}_2$.

Consequently, if there is a finite number of attractors in the system, we can always consider only their sum as a common attractor.

Solutions of some parabolic equations have a natural tendency to approach a stationary solution (see e.g. [13,21,34]), which is the simplest local attractor. Below we observe that if a global solution to a semilinear sectorial equation is convergent, then it must tend to an equilibrium.

Proposition 7.3 *Let Assumption 2.1 hold and assume that $u(t, u_0)$ is a global X^α solution of* (1) *and there exists $v \in X^\alpha$ such that $\lim_{t\to\infty} u(t, u_0) = v$ in X^α. Then v is a stationary solution of* (1), *that is, $v \in X^1 \subset X^\alpha$ and $Av = F(v)$.*

Proof. By (11), for any $0 < T < \tau_v$, we have $u(T, u(t, u_0)) \to u(T, v)$ as $t \to \infty$. On the other hand, by assumption, $u(T, u(t, u_0)) = u(T + t, u_0)$ converges to v as $t \to \infty$. Thus $u(T, v) = v$ for any $0 < T < \tau_v$, so v is a stationary solution of (1). □

Therefore, under Assumption 2.1, the following alternative holds: either the solution u of (1) converges to a single stationary solution v or the solution u is not convergent in X^α as $t \to \infty$. In the second case, other forms of behavior are possible: the solution may grow up, blow up in a finite time, or eventually approach an attractor having more complicated structure (not reduced to a single equilibrium).

In literature, a common description of the behavior of dynamical systems generated by parabolic equations or systems was given using the notion of the *Lyapunov function*, see e.g. [12, 18, 34]. In the last two references, the semilinear and even fully nonlinear problems in one space dimension were analyzed within that approach. In Chapter 5 of [2], the connection of the existence of a global attractor and the Lyapunov function was described in the case of the so-called *gradient semigroups.*

Definition 7.3 A semigroup $\{S(t)\colon t \geq 0\}$ on a metric space (M, d) is called *gradient* if there exists a continuous function $V\colon M \to \mathbb{R}$ such that $V(S(t)u_0)$ is non-increasing along the trajectories of $u_0 \in M$ and, whenever $V(S(t)u_0) = V(u_0)$ for all $t \geq 0$, u_0 must be an equilibrium.

Note that in the above definition we do not require that V is bounded from below.

Remark 7.3 A semigroup $\{S(t)\colon t \geq 0\}$ on a metric space (M, d) is gradient if there exists a continuous function $V\colon M \to \mathbb{R}$ such that

$$\dot{V}(v) := \limsup_{t\to 0^+} \frac{V(S(t)v) - V(v)}{t} \leq 0, \ v \in M,$$

and for any $u_0 \in M$ if $V(v) = V(u_0)$, $v \in \gamma^+(u_0)$, then $u_0 \in \mathcal{E}$, where $\gamma^+(u_0) = \{S(t)u_0\colon t \geq 0\}$ and $\mathcal{E}$ denotes the set of equilibria in M. A function V having these properties or, equivalently, those from Definition 7.3, is called a *Lyapunov function.*

The following *LaSalle's Invariance Principle* holds, for the proof, see [15, Theorem 4.3.4].

Theorem 7.1 *Let $\{S(t)\colon t \geq 0\}$ be a gradient semigroup on a metric space M. If the positive orbit $\gamma^+(u_0) = \{S(t)u_0\colon t \geq 0\}$ of $u_0 \in M$ is a subset of a compact set K contained in M, then $\omega(u_0) \subset \mathcal{E}$ is a nonempty compact invariant subset of M, which attracts u_0, and $\operatorname{dist}(S(t)u_0, \mathcal{S}) \to 0$ as $t \to \infty$, where $\mathcal{S}$ is the maximal invariant subset of $\{v \in M\colon \dot{V}(v) = 0\}$.*

We apply LaSalle's Invariance Principle to the sectorial equation (1) (see [6]).

Corollary 7.1 *Consider the problem (1) under Assumptions 2.1 and 2.2 and let $\{S(t)\colon t \geq 0\}$ be the semigroup of X^α solutions on $M = X^\alpha_D \cup X^\alpha_G$, where we assume X^α_D to be nonempty (see Definition 2.2). Assume also that there exists a continuous function $V\colon X^\alpha_D \to \mathbb{R}$ such that*

$$\dot{V}(v) := \limsup_{t\to 0^+} \frac{V(S(t)v) - V(v)}{t} \leq 0, \ \ v \in X^\alpha_D,$$

and for any $u_0 \in X^\alpha_D$ if $V(v) = V(u_0)$, $v \in \gamma^+(u_0)$, then $u_0 \in \mathcal{E}$. Then, for any $u_0 \in X^\alpha_D$, the set $\operatorname{cl}_{X^\alpha} \gamma^+(u_0)$ is a compact subset of X^α_D and, by LaSalle's Invariance Principle, we obtain $\omega(u_0) \subset \mathcal{E}$. Thus the solutions $u(t, u_0)$ of (1) starting from $u_0 \in X^\alpha_D$ approach the set of equilibria $\mathcal{E}$ of (1).

Proof. Since X^α_D is positively invariant under the semigroup $\{S(t)\colon t \geq 0\}$, we may consider it only in the metric space X^α_D (with a metric inherited from X^α).

We first show that $\operatorname{cl}_{X^\alpha} \gamma^+(u_0)$ is a subset of X^α_D for any $u_0 \in X^\alpha_D$. Indeed, note that $B = \gamma^+(u_0)$ is a bounded subset of X^α_D. Let $v \in \operatorname{cl}_{X^\alpha} \gamma^+(u_0)$. Then there exists $t_n \geq 0$ such that $S(t_n)u_0 \to v$ in X^α. Since $\|u(t, S(t_n)u_0)\|_{X^\alpha} = \|u(t + t_n, u_0)\|_{X^\alpha} \leq R_B$ for all $t \geq 0$ and $u(t, S(t_n)u_0) \to u(t, v)$ in X^α for all $t \in [0, \tau_v)$ (see Theorem 4.1), it follows that the solution starting from v has an X^α norm bounded by R_B, hence $v \in X^\alpha_D$.

Observe also that the boundedness of B in X^α implies that $S(t)B$ with $t > 0$ is bounded in $X^{\alpha+\varepsilon}$ for $\alpha + \varepsilon < 1$. By Assumption 2.2, $X^{\alpha+\varepsilon}$ is compactly embedded in X^α, which yields the compactness of $\operatorname{cl}_{X^\alpha} S(t)\gamma^+(u_0)$ for any $t > 0$. Finally, we have

$$\operatorname{cl}_{X^\alpha} \gamma^+(u_0) = \operatorname{cl}_{X^\alpha} \bigcup_{s\in[0,1]} S(s)u_0 \cup \operatorname{cl}_{X^\alpha} S(1)\gamma^+(u_0),$$

which proves the compactness of $\operatorname{cl}_{X^\alpha} \gamma^+(u_0)$. □

Remark 7.4 A particularly complete description of Lyapunov functions is possible in one space dimension (see [18, 34, 35]). For a general quasi-linear problem of the type

$$\begin{cases} u_t = a(x, u, u_x)u_{xx} + b(x, u, u_x), \\ \alpha_i u_x(t, i) + \psi_i(u(t, i)) = 0, \ t > 0, \ i = 0, 1, \quad u(0, x) = u_0(x), \end{cases}$$

considered for $(t, x) \in [0, \infty) \times [0, 1]$ with $a, b, \psi_i \in C^3$, one constructs a pair of functions $\rho, \Phi(x, \xi, \eta)$ as in [35, Chapter 2, Theorem 1.1]. Then, after multiplying the first equation by $\rho(u, u, u_x)u_t$, they generate a Lyapunov function V through the relations

$$\frac{d}{dt} \int_0^1 \Phi(x, u, u_x)dx = -\int_0^1 \rho(x, u, u_x)u_t^2 dx, \quad V(u) = \int_0^1 \Phi(x, u, u_x)dx.$$

It is especially easy to indicate a Lyapunov function for the problem (24). Namely,

$$V(u) = \int_\Omega (|\nabla u|^2 - bu^2 - 2G(u))dx \quad \text{with} \quad G(u) = \int_0^u g(s)dx,$$

is a Lyapunov function for (24) on $X^\alpha = D((-\Delta_{\mathcal{N},p})^\alpha)$ with $\alpha > \frac{1}{2}$ and $p > N$ and $p \geq 2$. Considering constant functions $u_n \equiv n$, $n \in \mathbb{N}$, we see that $V(u_n) \to -\infty$ as $n \to \infty$. Hence V is not bounded from below. For (24), we have $X^\alpha = X^\alpha_D \cup X^\alpha_G$ and the resolvent of $-\Delta_{\mathcal{N},p}$ is compact for a sufficiently regular domain Ω. Thus, if the set of equilibria $\mathcal{E}$ of (24) is nonempty, then by Corollary 7.1, for any $u_0 \in X^\alpha_D$ we have $\omega(u_0) \subset \mathcal{E}$, whereas for $u_0 \in X^\alpha_G$ the solutions become unbounded in an infinite time.

8 Concluding Remarks

In summary, the picture sketched in this paper in the case of a semilinear parabolic problem, or even its generalization in the form of the abstract sectorial Cauchy problem (1) under Assumption 2.1, reveals that, typically, we have three potential forms of behavior of solutions as specified in Definition 2.2.

Considering a particular example of an abstract semilinear Cauchy problem (1), we first need to check which a priori estimates are available for its solutions in order to use them eventually in the subordination condition (see Theorem 4.2). More precisely, we shall find the strongest a priori estimate. In case this a priori estimate is too weak to guarantee the global in time extendibility of the local solutions, via the subordination condition (18), we need to find regions of the phase space (e.g. for small initial data) in which the existing a priori estimates are sufficient to extend solutions globally.

Furthermore, the stationary, time independent solutions should be detected and their (linearized) stability be determined. Local attractors will be next constructed for the stable stationary points, together with their basins of attraction.

For many dissipative equations, we can show the existence of a global attractor, that is, a compact maximal invariant subset of the phase space which attracts all bounded subsets. In the ideal situation, we will be even able to determine the structure of this object. However, generally, we should expect that some solutions run away to infinity. Some of them may grow up still being defined globally in time, whereas the rest of the phase space will be occupied by locally existing solutions, which blow up in a finite time.

The coexistence of at least two behavior types of solutions leads to the corresponding separation of the phase space, which is hard to be characterized in general. Moreover, most of the above procedures, while formally possible, still remain rather only theoretical for many practical problems arising from the Applied Sciences since, for instance, we cannot precisely locate all the stationary points or periodic solutions.

Nevertheless, the questions raised above should be addressed. In particular situations, they have already gained positive feedback. For example, the asymptotics of equations possessing grow-up solutions was described in terms of non-compact attractors for slowly non-dissipative reaction-diffusion equations. For specific equations, the profiles of blow-up solutions were determined via comparison techniques. We have also shown that the existence of a Lyapunov function for a general semilinear evolution equation with a main sectorial operator having compact resolvent guarantees the attraction of each bounded solution by the set of stationary solutions.

A Reaction-Diffusion Neumann Boundary Problem

We place here some auxiliary results that are connected with the applications presented in the paper, but do not belong to its main topic. They concern the existence of smooth solutions and their global extendibility in time to the reaction-diffusion Neumann boundary problem with gradient-dependent nonlinearity of the form

$$\begin{cases} u_t = \Delta u + f(u, \nabla u), & t > 0, \ x \in \Omega, \\ \frac{\partial u}{\partial \nu} = 0 \text{ on } \partial\Omega, & u(0,x) = u_0(x), \ x \in \Omega. \end{cases} \tag{37}$$

We start with sketching out the proof of existence of a smooth solution having bounded first derivatives ∇u. We will construct a local mild solution to (37) in the sense of [4,15] in the base space $D((-\Delta_{\mathcal{N},p})^{\frac{1}{2}}) \subset W^{1,p}(\Omega)$ with $p > N$ (here $\Delta_{\mathcal{N},p}$ denotes the Neumann Laplacian in $L^p(\Omega)$). The following proposition extends the result from [33, Section 11.10 (5)].

Proposition A.1 *Assume that $f\colon \mathbb{R} \times \mathbb{R}^N \to \mathbb{R}$ is a C^1 function and let $p > N$ and Ω be a bounded domain in $\mathbb{R}^N$ with the boundary $\partial\Omega$ of class C^1 if $N \geq 2$. Then the Nemytskii operator $u \mapsto f(u, \nabla u)$ acts from $W^{2,p}(\Omega)$ into $W^{1,p}(\Omega)$, and*

$$\|f(u, \nabla u)\|_{W^{1,p}(\Omega)} \leq q(\|u\|_{W^{2,p}(\Omega)}), \quad u \in W^{2,p}(\Omega), \tag{38}$$

with some non-decreasing function q. Moreover, if f is a C^2 function, then that Nemytskii operator is Lipschitz continuous on the bounded subsets B of $W^{2,p}(\Omega)$, i.e.,

$$\|f(u, \nabla u) - f(v, \nabla v)\|_{W^{1,p}(\Omega)} \leq C(B)\|u - v\|_{W^{2,p}(\Omega)}, \ u, v \in B.$$

Proof. The key point for the first claim is the inclusion $W^{2,p}(\Omega) \subset C^1(\overline{\Omega})$, which holds since $p > N$. To shorten the calculation, we will show the estimate for one component of the $W^{1,p}(\Omega)$ norm only. We note that the argument $(u, \nabla u)$ of f and its partial derivatives is varying in a compact subset of $\mathbb{R}^{N+1}$, provided that $\|u\|_{W^{2,p}(\Omega)}$ is bounded. Also, the norms $\|\frac{\partial u}{\partial x_j}\|_{L^\infty(\Omega)}$ are bounded, so that we have an estimate

$$\|\frac{\partial}{\partial x_j} f(u, \nabla u)\|_{L^p(\Omega)} \leq c(\|u\|_{W^{2,p}(\Omega)}).$$

The proof of the second statement follows from (38) for the first derivatives of f and the fact that $W^{1,p}(\Omega)$ is a Banach algebra. □

The above proposition almost immediately translates into the local existence result; we only need to verify that the composite function $f(u, \nabla u) \in D((-\Delta_{\mathcal{N},p})^{\frac{1}{2}})$ whenever u varies in $D(-\Delta_{\mathcal{N},p})$, $p > N$. To this end, let us recall the *characterization of the fractional power spaces* connected with the Neumann Laplacian considered on $L^p(\Omega)$. Considering fractional powers up to the exponent $\theta = 1$, we will assume that $\partial\Omega \in C^2$ if $N \geq 2$. Using the description in [33, pp. 474, 554], for $1 < p < \infty$, we have

$$D((-\Delta_{\mathcal{N},p})^\theta) = \begin{cases} W^{2\theta,p}(\Omega) & \text{for} \quad 0 \leq \theta < \frac{1}{2} + \frac{1}{2p}, \\ W^{2\theta,p}_{\mathcal{N}}(\Omega) & \text{if} \quad \frac{1}{2} + \frac{1}{2p} < \theta < \frac{3}{2} + \frac{1}{2p}, \end{cases}$$

where we denote $W^{s,p}_{\mathcal{N}}(\Omega) := \{\phi \in W^{s,p}(\Omega)\colon \frac{\partial \phi}{\partial \nu} = 0 \text{ at } \partial\Omega\}$. Proposition A.1 together with the above characterization imply that the Nemytskii operator $u \mapsto f(u, \nabla u)$ from $D(-\Delta_{\mathcal{N},p})$ into $D((-\Delta_{\mathcal{N},p})^{\frac{1}{2}})$ is a Lipschitz continuous mapping on the bounded subsets of $D(-\Delta_{\mathcal{N},p})$. By the semigroup approach (see [4,5,15]), we obtain the local solutions.

Proposition A.2 *Let $u_0 \in D(-\Delta_{\mathcal{N},p})$ and $f\colon \mathbb{R}\times\mathbb{R}^N \to \mathbb{R}$ be C^2. Then there exists a unique local in time mild solution u to* (37) *having the following regularity properties:*

$$u \in C([0,\tau); D(-\Delta_{\mathcal{N},p})) \cap C((0,\tau); D((-\Delta_{\mathcal{N},p})^{\frac{3}{2}}),\;\; u_t \in C((0,\tau); D((-\Delta_{\mathcal{N},p})^{\frac{3}{2}-\varepsilon})),$$

with arbitrary $\varepsilon > 0$.

Following [20], we will now recall an a priori estimate of solutions to (37) leading to the global in time extendibility of the local solutions. Consider the Neumann semilinear problem (37) in a bounded domain $\Omega \subset \mathbb{R}^N$ with $\partial\Omega$ of class C^2 if $N \geq 2$, where the function $f\colon \mathbb{R}\times\mathbb{R}^N \to \mathbb{R}$ is C^2 and satisfies the following growth restriction:

$$f(v,q)v \leq c_0|q|^2 + c_1 v^2 + c_2,\;\; v \in \mathbb{R},\;\; q \in \mathbb{R}^N \tag{39}$$

with non-negative constants c_0, c_1, c_2. Then, for classical solutions of (37) having continuous in $[0,T]\times\overline{\Omega}$ spatial derivatives ∇u, the following a priori estimate in $L^\infty(\Omega)$ is valid:

$$\max_{(t,x)\in[0,T]\times\overline{\Omega}} |u(t,x)| \leq \kappa e^{\lambda T} \max\{\sqrt{c_2}; \max_{x\in\overline{\Omega}} |u_0(x)|\}, \tag{40}$$

where $\kappa, \lambda > 0$ are constants dependent only on c_0, c_1 and the domain Ω. The proof of that estimate can be found in [20, Ch. V, Theorem 7.3].

Having an a priori $L^\infty(\Omega)$ estimate as in (40) for all classical solutions to (37) under the assumption (39), we can thus eliminate the possibility of the blow-up in that case whenever f grows less than quadratically with respect to ∇u. Indeed, assume that the *sub-quadratic growth condition* with respect to the gradient is satisfied (compare [20, Chapter I, (3.31)]):

$$\begin{aligned} &|f(u,\nabla u)| \leq c(|u|)(1+|\nabla u|^{2-\varepsilon}), \quad |D_1 f(u,\nabla u)| \leq c(|u|)(1+|\nabla u|^{2-\varepsilon}),\\ &|D_{i+1} f(u,\nabla u)| \leq c(|u|)(1+|\nabla u|^{1-\varepsilon}), \quad i=1,\dots,N, \end{aligned} \tag{41}$$

where $c\colon \mathbb{R}^+ \to \mathbb{R}^+$ is a non-decreasing function and $\varepsilon \in (0,1)$.

Note first that whenever $\frac{(2-\varepsilon)p-N}{(2-\delta)p-N} < \theta(2-\varepsilon)$, where $0<\delta<\varepsilon$ and $0<\theta<1$, the Nirenberg-Gagliardo type estimate

$$\|\phi\|_{W^{1,(2-\varepsilon)p}(\Omega)} \leq c\|\phi\|^{\theta}_{W^{2-\delta,p}(\Omega)}\|\phi\|^{1-\theta}_{L^\infty(\Omega)}$$

holds. Further, since $\frac{(2-\varepsilon)p-N}{(2-\delta)p-N} < 1$, we can also assume that $\theta(2-\varepsilon) < 1$. Thus we get

$$\begin{aligned} &\|f(u,\nabla u)\|_{L^p(\Omega)} \leq c(\|u\|_{L^\infty(\Omega)})\|1+|\nabla u|^{2-\varepsilon}\|_{L^p(\Omega)}\\ &\leq c(\|u\|_{L^\infty(\Omega)})\big(|\Omega| + \|u\|^{2-\varepsilon}_{W^{1,(2-\varepsilon)p}(\Omega)}\big) \leq c'(\|u\|_{L^\infty(\Omega)})\big(1+\|u\|^{\theta(2-\varepsilon)}_{W^{2,p}(\Omega)}\big). \end{aligned}$$

We further consider the components of the norm $\|f(u,\nabla u)\|_{W^{1,p}(\Omega)}$:

$$\|\frac{\partial}{\partial x_j} f(u,\nabla u)\|_{L^p(\Omega)} \leq \|D_1 f \frac{\partial u}{\partial x_j}\|_{L^p(\Omega)} + \sum_{i=1}^N \|D_{i+1} f \frac{\partial^2 u}{\partial x_j \partial x_i}\|_{L^p(\Omega)}. \tag{42}$$

We will estimate the second component in (42), the first one can be treated analogously. Using the Hölder inequality (with $\frac{1}{r}+\frac{1}{s}=1$) and (41), we obtain

$$\begin{aligned} \|D_{i+1} f \frac{\partial^2 u}{\partial x_j\partial x_i}\|_{L^p(\Omega)} &\leq \|D_{i+1} f(u,\nabla u)\|_{L^{pr}(\Omega)} \|\frac{\partial^2 u}{\partial x_j \partial x_i}\|_{L^{ps}(\Omega)}\\ &\leq c'(\|u\|_{L^\infty(\Omega)})\big(1+\|\nabla u\|^{1-\varepsilon}_{L^{(1-\varepsilon)pr}(\Omega)}\big)\|u\|_{W^{2,ps}(\Omega)}. \end{aligned}$$

The last estimate, by the Nirenberg-Gagliardo type inequalities

$$\|\phi\|_{W^{1,(1-\varepsilon)pr}(\Omega)} \leq c\|\phi\|^{\theta}_{W^{3-\delta,p}(\Omega)}\|\phi\|^{1-\theta}_{L^\infty(\Omega)}, \quad \|\phi\|_{W^{2,ps}(\Omega)} \leq \bar{c}\|\phi\|^{\overline{\theta}}_{W^{3-\delta,p}(\Omega)}\|\phi\|^{1-\overline{\theta}}_{L^\infty(\Omega)},$$

extends to

$$\|D_{i+1}f\frac{\partial^2 u}{\partial x_j \partial x_i}\|_{L^p(\Omega)} \leq C(\|u\|_{L^\infty(\Omega)})\big(1+\|u\|^{\overline{\theta}+(1-\varepsilon)\theta}_{W^{3-\delta,p}(\Omega)}\big),$$

where we need to fulfill two conditions

$$1-\frac{N}{(1-\varepsilon)pr} < \theta\big(3-\delta-\frac{N}{p}\big) \ \text{ and } \ 2-\frac{N}{ps} < \overline{\theta}\big(3-\delta-\frac{N}{p}\big),$$

or, jointly, $3-\varepsilon-\frac{N}{p} < \big(\overline{\theta}+(1-\varepsilon)\theta\big)\big(3-\delta-\frac{N}{p}\big)$. Note that, for a given $\varepsilon \in (0,1)$ and $0<\delta<\varepsilon$, the sum $(\overline{\theta}+(1-\varepsilon)\theta)$ will be made strictly less than 1. We thus obtained a *subordination type condition*

$$\|f(u,\nabla u)\|_{W^{1,p}(\Omega)} \leq c(\|u\|_{L^\infty(\Omega)})\big(1+\|u\|^{\overline{\theta}+(1-\varepsilon)\theta}_{W^{3-\delta,p}(\Omega)}\big)$$

allowing to extend a local solution to (37), varying in the phase space $W^{3-\delta,p}_{\mathcal{N}}(\Omega)$ globally in time (see Theorem 4.2 and [4, Section 4.3] for details).

References

[1] N. Ben-Gal. Non-compact global attractors for slowly non-dissipative PDEs I: The asymptotics of bounded and grow-up heteroclinics. Preprint, 2011.

[2] A.N. Carvalho, J.A. Langa and J.C. Robinson. *Attractors for Infinite-dimensional Non-autonomous Dynamical Systems*. Springer, New York, 2013.

[3] V.V. Chepyzhov and A.Yu. Goritskii. Unbounded attractors of evolution equations. *Adv. Soviet Math.* **10** (1992) 85–128.

[4] J.W. Cholewa and T. Dlotko. *Global Attractors in Abstract Parabolic Problems*. Cambridge University Press, Cambridge, 2000.

[5] J.W. Cholewa, C. Quesada and A. Rodríguez-Bernal. Nonlinear evolution equations in scales of Banach spaces and applications to PDEs. *J. Abstr. Differ. Equ. Appl.* **8** (2017) 1–69.

[6] R. Czaja. Asymptotics of parabolic equations with possible blow-up. *Colloq. Math.* **99** (2004) 61–73.

[7] T. Dlotko. Examples of parabolic problems with blowing-up derivatives. *J. Math. Anal. Appl.* **154** (1991) 226–237.

[8] B. Fiedler and C. Rocha. Sturm 3-ball global attractors 3: Examples of Thom-Smale complexes. *Discrete Contin. Dyn. Syst.* **38** (2018) 3479–3545.

[9] B. Fiedler, C. Rocha and M. Wolfrum. A permutation characterization of Sturm global attractors of Hamiltonian type. *J. Differential Equations* **252** (2012) 588–623.

[10] D. Gilbarg and N.S. Trudinger. *Elliptic Partial Differential Equations of Second Order*. Springer-Verlag, Berlin, 1983.

[11] J.K. Hale. *Ordinary Differential Equations*. Krieger Publishing Company, Malabar, 1980.

[12] J.K. Hale. *Asymptotic Behavior of Dissipative Systems*. AMS, Providence, R.I., 1988.

[13] A. Haraux and P. Poláčik. Convergence to a positive equilibrium for some nonlinear evolution equations in a ball. *Acta Math. Univ. Comenianae* **61** (2) (1992) 129–141.

[14] Ph. Hartman. *Ordinary Differential Equations.* John Wiley & Sons, New York, 1964.

[15] D. Henry. *Geometric Theory of Semilinear Parabolic Equations.* Springer-Verlag, Berlin, 1981.

[16] Bei Hu. *Blow-up Theories for Semilinear Parabolic Equations.* Springer-Verlag, Berlin, 2011.

[17] M. Kania. Solution to the critical Burgers equation for small data in a bounded domain. *Nonlinear Dyn. Syst. Theory* **20** (4) (2020) 397–409.

[18] P. Lappicy and B. Fiedler. A Lyapunov function for fully nonlinear parabolic equations in one spatial variable. *Sao Paulo J. Math. Sci.* **13** (2019) 283–291.

[19] O.A. Ladyzhenskaya. *Attractors for Semigroups and Evolution Equations.* Cambridge University Press, Cambridge, 1991.

[20] O.A. Ladyzhenskaya, V.A. Solonnikov and N.N. Ural'ceva. *Linear and Quasi-linear Equations of Parabolic Type.* Nauka, Moscow, 1967.

[21] H. Matano. Convegence of solutions of one-dimensional semilinear parabolic equations. *J. Math. Kyoto Univ.* **18** (1978) 221–227.

[22] J. Pimentel and C. Rocha. Noncompact global attractors for scalar reaction–diffusion equations. *São Paulo J. Math. Sci.* **9** (2015) 299–310.

[23] J. Pimentel and C. Rocha. A permutation related to non-compact global attractors for slowly non-dissipative systems. *J. Dynam. Differential Equations* **28** (2016) 1–28.

[24] P. Quittner and Ph. Souplet. *Superlinear Parabolic Problems - Blow-up, Global Existence and Steady States.* Birkhäuser Advanced Texts Basler Lehrbücher, 2019.

[25] J.C. Robinson. *Infinite-Dimensional Dynamical Systems: An Introduction to Dissipative Parabolic PDEs and the Theory of Global Attractors.* Cambridge University Press, 2001.

[26] A.A. Samarskii, V.A. Galaktionov, S.P. Kurdyumov and A.P. Mikhailov. *Blow-up in Quasilinear Parabolic Equations.* De Gruyter, Berlin, 2011.

[27] G.R. Sell and Y. You. *Dynamics of Evolutionary Equations.* Springer Science+Business Media, New York, 2002.

[28] J. Smoller. *Shock Waves and Reaction-Diffusion Equations.* Springer-Verlag, New York, 1983.

[29] Ph. Souplet. Gradient blow-up for multidimensional nonlinear parabolic equations with general boundary conditions. *Differ. Integral Equ.* **15** (2002) 237–256.

[30] Ph. Souplet. The influence of gradient perturbations on blow-up asymptotics in semilinear parabolic problems: a survey. In: *Progress in Nonlinear Differential Equations and Their Applications.* Birkhäuser Verlag, Basel, 2005, pp. 473–495.

[31] R. Temam. *Infinite-Dimensional Dynamical Systems in Mechanics and Physics.* Springer-Verlag, New York, 1988.

[32] W. von Wahl. Global solutions to evolution equations of parabolic type. In: *Differential Equations in Banach Spaces, Proceedings, 1985*, edited by A. Favini and E. Obrecht. Springer-Verlag, Berlin, 1986, pp. 254–266.

[33] A. Yagi. *Abstract Parabolic Evolution Equations and their Applications.* Springer-Verlag, Heidelberg, 2010.

[34] T.I. Zelenyak. Stabilization of solutions of boundary-value problems for a second order parabolic equation with one space variable. *Differ. Uravn.* **4** (1968) 34–45.

[35] T.I. Zelenyak, M.M. Lavrentiev Jr. and M.P. Vishnevskii. *Qualitative Theory of Parabolic Equations, Part 1.* VSP, Utrecht, 1997.

Nonlinear Dynamics and Systems Theory, **22** (1) (2022) 46–57

A Geometric Study of Relative Operator Entropies

A. El Hilali [1], B. El Wahbi [1] and M. Chergui [2*]

[1] *Department of Mathematics, Faculty of Sciences, Ibn Tofail University, LAGA-Lab Kenitra, Morocco.*
[2] *Department of Mathematics, CRMEF-Kenitra, EREAM Team, LaREAMI-Lab, Kenitra, Morocco.*

Received: August 6, 2021; Revised: January 22, 2022

Abstract: This paper investigates geometrical properties for relative operator entropies acting on positive definite matrices by the use of the log-determinant metric. Particularly, we prove that both entropies $S_p(A|B)$ and $T_p(A|B)$ lie inside the sphere centered at the geometric mean of A and B with the radius equal to half the log-determinant distance between A and B.

Keywords: *parametric relative operator entropy; Tsallis relative operator entropy; general perturbation schemes; general systems.*

Mathematics Subject Classification (2010): 54C70, 47A63, 70K60, 93A10.

1 Introduction

Let $\mathcal{M}_n$ be the algebra of $n \times n$ matrices over $\mathbb{R}$, and $\mathbb{P}_n$ denote the cone of symmetric positive definite elements of $\mathcal{M}_n$. The identity matrix will be denoted by I. We recall that for any two matrices A and B from $\mathbb{P}_n$, we set $A \leq B$ to mean that $B - A \geq 0$, i.e., $B - A$ is a positive semi-definite matrix. This order, known in the literature by the Löwner order, is partial.

Kamei and Fujii introduced in [7, 8] the relative operator entropy $S(A|B)$ for two positive definite matrices A and B, by the following formula:

$$S(A|B) = A^{\frac{1}{2}} \log\left(A^{\frac{-1}{2}} B A^{\frac{-1}{2}}\right) A^{\frac{1}{2}}, \tag{1}$$

which represents an extension of the operator entropy defined by Nakamura and Umegaki [18] and of the relative operator entropy introduced by Umegaki [21]. Later, a generalized parametric extension of the relative operator entropy was stated by Furuta in [10] as

$$S_p(A|B) = A^{\frac{1}{2}} \left(A^{\frac{-1}{2}} B A^{\frac{-1}{2}}\right)^p \log(A^{\frac{-1}{2}} B A^{\frac{-1}{2}}) A^{\frac{1}{2}}, \qquad p \in \mathbb{R}. \tag{2}$$

* Corresponding author: mailto:chergui_m@yahoo.fr

The last generalization is to be understood as follows:

$$\lim_{p\to 0} S_p(A|B) = S_0(A|B) = S(A|B).$$

Applying the concept of the Tsallis relative entropy for matrices, Yanagi, Kuriyama and Furuichi presented in [20] another parametric extension of relative operator entropy as follows:

$$T_p(A|B) = \frac{A\sharp_p B - A}{p}, \qquad p \in [-1,1] \setminus \{0\}, \tag{3}$$

where $A\sharp_p B := A^{\frac{1}{2}} \left(A^{\frac{-1}{2}} B A^{\frac{-1}{2}}\right)^p A^{\frac{1}{2}}$ for all $p \in \mathbb{R}$ is the p-weighted geometric mean of A and B, which coincides, when taking $p = 1/2$, with the well known geometric mean that will be simply denoted in the sequel by $A\sharp B$. The last extension is justified by the following result proved in [8]:

$$\lim_{p\to 0} T_p(A|B) = S(A|B).$$

Some algebraic properties and inequalities involving the two parametric extensions of the relative operator entropy can be found, for instance, in [6, 9, 15, 16]. The representation of the Tsallis relative operator by means has allowed to derive some inequalities related to this operator.

Following the Kubo-Ando theory [12], it is known that for the representing function $f_\sigma(x) = 1\sigma x$ for an operator mean σ acting on positive matrices, the scalar inequality $f_{\sigma_1}(x) \le f_{\sigma_2}(x),\ (x > 0)$ is equivalent to the operator one $A\sigma_1 B \le A\sigma_2 B$, for all positive definite matrices A and B. It is also worth recalling that for any non-negative monotone function f on $(0, +\infty)$, the binary map defined for two positive matrices A and B by $A\sigma B = A^{\frac{1}{2}} f\left(A^{\frac{-1}{2}} B A^{\frac{-1}{2}}\right) A^{\frac{1}{2}}$ is a Kubo-Ando mean in the sense stated in [12].

The concept of entropy is widely used in estimating uncertainty existing in the state of a dynamic system and in measuring the degree of chaos in a deterministic system. Further details and approaches related to these notions can be found in [3, 11, 19], for example. Another very interesting topic in this field is the measure of the distance between the states of a dynamic system. It represents an essential tool to describe the evolution of quantum systems. Intensive studies have been carried out in the last few years concerning this point, see [1, 13, 14] for instance.

There are many definitions of the distance between states. Among those, we recall the log-determinant metric d_l, widely used in machine learning and quantum information, and defined for any matrices A and B from $\mathbb{P}_n$ as follows [17]:

$$d_l(A, B) = \log\det(A\nabla B) - \frac{1}{2}\log\det(AB), \tag{4}$$

where $A\nabla B := \dfrac{A+B}{2}$ denotes the arithmetic mean of A and B. We recall the following property [17] that holds true for every three matrices A, B and C from $\mathbb{P}_n$:

$$d_l(C\,A\,C, C\,B\,C) = d_l(A, B). \tag{5}$$

Recently, many authors employ this metric in developing various concepts and establishing interesting properties concerning some parametric means. For details, we refer the reader to [2, 4, 5] and the references therein.

In this paper, by the use of the log-determinant metric, we estimate some distances involving the relative operator entropies recalled in (1), (2) and (3). The present paper is organized in the following manner. In the second section, we present some preliminary tools and in the third one, we focus on stating our main results with respect to the log-determinant metric. The findings presented in this paper have geometric interpretations.

2 Preliminaries

In this section, we set out some preliminary results that will be needed in the sequel. We begin by presenting some results about some real functions that will be used as ingredients for our main results.

Lemma 2.1 *We have the following results:*

i) $\forall t > 0\,, \quad 1 - \dfrac{1}{t} \leq \log t \leq t - 1.$

ii) *The function* $p \longmapsto \dfrac{x^p - 1}{p}$ *is increasing on* $(0, 1]$ *for each* $x > 0$.

iii) *The function* $p \longmapsto (1+p)^{\frac{1}{p}}$ *is decreasing on* $(0, 1]$ *and* $\sup_{p \in (0,1]} (1+p)^{\frac{1}{p}} = e$.

Proof. These statements are routine exercises in mathematical real analysis.

The following proposition will give an efficient tool in determining some results for the Tsallis relative operator entropy with respect to the log-determinant metric.

Proposition 2.1 *Let* C *be a positive definite matrix. If* $e\, I \leq C$*, then the map defined by*

$$p \longmapsto \left(\frac{C^p - I}{p}\right)^{1/2} \nabla \left(\frac{C^p - I}{p}\right)^{-1/2}$$

is increasing on $(0, 1]$.

Proof. Let $x \geq e$. The functions $t \overset{h}{\longmapsto} t^{1/2} \nabla t^{-1/2}$ and $p \overset{k}{\longmapsto} \dfrac{x^p - 1}{p}$ are both increasing on $[1, \infty)$ and $(0, 1]$, respectively. Since $x \geq e$ and using the third assertion in Lemma 2.1, we can set $x \geq (p+1)^{1/p}$ for every p in $(0, 1]$.

So, for all $p \in (0, 1]$, we get $\dfrac{x^p - 1}{p} \geq 1$. By taking the appropriate composition of the functions h and k, we deduce that the function

$$p \longmapsto \left(\frac{x^p - 1}{p}\right)^{1/2} \nabla \left(\frac{x^p - 1}{p}\right)^{-1/2}$$

is increasing on $(0, 1]$.

Finally, if the condition $C \geq e\, I$ is satisfied, then the map $p \longmapsto \left(\dfrac{C^p - I}{p}\right)^{1/2} \nabla \left(\dfrac{C^p - I}{p}\right)^{-1/2}$ is increasing on $(0, 1]$, thanks to the connection well known in the theory of Kubo-Ando between the inequalities satisfied by the representing functions and associate means operators. (For simplicity, this detail will be omitted in the following proofs.)

The main goal of the next three lemmas is to characterize some constants which will be needed in establishing appropriate conditions for our main results.

Lemma 2.2 *The function f defined on $(1,\infty)$ by $f(x) = x^{\frac{1}{2}} + x^{\frac{-1}{2}} - (\log x)^{\frac{1}{2}} - (\log x)^{\frac{-1}{2}}$ is strictly increasing. Moreover, there exists a unique α satisfying $f(\alpha) = 0$ and $1,76 < \alpha < 1,77$.*

Proof. For all $x > 1$, we have

$$f'(x) = \frac{(x-1)\sqrt{\log x}\log x + \sqrt{x}(1-\log x)}{2x\sqrt{x}\sqrt{\log x}\log x}.$$

For $1 < x \leq e$, the inequality $(x-1)\sqrt{\log x}\log x + \sqrt{x}(1-\log x) \geq 0$ is simple to deduce.
If $x > e$, then we have

$$\begin{aligned}(x-1)\sqrt{\log x}\log x + \sqrt{x}(1-\log x) &> (x-1)\log x + \sqrt{x}(1-\log x) \\ &= (x-\sqrt{x})\log x + \sqrt{x} - \log x.\end{aligned}$$

One can easily check that $(x-\sqrt{x})\log x > 0$ and $\sqrt{x} - \log x > 0$. This implies that f increases strictly on $(1,\infty)$. In addition, since f is continuous on $(1,\infty)$, there is a bijection from $(1,\infty)$ onto $(\lim_{x\downarrow 1} f(x), \lim_{x\to+\infty} f(x)) = (-\infty,+\infty)$. This confirms the existence and uniqueness of α. Finally, by checking that $f(1,76) < 0 < f(1,77)$, the proof is ended.

Lemma 2.3 *The function g defined on $[1,\infty)$ by $g(x) = \log x - 1 + \dfrac{1}{x+1}$ is strictly increasing and there exists a unique $\beta > 1$ such that $g(\beta) = 0$. Moreover, $1,93 < \beta < 1,94$.*

Proof. It suffices to study the variations of the function g on $[1,\infty)$ and to deduce the results in a similar way as in the proof of Lemma 2.2.

Lemma 2.4 *The function h defined on $(1,\infty)$ by $h(x) = x + \dfrac{1}{x} - x^{\frac{1}{2}}\log x - (\log x)^{-1}$ is strictly increasing and there exists a unique $\sigma > 1$ satisfying $h(\sigma) = 0$. Moreover, $1,91 < \sigma < 1,92$.*

Proof. For all $x > 1$, we have

$$h'(x) = \frac{2\sqrt{x} - \log x - 2}{2\sqrt{x}} + \frac{1}{x(\log x)^2} - \frac{1}{x^2}.$$

By simple computations, one can check that

$$\frac{2\sqrt{x} - \log x - 2}{2\sqrt{x}} \geq 0 \quad \text{and} \quad \frac{1}{x(\log x)^2} - \frac{1}{x^2} \geq 0.$$

So h increases strictly on $(1,\infty)$. On the other hand, h is continuous on $(1,\infty)$, so it establishes a bijection from $(1,\infty)$ onto $\big(\lim_{x\downarrow 1} h(x), \lim_{x\to\infty} h(x)\big) = (-\infty,\infty)$. This proves the existence and the uniqueness of σ. To end the proof, it suffices to note that $h(1,91) < 0 < h(1,92)$.

Now we are in a position to state our findings, and hereafter, for any given two positive definite matrices A and B, we will constantly set $C = A^{-1/2}\,B\,A^{-1/2}$.

3 Statement of Findings

In this section, we aim to establish inequalities for the relative operator entropy and its generalizations with respect to the log-determinant metric.

Theorem 3.1 *Let $A, B \in \mathbb{P}_n$ be two positive definite matrices such that $\alpha A \leq B$. We have the following inequality:*

$$d_l\big(A, S(A|B)\big) \leq d_l(A, B), \tag{6}$$

where α is the fixed real number defined in Lemma 2.2.

Proof. Using Lemma 2.2, for every $x \geq \alpha$, we have

$$(\log x)^{\frac{1}{2}} + (\log x)^{\frac{-1}{2}} \leq x^{\frac{1}{2}} + x^{\frac{-1}{2}}.$$

So, if $\alpha A \leq B$, then $\alpha\, I \leq C$ and we get

$$(\log C)^{\frac{1}{2}} + (\log C)^{\frac{-1}{2}} \leq C^{\frac{1}{2}} + C^{\frac{-1}{2}}.$$

The last inequality combined with the monotonicity of the logarithm and the determinant gives

$$\log\det\left(\frac{1}{2}\big((\log C)^{\frac{1}{2}} + (\log C)^{\frac{-1}{2}}\big)\right) \leq \log\det\left(\frac{1}{2}\big(C^{\frac{1}{2}} + C^{\frac{-1}{2}}\big)\right),$$

that is,

$$d_l(I, \log C) \leq d_l(I, C),$$

or

$$d_l\big(A, S(A|B)\big) \leq d_l(A, B).$$

By this, the proof is concluded.

Now we will deal with the generalization of the last result for any operator $S_p(A|B)$ with $p \in (0, \frac{1}{2}]$.

Theorem 3.2 *Let A and B be two positive definite matrices such that $\sigma A \leq B$. The following inequality holds true:*

$$d_l(A, S_p(A|B)) \leq d_l(A, B) \tag{7}$$

for all $p \in (0, \frac{1}{2}]$. σ denotes the constant number in Lemma 2.4.

Proof. By the condition $\sigma A \leq B$ and for all $0 < p \leq \dfrac{1}{2}$, we have

$$\log C \leq C^p \log C \leq C^{\frac{1}{2}} \log C,$$

so

$$(C^p \log C)^{-1} \leq (\log C)^{-1}.$$

Hence

$$C^p \log C + (C^p \log C)^{-1} \leq C^{\frac{1}{2}} \log C + (\log C)^{-1}.$$

Since $C \geq \sigma\, I$, thanks to Lemma 2.4 we obtain the following inequalities:

$$C^p \log C + (C^p \log C)^{-1} \leq C^{\frac{1}{2}} \log C + (\log C)^{-1} \leq C + C^{-1},$$

and we can deduce that

$$(C^p \log C) + (C^p \log C)^{-1} + 2I \leq C + C^{-1} + 2I,$$

or equivalently,

$$\frac{(C^p \log C)^{\frac{1}{2}} + (C^p \log C)^{\frac{-1}{2}}}{2} \leq \frac{C^{\frac{1}{2}} + C^{\frac{-1}{2}}}{2}.$$

Thus,

$$\log \det \left(\frac{\big(C^p \log C\big)^{\frac{1}{2}} + \big(C^p \log C\big)^{\frac{-1}{2}}}{2} \right) \leq \log \det \left(\frac{C^{\frac{1}{2}} + C^{\frac{-1}{2}}}{2} \right),$$

that is,

$$d_l(I, C^p \log C) \leq d_l(I, C).$$

The last inequality is equivalent to (2.4).

Remark 3.1 The proof of Theorem 3.2 is also valid for $p = 0$. So, it gives $d_l\big(A, S(A|B)\big) \leq d_l(A, B)$ for two definite positive matrices A and B when $\sigma A \leq B$. But since $\sigma > \alpha$, the result given by Theorem 3.1 is better than the one given in Theorem 3.2 for this case.

Theorem 3.3 *Let A and B be two positive definite matrices such that $eA \leq B$. For all two positive numbers $p, q \in [0, 1]$ such that $p \leq q$, we have*

$$d_l\big(A, S_p(A|B)\big) \leq d_l\big(A, S_q(A|B)\big). \tag{8}$$

Proof. One can easily check that for a given $x \geq e$, the function $p \longmapsto \big(x^p(\log x)\big)^{\frac{1}{2}} + \big(x^p(\log x)\big)^{\frac{-1}{2}}$ is increasing on $[0, 1]$. So, if $eA \leq B$, then for all $p, q \in [0, 1]$ such that $p \leq q$, we have

$$\frac{\big(C^p(\log C)\big)^{\frac{1}{2}} + \big(C^p(\log C)\big)^{\frac{-1}{2}}}{2} \leq \frac{\big(C^q(\log C)\big)^{\frac{1}{2}} + \big(C^q(\log C)\big)^{\frac{-1}{2}}}{2}.$$

Thus,

$$\log \det \left(\frac{\big(C^p(\log C)\big)^{\frac{1}{2}} + \big(C^p(\log C)\big)^{\frac{-1}{2}}}{2} \right) \leq \log \det \left(\frac{\big(C^q(\log C)\big)^{\frac{1}{2}} + \big(C^q(\log C)\big)^{\frac{-1}{2}}}{2} \right),$$

which means that the following inequalities hold:

$$d_l\big(I, C^p(\log C)\big) \leq d_l\big(I, C^q(\log C)\big),$$

or equivalently,

$$d_l\big(A, S_p(A|B)\big) \leq d_l\big(A, S_q(A|B)\big).$$

Remark 3.2 If the conditions stated in Theorems 3.1, 3.2 and 3.3 are not fulfilled by the matrices A and B, then the inequalities (6), (7) and (8) are no longer valid. This fact can be highlighted by the following counter-example.

Let us consider the following two positive definite matrices:

$$A = \begin{pmatrix} 4 & 1 \\ 1 & 4 \end{pmatrix} \text{ and } B = \begin{pmatrix} 5 & 1 \\ 1 & 5 \end{pmatrix}.$$

Computing with Matlab software, we find the following values:

- $d_l(A,B)=0,0145<d_l(A,S(A|B))=0,5080.$

- $d_l(A,B)<d_l\big(A,S_{1/2}(A|B)\big)=0.4391<d_l\big(A,S_{1/4}(A|B)\big)=0,4729.$

Theorem 3.4 *Let A and B be two positive definite matrices such that $\beta\,A\le B$. The following inequality holds for any $0<p\le 1$:*

$$d_l\big(A,T_p(A|B)\big)\le d_l(A,B) \tag{9}$$

with β being the constant defined in Lemma 2.3.

Proof. Inequality (9) is equivalent to the following:

$$\log\det\left(\frac{(\frac{C^p-I}{p})^{\frac{1}{2}}+(\frac{C^p-I}{p})^{\frac{-1}{2}}}{2}\right)\le\log\det\left(\frac{C^{\frac{1}{2}}+C^{\frac{-1}{2}}}{2}\right). \tag{10}$$

So, let us prove that we have, for any $x\ge\beta$,

$$\left(\frac{x^p-1}{p}\right)^{\frac{1}{2}}+\left(\frac{x^p-1}{p}\right)^{\frac{-1}{2}}\le x^{\frac{1}{2}}+x^{\frac{-1}{2}}, \tag{11}$$

or equivalently,

$$\frac{x^p-1}{p}+(\frac{x^p-1}{p})^{-1}\le x+\frac{1}{x}.$$

For any $x\ge\beta$, we have $\log x\le\dfrac{x^p-1}{p}\le x-1$ and, consequently, we get

$$\frac{x^p-1}{p}+\left(\frac{x^p-1}{p}\right)^{-1}\le x-1+(\log x)^{-1}.$$

Furthermore, according to Lemma 2.3, we have

$$x-1+(\log x)^{-1}\le x+\frac{1}{x}.$$

So, if $\beta\,A\le B$, then $\beta\,I\le C$ and, consequently, the inequality (11) is established. This ends the proof.

Theorem 3.5 *Let A and B be two matrices from $\mathbb{P}_n$. If $e\,A\le B$, then the following inequality*

$$d_l(A,T_p(A|B))\le d_l(A,T_q(A|B)) \tag{12}$$

holds true if $0<p\le q\le 1$.

Proof. If $e\,A\le B$, then $e\,I\le C$. Employing Proposition 2.1, we get

$$\left(\frac{C^p-I}{p}\right)^{1/2}\nabla\left(\frac{C^p-I}{p}\right)^{-1/2}\le\left(\frac{C^q-I}{p}\right)^{1/2}\nabla\left(\frac{C^q-I}{p}\right)^{-1/2}$$

for every $p, q \in (0, 1]$ and $p \leq q$. So,

$$\log\det\left[\left(\frac{C^p - I}{p}\right)^{1/2} \nabla \left(\frac{C^p - I}{p}\right)^{-1/2}\right] \leq \log\det\left[\left(\frac{C^q - I}{q}\right)^{1/2} \nabla \left(\frac{C^q - I}{q}\right)^{-1/2}\right].$$

After some minor computations the last inequality implies

$$d_l\left(I, \frac{C^p - I}{p}\right) \leq d_l\left(I, \frac{C^q - I}{q}\right)$$

which is equivalent to the desired one (12).

In what follows we focus on estimating the log-determinant distance between the geometric mean and different relative entropy operators.

Theorem 3.6 *Let A and B be two positive definite matrices such that $e\,A \leq B$. We have the following inequality:*

$$d_l(A \sharp B, S(A|B)) \leq \frac{1}{2} d_l(A, B). \tag{13}$$

Proof. The inequality

$$d_l(A \sharp B, S(A|B)) \leq \frac{1}{2} d_l(A, B)$$

is equivalent to

$$\log\det\left(\frac{\left(C^{\frac{-1}{4}}(\log C)C^{\frac{-1}{4}}\right)^{\frac{1}{2}} + \left(C^{\frac{-1}{4}}(\log C)C^{\frac{-1}{4}}\right)^{\frac{-1}{2}}}{2}\right) \leq \log\det\left(\frac{C^{\frac{1}{2}} + C^{\frac{-1}{2}}}{2}\right)^{\frac{1}{2}}.$$

So, let us prove that if $C \geq e\,I$, then we have

$$\frac{\left(C^{\frac{-1}{4}}(\log C)C^{\frac{-1}{4}}\right)^{\frac{1}{2}} + \left(C^{\frac{-1}{4}}(\log C)C^{\frac{-1}{4}}\right)^{\frac{-1}{2}}}{2} \leq \left(\frac{C^{\frac{1}{2}} + C^{\frac{-1}{2}}}{2}\right)^{\frac{1}{2}},$$

or equivalently,

$$C^{\frac{-1}{4}}(\log C)C^{\frac{-1}{4}} + \left(C^{\frac{-1}{4}}(\log C)C^{\frac{-1}{4}}\right)^{-1} + 2I \leq 2(C^{\frac{1}{2}} + C^{\frac{-1}{2}}). \tag{14}$$

Let us set for $x \geq e$, $\varphi(x) = 2x^{\frac{1}{2}} + 2x^{\frac{-1}{2}} - x^{\frac{-1}{2}} \log x - \left(x^{\frac{-1}{2}} \log x\right)^{-1} - 2$.

One can simply check that

$$\varphi'(x) = \frac{2(x - \log^2 x) + (\log x - 1)\log^2 x + (x-1)\log^2 x + x\,\log x\,(\log x - 1)}{2x\sqrt{x}(\log x)^2}.$$

It is clear that for $x \geq e$ one has $\varphi'(x) \geq 0$. So φ is increasing on $[e, \infty)$ and this implies that

$$\varphi(x) \geq \varphi(e) \geq 0.$$

Thus we get the inequality

$$\left(x^{\frac{-1}{2}} \log x\right) + \left(x^{\frac{-1}{2}}(\log x)\right)^{-1} + 2 \leq 2(x^{\frac{1}{2}} + x^{\frac{-1}{2}}),$$

which can be rephrased as follows:

$$x^{\frac{-1}{4}}(\log x)x^{\frac{-1}{4}} + \left(x^{\frac{-1}{4}}(\log x)x^{\frac{-1}{4}}\right)^{-1} + 2 \leq 2(x^{\frac{1}{2}} + x^{\frac{-1}{2}}).$$

By this, the inequality (14) is established and the proof of the desired result is ended.

A generalization of this result will be recited in the following theorem.

Theorem 3.7 *Let A and B be two positive definite matrices such that $\mu A \leq B$. If $\mu \geq 3,3$, then we have for all $p \in (0, \frac{1}{2}]$ the following inequality:*

$$d_l(A\sharp B, S_p(A|B)) \leq \frac{1}{2} d_l(A, B). \tag{15}$$

Proof. We consider the function l defined on $[3, \infty[$ by

$$l(x) = 2x^{\frac{1}{2}} + 2x^{\frac{-1}{2}} - \log x - \left(x^{\frac{-1}{2}} \log x\right)^{-1} - 2.$$

Let $x \geq 3,3$. We have

$$l'(x) = \frac{2(x - \log^2 x) + \sqrt{x}\log x[\,2(\sqrt{x} - 1)\,\log x - \sqrt{x}\,]}{2x\sqrt{x}(\log x)^2}.$$

We can by routine computations show that $x - \log^2 x \geq 0$ and $2(\sqrt{x} - 1)\,\log x - \sqrt{x} \geq 0$. So, the function l is increasing on $[\mu, \infty)$. Consequently, for all $x \geq \mu$, we get

$$2x^{\frac{1}{2}} + 2x^{\frac{-1}{2}} \geq \log x + \left(x^{\frac{-1}{2}} \log x\right)^{-1} + 2. \tag{16}$$

On the other hand, since the map $p \mapsto x^p$ is increasing on $(0, \frac{1}{2}]$, we have for any $x \geq \mu$ that

$$\left(x^{p-\frac{1}{4}}(\log x)x^{\frac{-1}{4}}\right) \leq \left(x^{\frac{1}{4}}(\log x)x^{\frac{-1}{4}}\right) \leq \log x.$$

These inequalities added to the following ones:

$$\left(x^{p-\frac{1}{4}}(\log x)x^{\frac{-1}{4}}\right)^{-1} \leq \left(x^{\frac{-1}{4}}(\log x)x^{\frac{-1}{4}}\right)^{-1} \leq \left(x^{\frac{-1}{2}} \log x\right)^{-1},$$

enable us via (16) to deduce that

$$\left(x^{p-\frac{1}{4}}(\log x)x^{\frac{-1}{4}}\right) + \left(x^{p-\frac{1}{4}}(\log x)x^{\frac{-1}{4}}\right)^{-1} + 2 \leq 2(x^{\frac{1}{2}} + x^{\frac{-1}{2}}).$$

So, if we suppose that $\mu A \leq B$, then we can deduce from the last inequality that

$$\left(C^{p-\frac{1}{4}}(\log C)C^{\frac{-1}{4}}\right) + \left(C^{p-\frac{1}{4}}(\log C)C^{\frac{-1}{4}}\right)^{-1} + 2I \leq 2\left(C^{\frac{1}{2}} + C^{\frac{-1}{2}}\right),$$

which is equivalent to

$$\frac{\left(C^{p-\frac{1}{4}}(\log C)C^{\frac{-1}{4}}\right)^{\frac{1}{2}} + \left(C^{p-\frac{1}{4}}(\log C)C^{\frac{-1}{4}}\right)^{\frac{-1}{2}}}{2} \leq \left(\frac{C^{\frac{1}{2}} + C^{\frac{-1}{2}}}{2}\right)^{\frac{1}{2}}.$$

So, this yields

$$\log\det\left(\frac{\left(C^{p-\frac{1}{4}}(\log C)C^{\frac{-1}{4}}\right)^{\frac{1}{2}} + \left(C^{p-\frac{1}{4}}(\log C)C^{\frac{-1}{4}}\right)^{\frac{-1}{2}}}{2}\right) \leq \log\det\left(\frac{C^{\frac{1}{2}} + C^{\frac{-1}{2}}}{2}\right)^{\frac{1}{2}},$$

that is,

$$d_l(A\sharp B, S_p(A|B)) \leq \frac{1}{2} d_l(A, B).$$

Now, to estimate the distance $d_l(A\sharp B, T_p(A|B))$, we need the result quoted in the following lemma.

Lemma 3.1 *The function v defined by*

$$v(x) = x^{\frac{1}{2}} + 3x^{\frac{-1}{2}} - \left(x^{\frac{-1}{2}} \log x\right)^{-1} - 2$$

is strictly increasing on $[3, \infty)$ and there exists a unique $\lambda \geq 3$ satisfying $v(\lambda) = 0$. Moreover, $3,61 < \lambda < 3,62$.

Proof. For every $x \in (3, \infty)$, we have $v'(x) = \dfrac{w(x)}{2x\sqrt{x}(\log x)^2}$, where

$$t \in [3, \infty) \longmapsto w(t) := 2t - t \log t + (t-3)(\log t)^2.$$

Computing the first derivative of w on $(3, \infty)$, we find

$$w'(x) = \log^2 x - \log x + 1 + \frac{2(x-3)}{x} \log x > 0.$$

So, $w(x) \geq w(3) > 0$ and we can deduce that u is strictly increasing on $[3, \infty)$.
This fact added to the continuity of v implies that there exists a unique $\lambda \geq 3$ satisfying $v(\lambda) = 0$. The boundedness of λ is easy to check.

Theorem 3.8 *Let A and B be two positive definite matrices such that $\lambda A \leq B$. We have for all $p \in (0, 1]$ the following inequality:*

$$d_l(A \sharp B, T_p(A|B)) \leq \frac{1}{2} d_l(A, B), \tag{17}$$

where λ is the constant defined in Lemma 3.1.

Proof. The inequality

$$d_l(A \sharp B, T_p(A|B)) \leq \frac{1}{2} d_l(A, B)$$

is equivalent to

$$\log\det\left(\frac{\left(\dfrac{C^{p-\frac{1}{2}} - C^{\frac{-1}{2}}}{p}\right)^{\frac{1}{2}} + \left(\dfrac{C^{p-\frac{1}{2}} - C^{\frac{-1}{2}}}{p}\right)^{\frac{-1}{2}}}{2}\right) \leq \log\det\left(\frac{C^{\frac{1}{2}} + C^{\frac{-1}{2}}}{2}\right)^{\frac{1}{2}}.$$

So, let us prove that if $C \geq \lambda\, I$, then we have

$$\frac{\left(\dfrac{C^{p-\frac{1}{2}} - C^{\frac{-1}{2}}}{p}\right)^{\frac{1}{2}} + \left(\dfrac{C^{p-\frac{1}{2}} - C^{\frac{-1}{2}}}{p}\right)^{\frac{-1}{2}}}{2} \leq \left(\frac{C^{\frac{1}{2}} + C^{\frac{-1}{2}}}{2}\right)^{\frac{1}{2}},$$

which is equivalent to the inequality

$$\frac{(\dfrac{C^{p-\frac{1}{2}} - C^{\frac{-1}{2}}}{p}) + (\dfrac{C^{p-\frac{1}{2}} - C^{\frac{-1}{2}}}{p})^{-1} + 2I}{4} \leq \frac{C^{\frac{1}{2}} + C^{\frac{-1}{2}}}{2},$$

or

$$\left(\frac{C^{p-\frac{1}{2}} - C^{\frac{-1}{2}}}{p}\right) + \left(\frac{C^{p-\frac{1}{2}} - C^{\frac{-1}{2}}}{p}\right)^{-1} + 2I \leq 2.\big(C^{\frac{1}{2}} + C^{\frac{-1}{2}}\big). \tag{18}$$

Using $i)$ in Lemma 2.1 and since the map $p \mapsto \dfrac{x^p - 1}{p}$ is increasing on $(0, 1]$, we have for any $x \geq \lambda$ that

$$\log x \leq \frac{x^p - 1}{p} \leq x - 1,$$

and we deduce

$$x^{\frac{-1}{2}} \log x \leq \frac{x^{p-\frac{1}{2}} - x^{\frac{-1}{2}}}{p} \leq x^{\frac{1}{2}} - x^{\frac{-1}{2}}. \tag{19}$$

So, by taking into account the result of Lemma 3.1, we get the following inequalities:

$$\left(\frac{x^{p-\frac{1}{2}} - x^{\frac{-1}{2}}}{p} \right)^{-1} \leq \left(x^{\frac{-1}{2}} \log x \right)^{-1} \leq x^{\frac{1}{2}} + 3x^{\frac{-1}{2}} - 2. \tag{20}$$

From (19) and (20), we can deduce

$$\frac{x^{p-\frac{1}{2}} - x^{\frac{-1}{2}}}{p} + \left(\frac{x^{p-\frac{1}{2}} - x^{\frac{-1}{2}}}{p} \right)^{-1} + 2 \leq 2(x^{\frac{1}{2}} + x^{\frac{-1}{2}}).$$

Finally, we can confirm that if $\lambda A \leq B$, which means that $\lambda I \leq C$, the desired inequality (18) is satisfied. With this, the proof is achieved.

We end this paper by stating the following remark.

Remark 3.3 $i)$ Thanks to Theorems 3.7 and 3.8, we deduce that for convenient values of the parameter p, the operators $S_p(A|B)$ and $T_p(A|B)$ lie inside the sphere centered at the geometric mean of A and B with the radius equal to half the log-determinant distance between A and B.
$ii)$ If the conditions stated for the matrices A and B from Theorem 3.4 to Theorem 3.8 are not fulfilled, then the related results are no longer true. This fact is ensured by counterexamples, that we omit here for this paper not to become heavier.

4 Conclusion

In this work, we established some properties of some classes of operator entropies by employing the log-determinant distance. In particular, some geometrical aspects have been highlighted such as the localization of the entropies of two positive matrices with respect to their geometric mean.

References

[1] J. Anandan and Y. Aharonov. Geometry of quantum evolution. *Phys. Rev. Lett* **65** (14) (1990) 1697–1700.

[2] K. M. R. Audenaert. In-betweenness, a geometrical monotonicity property for operator means. *Linear Algebra Appl., 16th ILAS Conference Proceedings*, **438** (4) (2013) 1769–1778.

[3] F. Derouiche and T. Hamaizia. An Enhanced Bi-Directional Chaotic Optimization Algorithm. *Nonlinear Dynamics and Systems Theory* **20** (4) (2020) 365–373.

[4] T. H. Dinh, B. K. T. Vo and T. Y. Tam. In-sphere property and reverse inequalities for matrix means. *Electron. J. Linear Algebra* **35** (1) (2019) 35–41.

[5] T. H. Dinh, R. Dumitru and J. A. Franco. Some geometric properties of matrix means with respect to different metrics. *Positivity* (2020). https://doi.org/10.1007/s11117-020-00738-w.

[6] S. S. Dragomir. Inequalities for relative operator entropy in terms of Tsallis entropy. *Asian-European Journal of Mathematics* **12**(4) (2019) 1950063.

[7] J. I. Fujii and E. Kamei. Relative operator entropy in noncommutative information theory. *Math. Japon* **34** (3) (1989) 341–348.

[8] J. I. Fujii and E. Kamei. Uhlmann's interpolational method for operator means. *Math. Japon* **34** (4) (1989) 541–547.

[9] N. Furuichi and N. Minculete. Inequalities for Relative Operator Entropies and Operator Means. *Acta Math. Vietnam* **43** (2018) 607–618. https://doi.org/10.1007/s40306-018-0250-7.

[10] T. Furuta. Parametric extensions of Shannon inequality and its reverse one in Hilbert space operators. *Linear Algebra Appl.* **381** (2004) 219–235.

[11] A. Khernane. Numerical Approximation of the Exact Control for the Vibrating Rod with Improvement of the Final Error by Particle Swarm Optimization. *Nonlinear Dynamics and Systems Theory* **20** (2) (2020) 179–190.

[12] F. Kubo and T. Ando. Means of positive linear operators. *Math. Ann.* **246** (3) (1980) 205–224.

[13] A.R. Kuzmak. Measuring distance between quantum states on a quantum computer. *Quantum Inf. Process* **20**, 269 (2021). https://doi.org/10.1007/s11128-021-03196-9.

[14] H. P. Laba and V. M. Tkachuk. Geometric characteristics of quantum evolution: curvature and torsion. *Cond. Matt. Phy.* **20**, 13003 (2017).

[15] I. Nikoufar. On operator inequalities of some relative operator entropies. *Advances in Mathematics* **259** (2014) 376–383.

[16] S. Kim. Operator entropy and fidelity associated with the geometric mean. *Linear Algebra and its Applications* **438** (2013) 2475–2483.

[17] S. Sra. A new metric on the manifold of kernel matrices with application to matrix geometric means. *Advances in Neural Information Processing Systems (NIPS)* **1** (2012) 144–152.

[18] M. Nakamura and H. Umegaki. A note on the entropy for operator algebras. *Proc. Japan Acad.* **37** (1967) 149–154.

[19] S. H. Strogatz. *Nonlinear Dynamics and Chaos*. Massachussets: Perseus Publishing, 2000.

[20] K. Yanagi, K. Kuriyama and S. Furuichi. Generalized Shannon inequalities based on Tsallis relative operator entropy. *Linear Algebra Appl.* **394** (2005) 109–118.

[21] H. Umegaki. Conditional expectation in operator algebra IV(entropy and information). *Kodai Math. Sem. Rep.* **14** (1962) 59–85.

Nonlinear Dynamics and Systems Theory, **22** (1) (2022) 58–65

On the Equivalence of Lorenz System and Li System

Lotfi Meddour * and Kheireddine Belakroum

Department of Mathematics, Faculty of Exact Sciences, Constantine 1 University, Algeria.

Received: July 21, 2021; Revised: December 18, 2021

Abstract: The question of the equivalence of various Lorenz-like systems has been recently discussed, it has been found that with the help of various transformations it is possible to reduce such systems to the same form. In this paper, we show that the Lorenz system and the Li system are topologically equivalent. However, in a recent work it was shown that there is a homothetic transformation which converts the Li system into the Lorenz system and, therefore, all the dynamical behavior exhibited by the Li system is also present in the Lorenz system. Consequently, the results obtained in the papers devoted to the study of the Li system unnecessarily duplicate the scientific literature, while it can be trivially derived from the corresponding results on the Lorenz system.

Keywords: *Lorenz system; Li system; homothetic transformation; topological equivalence.*

Mathematics Subject Classification (2010): 93C10, 34C41, 34C20, 37C15.

1 Introduction

In 1963, E.N. Lorenz [9] discovered chaos in a simple system of three autonomous ordinary differential equations

$$\begin{cases} X' = \sigma(Y - X), \\ Y' = \rho X - Y - XZ, \\ Z' = -\beta Z + XY, \end{cases} \tag{1}$$

where σ, ρ and β are real parameters, the system is chaotic on a small subset $\{\sigma, \rho, \beta\} = \{10, 28, \frac{8}{3}\}$. The Lorenz system is the first mathematical and physical model of chaos. Since the introduction of the Lorenz system, which attracted much attention from research teams, many other chaotic systems (generally called Lorenz-like systems) have

* Corresponding author: mailto:meddour_lotfi@umc.edu.dz

been analyzed (see, for instance, [13–18]). Among them, we mainly focus on the autonomous chaotic system proposed by X.F. Li et al. [15], which has been the subject of some study (see, for example, [20–22]).

For several years great effort has been devoted to the study of the question of the equivalence of various Lorenz-like systems, as discussed in [1–8], thus, with the help of various transformations, it is possible to reduce such systems to the same form. However, Algaba et al. showed that the Chen and the Lü systems are a special case of the Lorenz system [1, 2].

The purpose of this paper is to show that the Lorenz system and the Li system are topologically equivalent. Moreover, in [8] it was shown that there is a homothetic transformation which converts the Li system into the Lorenz system.

The Li system has the following form [15]:

$$\begin{cases} x' = -ax + ay, \\ y' = -y + xz, \\ z' = b - cz - xy, \end{cases} \tag{2}$$

where a, b and c are positive real parameters. With the following transformation:

$$x = X,\ y = Y,\ z = -Z + \frac{b}{c},\ \ (c \neq 0)\,, \tag{3}$$

the system (2) becomes

$$\begin{cases} X' = a\,(Y - X)\,, \\ Y' = \frac{b}{c}X - Y - XZ, \\ Z' = -cZ + XY. \end{cases} \tag{4}$$

Note that system (4) corresponds to the Lorenz system with parameters

$$\sigma = a,\ \rho = \frac{b}{c},\ \beta = c. \tag{5}$$

Therefore, if $c \neq 0$, the Li system is equivalent to the Lorenz system. Thus, for each Lorenz system, there are infinitely many Li systems, parameterized by c. In this case, the two systems are homothetic copies, i.e., all the dynamics found in the Li system with $c \neq 0$ is also present in the Lorenz system.

Moreover, if $c = 0$ and $a \neq 0$ (for $a = 0$, the Li system is linear and then trivially solvable), with the linear scaling

$$x = aX,\ y = aY,\ z = -aZ,\ \tau = at,$$

the Li system is transformed into the system

$$\begin{cases} X' = -X + Y, \\ Y' = -\frac{1}{a}Y - XZ, \\ Z' = -\frac{b}{a^2} + XY. \end{cases} \tag{6}$$

Consequently, the system (6) is a particular case of a system, which has been proposed and analysed by Pehlivan and Uyaroğlu [19].

2 Dynamics Found in the Lorenz and the Li Systems

In this section, we give some examples to illustrate how we can trivially deduce the dynamics that appears in the Li system from the dynamics found in the Lorenz system.

2.1 Equilibria and local bifurcations

It is clear that the Lorenz system has three equilibrium points if $\beta(\rho-1)>0$, i.e.,

$$P_1(0,0,0),\ P_2(-\sqrt{\beta(\rho-1)},-\sqrt{\beta(\rho-1)},\rho-1),$$

$$P_3(\sqrt{\beta(\rho-1)},\sqrt{\beta(\rho-1)},\rho-1).$$

Simply use equations (3) and (5) to obtain that the corresponding equilibrium points of the Li system are

$$Q_1(0,0,b/c),\ Q_2(\sqrt{b-c},\sqrt{b-c},1),$$

$$Q_3(-\sqrt{b-c},-\sqrt{b-c},1),$$

when $b-c>0$.

Denote the vector fields on the right-hand sides of (1) and (2) by $\overrightarrow{U}(X,Y,Z)$ and $\overrightarrow{V}(x,y,z)$, respectively. It is clear that the Jacobian of (1) is

$$D\overrightarrow{U}(X,Y,Z)=\begin{pmatrix}-\sigma & \sigma & 0\\ \rho-Z & -1 & -X\\ Y & X & -\beta\end{pmatrix}.$$

Simply use equations (3) and (5) to obtain that the corresponding Jacobian of the system (2) is

$$D\overrightarrow{V}(x,y,z)=\begin{pmatrix}-a & a & 0\\ z & -1 & -x\\ y & x & -c\end{pmatrix}.$$

For $\rho>1$, the origin is unstable. A pitchfork bifurcation of equilibria in the Lorenz system appears for $\beta(\rho-1)=0$, and, consequently, a pitchfork bifurcation in the Li system occurs when $b=c$. The Hopf bifurcation of the nontrivial equilibria occurs in the Lorenz system at

$$\rho=\frac{\sigma(\sigma+\beta+3)}{\sigma-\beta-1}\equiv\rho_h>1,\qquad \sigma-\beta-1>0, \tag{7}$$

using equations (5), that corresponds to the Hopf bifurcation of the nontrivial equilibria in the Li system [15]

$$b_h=\frac{ac(a+c+3)}{a-c-1},\qquad a>c+1.$$

In [15], the following statement appears: "If we fix $c=1$ and vary a and b, we can observe a continuous Hopf bifurcation, as shown in Fig.1. It is similar to that of the Lorenz and Chen systems, all of them have quadratic functions of parameter a". This fact is very easy to obtain in the dynamic of the Lorenz system: if we use equations (5) in the expression (7) with $\beta=1$.

2.2 Invariant algebraic surfaces

Invariant algebraic surfaces in the Lorenz system were discussed in [10–12]. From the invariant algebraic surfaces of the Lorenz system, using equations (3) and (5), the invariant algebraic surfaces of the Li system for $c\neq 0$ are trivially obtained.

The Lorenz system, when $\beta = 2\sigma$, has the invariant algebraic surface

$$X^2 - 2\sigma Z,$$

using equations (3) and (5) we get, when $c = 2a$, the invariant algebraic surface of the Li system is written as

$$2ax^2 + 4a^2 z - 2ab.$$

The Lorenz system, when $\beta = 6\sigma - 2$ and $\rho = 2\sigma - 1$, has the invariant algebraic surface

$$X^4 - 4\sigma X^2 Z - 4\sigma^2 Y^2 + 8\rho\sigma XY + 4\rho^2 X^2,$$

using equations (3) and (5) we get, when $c = 6a - 2$ and $b = 2ac - c$, the invariant algebraic surface of the Li system is written as

$$c^2x^4 + 4ac^2x^2z + \left(4b^2 - 4abc\right)x^2 - 4a^2c^2y^2 + 8abcxy.$$

The Lorenz system, when $\beta = 1$ and $\rho = 0$, has the invariant algebraic surface

$$Y^2 + Z^2,$$

using equations (3) and (5) we get, when $b = 0$ and $c = 1$, the Li system has the invariant algebraic surface

$$y^2 + z^2.$$

The Lorenz system, when $\beta = 4$ and $\sigma = 1$, has the invariant algebraic surface

$$X^4 - 4X^2Z - 4Y^2 - 8XY + 4\rho X^2 - 16\left(1 - \rho\right)Z,$$

using equations (3) and (5) we get, when $c = 4$ and $a = 1$, the Li system has the invariant algebraic surface

$$x^4 + 4x^2z - 4y^2 - 8xy - (4 - b)\left(-4z + b\right).$$

The Lorenz system, when $\beta = 1$ and $\sigma = 1$, has the invariant algebraic surface

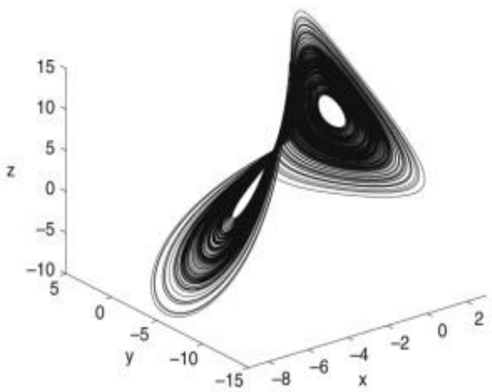

Figure 1: A chaotic attractor that exists in the Li system for $a = 5,\ b = 16,\ c = 1$.

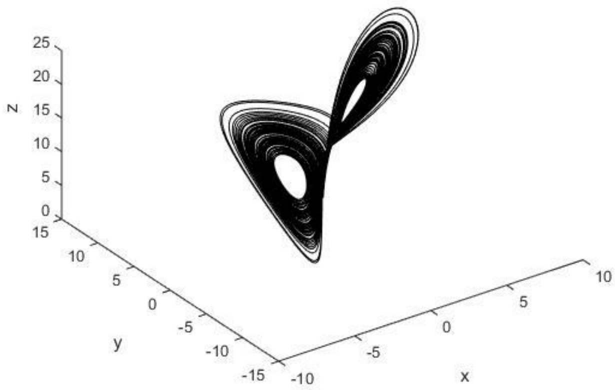

Figure 2: A chaotic attractor that exists in the Lorenz system for $\sigma = 5,\ \rho = 16,\ \beta = 1$.

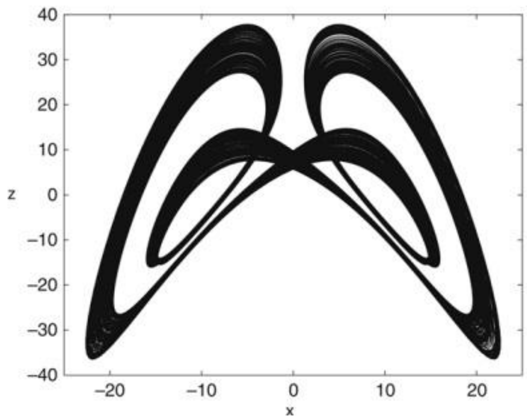

Figure 3: Projections onto two coordinate planes of a chaotic attractor that exists in the Li system for $a = 5,\ b = 115,\ c = 1$.

$$Y^2 + Z^2 - \rho X^2,$$

using equations (3) and (5) we get, when $c = 1$ and $a = 1$, the Li system has the invariant algebraic surface

$$y^2 + z^2 - bx^2 - 2bz + b^2.$$

The case when $\beta = 0$ and $\sigma = \frac{1}{3}$ has no companion case in the Li system, is the case when $c = 0$.

2.3 Chaotic attractors

The celebrated method developed by Tucker to demonstrate the existence of Lorenz's attractor can also be used to prove the existence of Li's attractor. We illustrate now the equivalence between both dynamical systems drawing a chaotic attractor. Thus, in

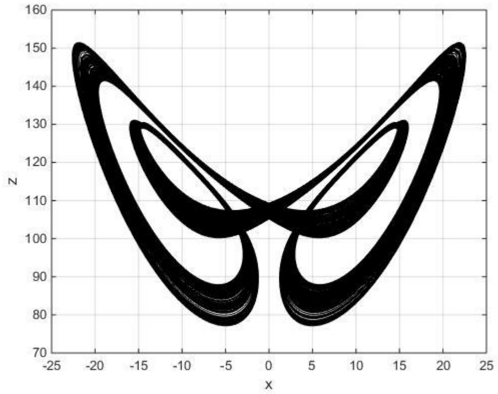

Figure 4: Projections onto two coordinate planes of a chaotic attractor that exists in the Lorenz system for $\sigma = 5,\ \rho = 115,\ \beta = 1$.

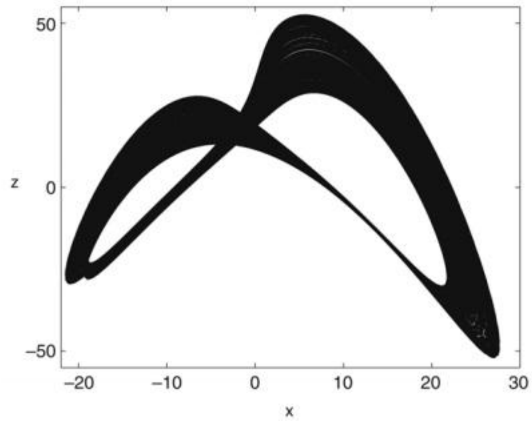

Figure 5: Projections onto two coordinate planes of a chaotic attractor that exists in the Li system for $a = 5,\ b = 167,\ c = 1$.

Figure 1, the chaotic attractor of the Li system is shown for the typical values $a = 5,\ b = 16,\ c = 1$ (Fig.2, [15]), in Figure 2, the companion chaotic attractor is presented that exists in the Lorenz system for $\sigma = 5,\ \rho = 16,\ \beta = 1$.

In Figure 3, we have a projection of the chaotic attractors of the Li system for the parameter values $a = 5,\ b = 115,\ c = 1$ (Fig.4(c), [15]), Figure 4, demonstrates the projections onto two coordinate planes of the companion chaotic attractor that exists in the Lorenz system for the parameter values $\sigma = 5,\ \rho = 16,\ \beta = 1$. In Figure 5, we have a projection of the chaotic attractors of the Li system for the parameter values $a = 5,\ b = 167,\ c = 1$ (Fig.4(h), [15]), Figure 6, displays the projections onto two coordinate planes of the companion chaotic attractor that exists in the Lorenz system for the parameter values $\sigma = 5,\ \rho = 167,\ \beta = 1$.

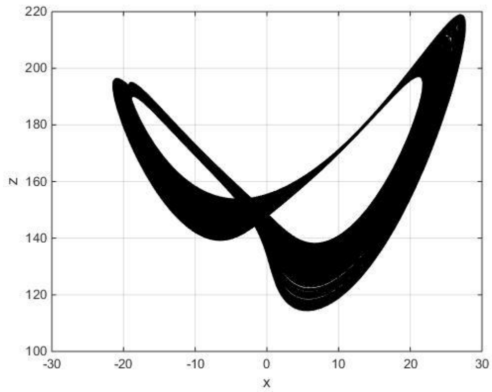

Figure 6: Projections onto two coordinate planes of a chaotic attractor that exists in the Lorenz system for $\sigma = 5,\ \rho = 167,\ \beta = 1$.

3 Conclusion

In conclusion, this study has shown with the help of a coordinate transform that the Li system is only a particular case of the Lorenz system from the dynamical point of view. Therefore, all the dynamical behavior exhibited by the Li system is present in the Lorenz system. From this, we conclude that most results obtained in the previous studies of the Li system (equilibria, bifurcations, periodic orbits, chaotic attractors, etc.) are a duplicate of the corresponding literatures on the Lorenz system.

References

[1] A. Algaba, F. Fernandez-Sanchez, M. Merino and A. J. Rodriguez-Luis. Chen's attractor exists if Lorenz repulsor exists: The Chen system is a special case of the Lorenz system. *Chaos* **23** (2013) 033108.

[2] A. Algaba, F. Fernandez-Sanchez, M. Merino and A. J. Rodriguez-Luis. The Lü system is a particular case of the Lorenz system. *Phys. Lett. A.* **377** (2013) 2771–2776.

[3] G.A. Leonov and N.V. Kuznetsov. On differences and similarities in the analysis of Lorenz, Chen, and Lü systems. *Applied Mathematics and Computation* **256** (2015) 334–343.

[4] G. Leonov. Criteria for the existence of homoclinic orbits of systems Lü and Chen. *Doklady Mathematics* **87** (2013) 220–223.

[5] J. Lü, G. Chen, D. Cheng and S. Celikovsky. Bridge the gap between the Lorenz system and the Chen system. *Int. J. Bifurcation and Chaos* **12** (2002) 2917–2926.

[6] Y. Chen and Q. Yang. The nonequivalence and dimension formula for attractos of Lorenz-type systems. *Int. J. Bifurcation and Chaos* **23** (2013) 1250200.

[7] Z. Hou, N. Kang, X. Kong, G. Chen and G. Yan. On the nonequivalence of Lorenz system and Chen system. *Int. J. Bifurcation and Chaos* **20** (2010) 557–560.

[8] L. Meddour and E. Zeraoulia. About the threedimensional quadratic autonomous system with two quadratic terms equivalent to the Lorenz system. Dyn. Contin. *Discrte Impuls. Syst. B.* **27** (2020) 133–143.

[9] E. N. Lorenz. Deterministic nonperiodic flow. *J. Atmos. Sci.* **20** (1963) 130–141.

[10] M. Kus. Integrals of motion for the Lorenz system. *J. Phys. A.* **16** (1983) L689–L691.

[11] J. Llibre and X. Zhang. Invariant algebraic surfaces of the Lorenz system. *J. Math. Phys.* **43** (2002) 1622–1645.

[12] J. Llibre, M. Messias and P.R. da Silva. Global dynamics of the Lorenz system with invariant algebraic surfaces. *Int. J. Bifurcation Chaos* **20** (2010) 3137–3155.

[13] G. Chen and T. Ueta. Yet another chaotic attractor. *Int. J. Bifurcation and Chaos* **9** (1999) 1465–1466.

[14] J. Lü, G. Chen. A new chaotic attractor coined. *Int. J. Bifurcation Chaos* **12** (2002) 659–661.

[15] X.F. Li, K.E. Chlouverakis and D.L. Xu. Nonlinear dynamics and circuit realization of a new chaotic flow: A variant of Lorenz, Chen and Lü. *Nonlinear Analysis* **10** (2009) 2357-2358.

[16] F. Hannachi. Adaptive Sliding Mode Control Synchronization of a Novel, Highly Chaotic 3-D System with Two Exponential Nonlinearities. *Nonlinear Dynamics and Systems Theory* **20** (1) (2020) 38–50.

[17] N. Djafri, T. Hamaizia and F. Derouiche. Boundedness and Dynamics of a Modified Discrete Chaotic System with Rational Fraction. *Nonlinear Dynamics and Systems Theory* **21** (1) (2021) 68–75.

[18] S. Rezzag. On the Boundedness of a Novel Four-Dimensional Hyperchaotic System. *Nonlinear Dynamics and Systems Theory* **20** (1) (2020) 72–77.

[19] I. Pehlivan and Y. Uyaroğlu. A new chaotic attractor from general Lorenz system family and its electronic experimental implementation. *Turkish Journal of Electrical Engineering and Computer Sciences* **18** (2010) 171–184.

[20] D. Wenju, Z. Jiangang and Q. Shuang. Bifurcation analysis in an autonomous chaotic system. *Information Technology, Networking, Electronic and Automation Control Conference* (2016) 1-5.

[21] F. Zhang, X. Liao, G. Zhang and C. Mu. Complex dynamics of a new 3D Lorenz-type autonomous chaotic system. *Pramana - J. Phys.* **89** (2017) 84.

[22] S. Vaidyanathan and K. Rajagopal. Anti-Synchronization of Tigan and Li Systems with Unknown Parameters via Adaptive Control. *An International Journal of Optimization and Control: Theories & Applications* **2** (2012) 17–28.

Nonlinear Dynamics and Systems Theory, **22** (1) (2022) 66–81

Similarities between the Lorenz Related Systems

C. Morel [1]*, R. C. Vlad [2] and J.-Y. Morel [3]

[1] *Aeronautical and Automobile Engineering School, ESTACA'Lab Paris Saclay, France.*
[2] *Technical University of Cluj-Napoca, 103-105 Bd. Muncii, 400641 Cluj-Napoca, Romanie.*
[3] *University of Angers, 4 Bd. Lavoisier, 49100 Angers, France.*

Received: July 9, 2021;   Revised: December 5, 2021

Abstract: In this paper, the dynamic behaviour of all the Lorenz related systems is examined in a previously unexplored region of parameter space. The Lorenz, hidden chaotic, Chen and broken butterfly attractors can be generated at any desired size, with different equilibria. We focus on the attractors smaller or larger than the original one, we call them *mini* and *maxi*, and study their global dynamic behaviour to demonstrate that they are similar or equivalent to the original chaotic attractor. We finally examine their phase portraits, bifurcation diagrams, the largest Lyapunov exponents and their multiscale entropy MSE_{1D}. The analysis results show that the mini, original and maxi Lorenz related attractors have the same MSE_{1D} values and are independent of the scale factor. We can conclude that the MSE_{1D} analysis can be used successfully to quantify the complexity of the dynamic response.

Keywords: *attractors; bifucation; equilibria; Lyapunov; entropy.*

Mathematics Subject Classification (2010): 37M22, 65P30, 70K42, 93D05, 94A17.

1 Introduction

Since the Lorenz system was discovered, chaos and many phenomena in nonlinear dynamic systems have been developed and studied. This allowed to explore more chaotic systems and to discover new chaotic systems with a more complex dynamic behaviour. Chen and Lü [1] found a similar but not equivalent chaotic attractor, the dual of the Lorenz system. After that, Lü [2] reported a new chaotic system which is the transition between the Lorenz and Chen systems. [3] presented a comparative analysis of the Lorenz and Chen systems in order to understand better what distinguishes them. It is

* Corresponding author: mailto:cristina.morel@estaca.fr

notable that for certain values of the parameters, the classical Lorenz butterfly attractor is broken into a symmetric pair of strange attractors [4].

Several complex dynamic systems, called multistable systems, are characterized by the existence of many coexisting attractors. In this kind of systems, the trajectory will eventually end in an attractor strongly influenced by the initial conditions. [5] introduced a new category of chaotic systems with a line of equilibria. The basin of attraction may intersect with the line of equilibria, in some sections. There are many examples of chaotic systems with no equilibrium [6], one stable equilibrium [7], a single unstable equilibrium [8], many equilibria, a line equilibrium [5], a surfaces of equilibria [9].

Most of the known chaotic attractors (like the Lorenz, Chua or Van der Pol ones) are located in the neighbourhood of unstable fixed points. Such attractors are called self-excited and their basins of attraction touch unstable equilibrium. The transient trajectory of the attractor starts in the neighbourhood of this unstable equilibrium, oscillates around and then traces it. The concept of hidden attractors has been suggested by the discovery of unexpected attractor in Chua's circuit. Recently, it has been shown that multistability is connected with the occurrence of hidden attractors. In multistable systems, particularly in the case of the existence of attractors with very small basins like in [9], the switching from one attractor to another unexpected attractor can be observed. Hidden attractors are important in engineering applications [10] because many physical structures can have disastrous responses to perturbations, as the crash of aircraft YF-22 Boeing in 1992. Other applications of chaos theory such as synchronization [11], [12] and chaos control of hyperchaotic financial model have become topics for research.

The Chen system, butterfly attractor broken into a symmetric pair and hidden attractor are named the Lorenz related systems because they are derived from the Lorenz system. We introduce a parameter γ in (2) describing these systems and study the influence of a variation of γ on the occurrence of such chaotic attractors and on their size. In this paper, we find that the chaotic attractors occurred are mini and maxi attractors. By changing the parameter γ, all the quantitative properties of the Chen, Lorenz, hidden and broken butterfly attractors are preserved. This is why, the Lorenz related systems are essentially the one-parameter systems.

The irregularity of time series can be studied through several measures, e.g., sample entropy ($SampEn_{1D}$), which improves the understanding of the nonlinear behaviour of complex systems. $SampEn_{1D}$ is the measure of the degree of irregularity and disorder of finite length time series; it evaluates the probability of finding similar patterns. $SampEn_{1D}$ is precisely the negative natural logarithm of the conditional probability that two sequences similar for m points remain similar at the next point, where self-matches are not included in the computation of the probability [13]. A lower value of $SampEn_{1D}$ indicates many similarities in time-series. However, $SampEn_{1D}$ is not adapted for structures at the multiple time scale. This is why the multiscale entropy MSE_{1D} has been proposed to extend the computation of $SampEn_{1D}$ over a range of time scales. The concept of multi-scale entropy is used to characterize the complexity of different research fields [14]. Serving as a quantification parameter, MSE_{1D} is based on the coarse-graining procedure that uses a coarse-grained time series, as an average of the original data points within not overlapping windows by increasing the scale factor τ.

In this paper, the dynamic behaviour of the Lorenz related systems is examined in a previously unexplored region of parameter space. By simulation, the attractors can be generated at different equilibria in the function of γ. Furthermore, the generated attractors (smaller than the original attractor called *mini* and bigger called *maxi*) are similar to it but are not identical because of their chaotic behaviour. According to the Jacobian matrix of the nonlinear system, the local stability of the generated attractors is studied. In order to study the global dynamic behaviour, firstly, bifurcation diagrams and Lyapunov exponents are used to investigate the presence of chaos in the Chen system. The simulations reveal the same value of the largest Lyapunov exponent of the attractor's size. Secondly, multiscale entropy MSE_{1D} is proposed to evaluate the complexity of these mini, original and maxi chaotic attractors. MSE_{1D} is applied to different time series of the chaotic attractors to determine their irregularity over a range of temporal scales. The results show that the mini, original and maxi chaotic attractors have the same irregularity values for all time scales (i.e., the same complexity of the time series). More precisely, all the quantitative properties are preserved.

2 The Lorenz Related Systems

The Lorenz related systems are described by the following set of differential equations:

$$\begin{cases} \dot{x} = \sigma(y - x), \\ \dot{y} = \rho x - \alpha y - xz, \\ \dot{z} = xy - \beta z. \end{cases} \tag{1}$$

Lorenz found the first canonical chaotic attractor in a three-dimensional autonomous system. The usual values of the classical Lorenz system parameters are $\sigma = 10$, $\rho = 28$, $\alpha = 1$, $\beta = 8/3$; this produces a chaotic attractor with a butterfly shape. Then, a similar looking but nonequivalent chaotic attractor was found out, which is the dual of the Lorenz system. Moreover, both attractors occur for different values of the parameters ($\sigma = 35$, $\rho = -7$, $\alpha = -28$, $\beta = 3$). The work of Lü [2] introduced a unified chaotic system (Lü system) which bridges the gap between the Lorenz system and the Chen system. A hidden chaotic attractor was illustrated in the classical Lorenz system depending on the values of both system parameters and initial conditions ($\sigma = 4$, $\rho = 29$, $\alpha = 1$, $\beta = 2$). For some values of the parameters ($\sigma = 0.12$, $\rho = 0$, $\alpha = 1$, $\beta = -0.6$), Li and Sprott [4] broke the classical butterfly attractor into a symmetric pair of strange attractors. In this paper, we introduce the parameter γ in (1)

$$\begin{cases} \dot{x} = \sigma(y - x), \\ \dot{y} = \rho x - \alpha y - \gamma xz, \\ \dot{z} = xy - \beta z. \end{cases} \tag{2}$$

Special sides of the system (2) are then pointed out: the attractor's size depends on the variation of the parameter γ in system (2). $\gamma \in (0,1)$ leads to a chaotic attractor (called maxi) with a larger size than the original chaotic attractor of system (1) (i.e., for $\gamma = 1$). Similarly, $\gamma > 1$ leads to a chaotic attractor (called mini) with a smaller size than the chaotic attractor of (1).

3 MSE_{1D} Algorithm

Complexity measures are important to understand and analyze systems with one dimensional data. One of the most well-known complexity measures is the multiscale sample entropy MSE_{1D}. For the time series, the computation of MSE_{1D} is defined as the following two steps:

– The first step is the coarse-graining (average) procedure, which consists in deriving a set of time series of the system dynamics on different time scales. Given a discrete time series of the form $\mathbf{x} = \{x_1, x_2, \ldots, x_i, \ldots, x_N\}$, the coarse-grained time series $\{\mathbf{y}^{(\tau)}\}$, at the scale τ, is

$$y_j^{(\tau)} = \frac{1}{\tau} \sum_{i=(j-1)\tau+1}^{i\tau} x_i, \tag{3}$$

where $1 \leq j \leq \lfloor N/\tau \rfloor$ and τ is the scale factor. If the scale factor τ is equal to one, the coarse-grained time series $\mathbf{y}^{(1)}$ corresponds to the original time series $\mathbf{x}$.

– The second step computes the sample entropy for each coarse-grained time series as the negative of the natural logarithm of the conditional probability that the sequences for m consecutive data points remain close to each other when one more point is added to each sequence $SampEn_{1D}(\mathbf{x}, m, r) = -\ln \frac{A^m(r)}{B^m(r)}$, where $A^m(r)$ is the probability that two sequences will match for $m+1$ points, whereas $B^m(r)$ is the probability that two sequences will match for m points. They are computed as

$$A^m(r) = \frac{1}{N-m} \sum_{i=1}^{N-m} A_i^m(r) \quad \text{and} \quad B^m(r) = \frac{1}{N-m} \sum_{i=1}^{N-m} B_i^m(r). \tag{4}$$

$A_i^m(r)$ is $\frac{1}{N-m-1}$ times the number of vectors $\mathbf{x}_{m+1}(j)$ within r of $\mathbf{x}_{m+1}(i)$, where j goes from 1 to $N-m$ and $j \neq i$ to exclude self-matches. $B_i^m(r)$ is $\frac{1}{N-m-1}$ times the number of vectors $\mathbf{x}_m(j)$ within r of $\mathbf{x}_m(i)$, where j goes from 1 to $N-m$ and $j \neq i$ for the same reason as above. The distance d between two vectors is defined as the maximum absolute difference of their corresponding scalar components. MSE_{1D} can be written as $MSE_{1D}(x, \tau, m, r) = -\ln \frac{A_\tau^m(r)}{B_\tau^m(r)}$, where $A_\tau^m(r)$ and $B_\tau^m(r)$ are calculated from the coarse-grained time series at the scale factor τ.

4 Equilibria and Stability

The system equilibria (2) can be found by solving the equations $\dot{x} = \dot{y} = \dot{z} = 0$. This leads to

$$\begin{cases} x - y = 0, \\ \rho x - \alpha y - \gamma xz = 0, \\ xy - \beta z = 0. \end{cases} \tag{5}$$

The first equation of the system (5) yields immediately $x = y$, so that the third one gives $z = x^2/\beta$. Therefore, the second equation leads to $z = (\rho - \alpha)/\gamma$. There are three equilibria: $X_0 = (0, 0, 0)$,

$$X_+^* = \left(+\sqrt{\frac{(\rho-\alpha)\beta}{\gamma}}, +\sqrt{\frac{(\rho-\alpha)\beta}{\gamma}}, \frac{\rho-\alpha}{\gamma} \right), \tag{6}$$

$$X_-^* = \left(-\sqrt{\frac{(\rho-\alpha)\beta}{\gamma}}, -\sqrt{\frac{(\rho-\alpha)\beta}{\gamma}}, \frac{\rho-\alpha}{\gamma} \right). \tag{7}$$

The three equilibrium points are indicated in Table 1, Table 2 and Table 3. The equilibrium points X^* depend on γ. For a variation of this parameter γ, they take place in the plane $x = y$ and on the precise curve $z = x^2/\beta$ at $(\rho - \alpha)/\gamma$.

	Classical Lorenz at. (10, 28, 1, 8/3)	Hidden attractor (4, 29, 1, 2)	Broken attractor (0.12, 0, 1, -0.6)	Chen attractor (35, -7, -28, 3)
X_0	(0, 0, 0)	(0, 0, 0)	(0, 0, 0)	(0, 0, 0)
X_+^*	(8.48, 8.48, 27)	(7.48, 7.48, 28)	(0.77, 0.77, -1)	(7.94, 7.94, 21)
X_-^*	(-8.48, -8.48, 27)	(-7.48, -7.48, 28)	(-0.77, -0.77, -1)	(-7.94, -7.94, 21)

Table 1: Three equilibrium points of the Lorenz related systems (σ, ρ, α, β, $\gamma = 1$).

	Classical Lorenz at. (10, 28, 1, 8/3)	Hidden attractor (4, 29, 1, 2)	Broken attractor (0.12, 0, 1, -0.6)	Chen attractor (35, -7, -28, 3)
X_0	(0, 0, 0)	(0, 0, 0)	(0, 0, 0)	(0, 0, 0)
X_+^*	(4.24, 4.24, 6.75)	(3.74, 3.74, 7)	(0.4, 0.4, -0.25)	(3.97, 3.97, 5.2)
X_-^*	(-4.24, -4.24, 6.75)	(-3.74, -3.74, 7)	(-0.4, -0.4, -0.25)	(-3.97, -3.97, 5.2)

Table 2: Three equilibrium points of the Lorenz related systems (σ, ρ, α, β, $\gamma = 4$).

	Classical Lorenz at. (10, 28, 1, 8/3)	Hidden attractor (4, 29, 1, 2)	Broken attractor (0.12, 0, 1, -0.6)	Chen attractor (35, -7, -28, 3)
X_0	(0, 0, 0)	(0, 0, 0)	(0, 0, 0)	(0, 0, 0)
X_+^*	(13.4, 13.4, 67.5)	(11.8, 11.8, 70)	(1.2, 1.2, -2.5)	(12.5, 12.5, 52.5)
X_-^*	(-13.4, -13.4, 67.5)	(-11.8, -11.8, 70)	(-1.2, -1.2, -2.5)	(-12.5, -12.5, 52.5)

Table 3: Three equilibrium points of the Lorenz related systems (σ, ρ, α, β, $\gamma = 0.4$).

	Classical Lorenz at. (10, 28, 1, 8/3, 1)	Hidden attractor (4, 29, 1, 2, 1)	Broken attractor (0.12, 0, 1, -0.6, 1)	Chen attractor (35, -7, -28, 3, 1)
λ_1	-8/3	-2	0.6	-3
λ_2	1.4462	8.3743	-0.12	23.836
λ_3	-12.4462	-13.3743	-1	-30.835

Table 4: Three eigenvalues of the Lorenz related systems (σ, ρ, α, β, γ) for X_0.

Linearizing (1) around X_0 provides an eigenvalue $\lambda_1 = -\beta$ along with the following characteristic equation: $\lambda^2 + (\alpha + \sigma) \cdot \lambda + \sigma \cdot (\alpha - \rho) = 0$. The two eigenvalues of this equation are indicated in Table 4, for the usual values of σ, ρ, α, β, γ. At the equilibrium point X_0, there are one positive real eigenvalue and two negative real eigenvalues. X_0 is therefore an unstable saddle point for the classical Lorenz, hidden, Chen and broken attractors. In order to study the stability of X^*, the Jacobian J_{X^*} is computed:

$$J_{X^*} = \begin{bmatrix} -\sigma & \sigma & 0 \\ \rho - \gamma z^* & -\alpha & -\gamma x^* \\ y^* & x^* & -\beta \end{bmatrix}. \tag{8}$$

Linearizing (1) around X^* yields the following characteristic equation:

$$\lambda I - J_{X^*} = \begin{bmatrix} \lambda+\sigma & -\sigma & 0 \\ -\alpha & \lambda+\alpha & \pm\sqrt{(\rho-\alpha)\beta\gamma} \\ \mp\sqrt{\frac{(\rho-\alpha)\beta}{\gamma}} & \mp\sqrt{\frac{(\rho-\alpha)\beta}{\gamma}} & \lambda+\beta \end{bmatrix} \tag{9}$$

with the characteristic polynomial $P(\lambda) = \lambda^3+(\alpha+\beta+\sigma)\lambda^2+(\rho+\sigma)\beta\lambda+2\beta\sigma(\rho-\alpha)$. This characteristic polynomial is equivalent to $P(\lambda) = \lambda^3+A\lambda^2+B\lambda+C$, where $A = \alpha+\beta+\sigma$, $B = (\rho+\sigma)\beta$, $C = 2\beta\sigma(\rho-\alpha)$. The exact values of the eigenvalues λ_1, λ_2, λ_3 can be determined by setting $\lambda = -A/3+\Lambda$. This yields $P(\Lambda) = \Lambda^3+p\Lambda+q$, where $p = -A^2/3+B$ and $q = (2A^3/27)-(AB/3)+C$. This third order polynomial in Λ can be solved using Cardan's formula, thus giving the unique real eigenvalue

$$\lambda_1 = -\frac{A}{3}+\Lambda_R = -\frac{A}{3}+\left(-\frac{q}{2}+\sqrt{\frac{q^2}{4}+\frac{p^3}{27}}\right)^{1/3}+\left(-\frac{q}{2}-\sqrt{\frac{q^2}{4}+\frac{p^3}{27}}\right)^{1/3}, \tag{10}$$

along with two complex conjugate eigenvalues

$$\lambda_{2,3} = -\frac{A}{3}-\frac{\Lambda_R}{2}\pm\frac{i}{2}\sqrt{4p+3(\Lambda_R)^2}. \tag{11}$$

The three eigenvalues of equilibrium points X^* of the classical Lorenz, Chen and broken attractors are indicated in Table 5. Since the pair of complex conjugate eigenvalues has a positive real part, the equilibrium points $X^*_\pm$ are unstable. For the equilibrium points $X^*_\pm$ of the hidden attractor, λ_1 is real and $\lambda_{2,3}$ are complex conjugates, all with negative real parts. Therefore, the equilibrium points $X^*_\pm$ are stable focus-node points.

	Classical Lorenz at. (10, 28, 1, 8/3, 1)	Hidden attractor (4, 29, 1, 2, 1)	Broken attractor (0.12, 0, 1, -0.6, 1)	Chen attractor (35, -7, -28, 3, 1)
λ_1	-13.8546	-6.8764	-0.8212	-18.4280
λ_2	$0.094+i\cdot 10.19$	$-0.062+i\cdot 8.07$	$0.1506+i\cdot 0.39$	$4.214+i\cdot 14.88$
λ_3	$0.094-i\cdot 10.19$	$-0.062-i\cdot 8.07$	$0.1506-i\cdot 0.39$	$4.214-i\cdot 14.88$

Table 5: Three eigenvalues of the Lorenz related systems (σ, ρ, α, β, γ) for $X^*_\pm$.

5 Numerical Simulations

5.1 One-parameter Lorenz related systems

Let study the Lorenz related systems, described by (2), where σ, ρ, α, β, γ are real parameters. Typically, when $\sigma = 10$, $\rho = 28$, $\alpha = 1$; $\beta = 8/3$ and $\gamma = 1$, the system is chaotic. Figure 1(a) is a graphical representation of the unique attractor on the $x-y$ plane using the *Matlab plot*(x, y) function. The magnitudes of x, y and z are $x_m = \max(x)-\min(x)$, $y_m = \max(y)-\min(y)$, $z_m = \max(z)-\min(z)$. Now, let us consider the following transformation of variables:

$$\bar{x} = \frac{x}{k}, \qquad \bar{y} = \frac{y}{k}, \qquad \bar{z} = \frac{z}{k}. \tag{12}$$

The Lorenz related system (2) can be reformulated via (12) as

$$\begin{cases} \dot{\bar{x}} = \sigma(\bar{y} - \bar{x}), \\ \dot{\bar{y}} = \rho\bar{x} - \alpha\bar{y} - (k\gamma)\bar{x}\bar{z}, \\ \dot{\bar{z}} = k\bar{x}\bar{y} - \beta\bar{z}. \end{cases} \tag{13}$$

After redefining x, y and z, the resulting system is identical to (2), but with the first term of the third equation multiplied by k. The Lorenz attractor is represented in Figure 1(b) on the $x-y$ plane with $\gamma = 1$, $k = 0.4$ ($Matlab$ $plot(\bar{x}, \bar{y})$). It can be observed that the $x-y$ representations of the systems (2) and (13) differ only by a scale factor. Furthermore, there is no scale difference with $plot(k\bar{x}, k\bar{y})$: the representation of the Lorenz attractor on $x-y$ is also identical (visual aspect and scale). Let us take again the system (2), where γ takes the value k. The unique attractor is represented graphically in Figure 1(c) on the $x-y$ plane using $plot(x, y)$. The magnitudes of x, y and z are

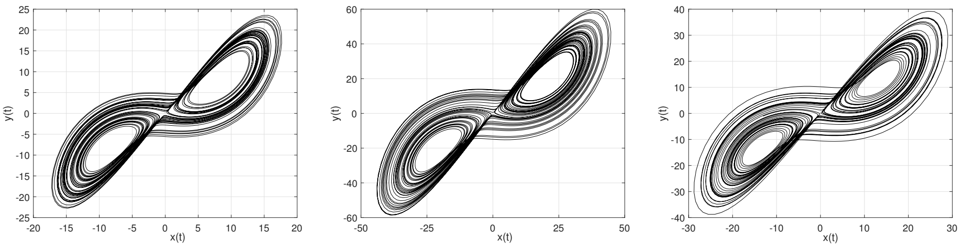

(a) (b) (c)

Figure 1: The Lorenz attractor of system (2) with $\sigma = 10$, $\rho = 28$, $\alpha = 1$, $\beta = 8/3$. (a) $\gamma = 1$, (b) $\gamma = 1$ and $k = 0.4$, (c) $\gamma = 0.4$.

$x_{m2} = \max(x) - \min(x)$, $y_{m2} = \max(y) - \min(y)$, $z_{m2} = \max(z) - \min(z)$. The $x-y$ representation of system (2) with $\gamma = 1$ and $\gamma = 0.4$ is identical, except for a scale factor. If the variables x, y and z are multiplied by x_m, y_m and z_m and divided by x_{m2}, y_{m2} and z_{m2} with $plot(x \cdot x_m/x_{m2}, y \cdot y_m/y_{m2})$, there is no more a scale difference. The two representations of the Lorenz attractor on $x-y$ and $y-z$ are also identical (visual aspect and scale).

5.2 Lorenz attractors

Figure 2(a) shows the original Lorenz attractor (grey) on the space $x-y-z$ with the initial conditions (x_0, x_0, $3 * x_0 * x_0/8$) = (1,1,3/8) and $\gamma = 1$. The result is the self-excited chaotic attractor. With a variation of γ, a mini and a maxi self-excited chaotic attractors appear in a similar manner as the well-known Lorenz attractor, but their sizes are different (Figure 2(a)). For $\gamma \in(0,1)$, a maxi self-excited chaotic red attractor is generated and if $\gamma > 1$, a mini self-excited chaotic blue attractor is generated. All three attractors, mini, original and maxi self-excited chaotic attractors, have two unstable equilibria X^* on the green curve $z = x^2/\beta$. With the parameter γ, the height of the attractors is selected on this curve, as well as their size. The positive Lyapunov exponent in Table 6 for the mini and maxi self-excited chaotic attractors confirms their chaoticity. The mini and maxi chaotic attractors have different sizes and their magnitudes depend on the parameter γ. The mini and maxi chaotic attractors are not identical with the original chaotic attractor because their chaotic behaviour differs. In order to prove the similarity and the equivalence with the original chaotic attractor, the use of multiscale entropy MSE_{1D} is proposed. Additionally, MSE_{1D} is sensitive to signal amplitude changes. A common practice to address this issue is to normalize the signal amplitude. The time series $\mathbf{x}(t)$ is rescaled along the signal amplitude axis with a factor, thus normalising the magnitude of the mini and maxi Lorenz attractors to the original Lorenz attractor. MSE_{1D} is applied to different time series of the chaotic attractors to determine their entropy over a range of temporal scales from 1 to 20. The results show (Figure 2(b)) that the MSE_{1D} increases with the variation of the scale factor for the mini, original and maxi chaotic attractors and that they have the same MSE_{1D} value. This indicates that the complexity of these attractors is at the same level.

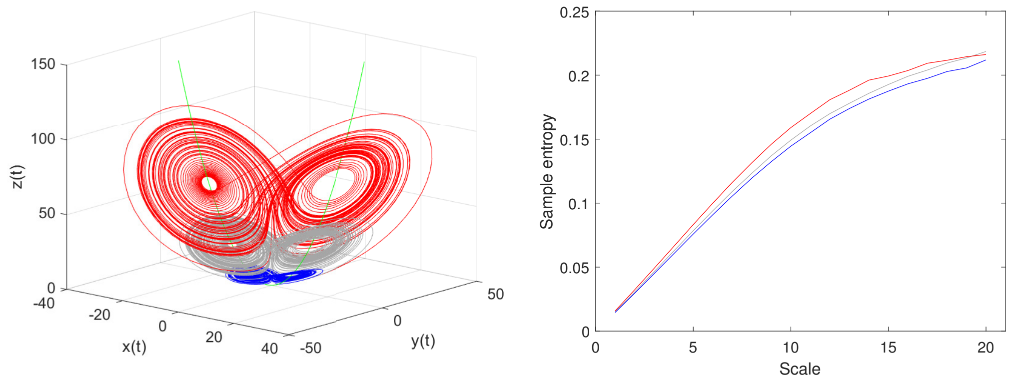

(a) Projection of phase portrait on space $x-y-z$. (b) MSE_{1D}.

Figure 2: (a) The mini ($\gamma = 4$, blue), original ($\gamma = 1$, gray) and maxi ($\gamma = 0.4$, red) Lorenz attractors with $\sigma = 10$, $\rho = 28$, $\alpha = 1$, $\beta = 8/3$; (b) MSE_{1D} of the time series of Lorenz attractors for different scales.

	Classical Lorenz at. (10, 28, 1, 8/3)	Hidden attractor (4, 29, 1, 2)	Broken attractor (0.12, 0, 1, -0.6)	Chen attractor (35, -7, -28, 3)
$\gamma = 0.4$	0.8878 0.0029 -14.5538	0.6537 0.0001 -7.6539	0.0497 0.0009 -0.57064	2.0499 0.0078 -12.0535
$\gamma = 1$	0.8904 0.0018 -14.555	0.6516 0.0005 -7.6522	0.037 -0.0025 -0.5545	2.0684 0.0015 -12.0657
$\gamma = 4$	0.8835 -0.00498 -14.5513	0.6691 0.00004 -7.6691	0.0548 0.0005 -0.668	2.0243 0.0002 -12.021

Table 6: The Lyapunov exponents of the Lorenz related systems (σ, ρ, α, β).

5.3 Hidden chaotic attractors

Figure 3(a) illustrates a hidden chaotic attractor in grey on the space $x-y-z$ using the initial conditions (x_0, y_0, z_0) = (5,5,5) and $\gamma = 1$. This attractor has the equilibria X^*

on the green curve $z = x^2/\beta$. As in the previous case, the variation of γ can generate a mini and a maxi hidden chaotic attractors. For $\gamma \in(0,1)$, a maxi hidden chaotic attractor is generated and if $\gamma > 1$, a mini hidden chaotic attractor is generated. The mini and maxi hidden attractors can be generated at any height on the z axis in the function of γ. As the parameter γ varies, an attractor appears with a periodic motion around the stable equilibrium points X^*. In this case, the rise of γ is accompanied by transformations of the attractors'size. The higher γ, the smaller the attractor (Figure 5). As we can see in Table 6, the Lyapunov exponents of the mini and maxi hidden chaotic attractors are positive. MSE_{1D} is now applied to different time series of the hidden chaotic attractor

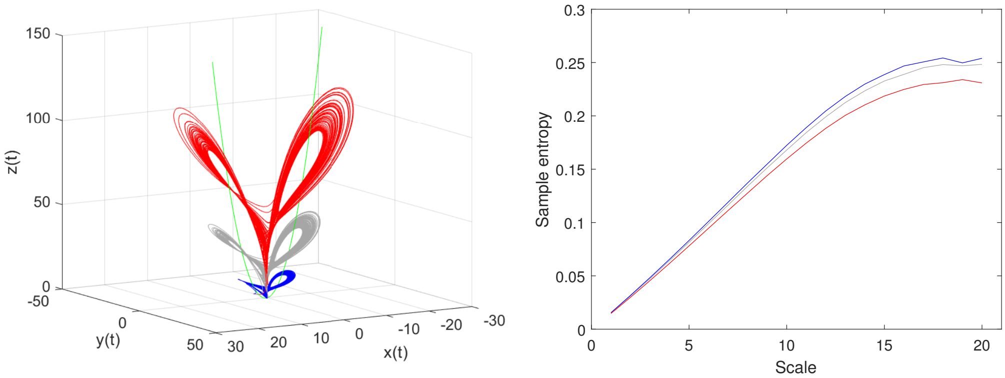

(a) Projection of phase portrait on space $x - y - z$. (b) MSE_{1D}.

Figure 3: (a) The mini ($\gamma = 4$, blue), original ($\gamma = 1$, gray) and maxi ($\gamma = 0.4$, red) hidden chaotic attractors with $\sigma = 4$, $\rho = 29$, $\alpha = 1$, $\beta = 2$, with (x_0, y_0, z_0) = (5,5,5); (b) MSE_{1D} of the time series of hidden chaotic attractors for different scales τ.

and of the one point attractor to qualify entropy over a range of temporal scales for $\tau =$ 1 to 20. The mini, original and maxi chaotic attractors have the same MSE_{1D} values for the small time scales (Figure 3(b)); very small differences appear for the large time scales. MSE_{1D} values of the mini, original and maxi one point attractors are identical at the begining of the scale, and with small differences in the end of the scale, as in Figure 3(b). The complexity of the chaotic sequences tends to be uniform, independently of γ.

5.4 Broken butterfly attractors

Figure 4(a) illustrates the broken butterfly attractors in grey on the space $x-y$, where two strange attractors coexist ((x_0, y_0, z_0) = (-0.8,3,0), (x_0, y_0, z_0) = (0.8,-3,0) and $\gamma = 1$). Starting from the same initial conditions, for $\gamma = 0.4$, two strange maxi broken butterfly chaotic attractors are generated. If $\gamma = 4$, two other strange mini broken butterfly chaotic attractors are also generated. The positive Lyapunov exponents of the mini and maxi self-excited chaotic butterfly attractors confirm their chaoticity. The magnitudes of the broken butterfly chaotic attractors of the mini ($\gamma = 4$), original ($\gamma = 1$) and maxi ($\gamma =$ 0.4) are different: they vary from 1 for the mini broken butterfly attractor to 4 for the maxi broken butterfly attractor on the x-axis. The irregularity values MSE_{1D} of the three broken butterfly attractors are identical for the small time scales, while very small differences appear for the large time scales, as shown in Figure 4(b).

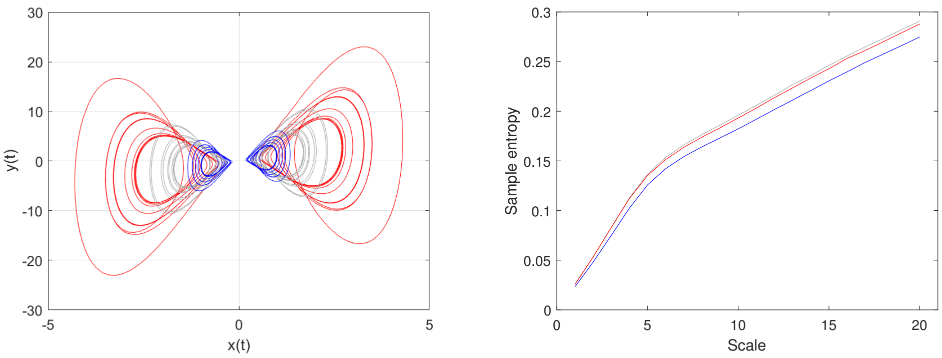

(a) Coexisting strange attractors on the $x-y$ plane for γ = 0.4, 1, 4 and two symmetric initial conditions ($\mp$0.8, $\pm$3, 0).

(b) MSE_{1D} of the time series of broken attractors for different scales τ.

Figure 4: Broken attractors with σ = 0.12, ρ = 0, α = 1, β = -0.6.

5.5 Chen chaotic attractors

Figure 5(b) illustrates the Chen attractor in grey on tri-dimensional space with γ = 1. For γ = 0.4, a maxi Chen red attractor is generated (Figure 5(a)) and if γ = 4, a mini Chen blue attractor is generated (Figure 5(c)). A graphical comparison is given in Figures 5(a), (b), (c), where the maxi, original and mini Chen attractors are represented on the $y-z$ plane. The mini and maxi Chen attractors are visually similar to the original Chen attractor (Figure 5(b)), but not identical. The chaotic behaviour of all attractors is proved by the positive Lyapunov exponents in Table 6.

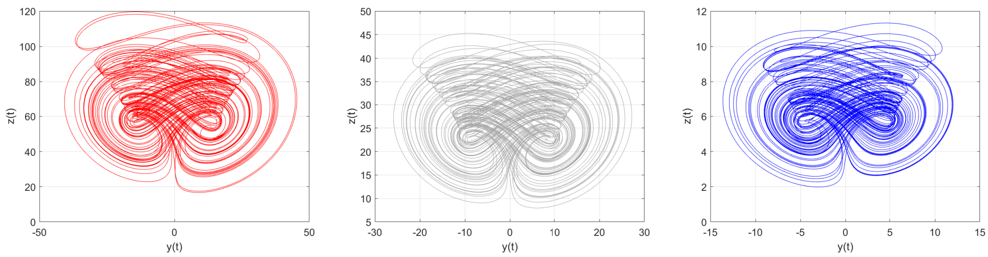

(a) Maxi attractor γ = 0.4. (b) Original attractor γ = 1. (c) Mini attractor γ = 4.

Figure 5: The Chen chaotic attractor for σ = 4, ρ = 29, α = 1, β = 2 with (x_0, y_0, z_0) = (0.1, 0, 0).

As shown in Figures 5(c), (b), (a), the magnitudes of the Chen attractors of the mini (γ = 4), original (γ = 1) and maxi (γ = 0.4) attractors are different. The magnitude of the original attractor is 40 (Figure 6 (a)), but for the mini and maxi attractors, the magnitudes are 10 and 100, respectively. The multiscale entropy MSE_{1D} is employed to quantify the complexity of the time series of mini and maxi Chen attractors over the same scales for τ = 1 to 20 with the original Chen attractor: the mini, original and maxi chaotic attractors have the same MSE_{1D} (Figure 6(b)).

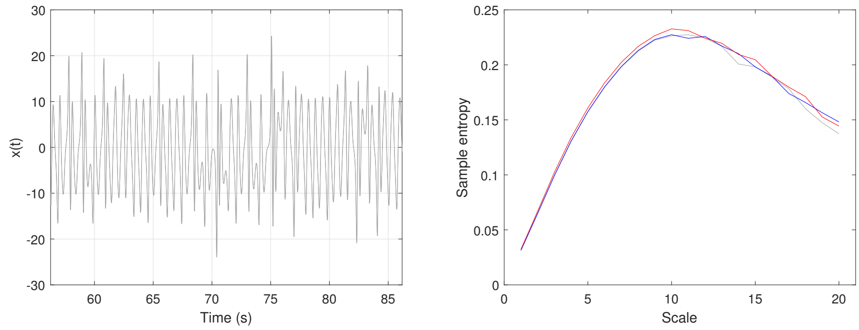

(a) Time series of $x(t)$ for $\gamma = 1$.

(b) MSE_{1D} of the time series of the Chen attractors for different scales.

Figure 6: The Chen attractors with the parameters $\sigma = 35$, $\rho = -7$, $\alpha = -28$, $\beta = 3$.

6 Bifurcation Diagrams, Lyapunov Exponents and Multiscale Entropy MSE_{1D} Analysis of Chen Attractors

In the previous section, three chaotic Chen attractors were presented for a unique value of the parameter $\beta = 3$. In this section, we are interested in the dynamic behaviour of Chen system for a large variation of this parameter β changing gradually from the lower to the upper values of $\beta = [1, 7]$. This system can generate chaotic dynamic behaviours in a wide region of β. Figures 7, 8 and 9 show the bifurcation diagrams and the largest Lyapunov exponent of the Chen system (with the parameters $\sigma = 35$, $\rho = -7$, $\alpha = -28$) for $\gamma = 0.4$, 1 and 4. In order to prove the similarity and the equivalence of different size Chen attractors ($\gamma > 1$ or $\gamma < 1$) with the original Chen attractor ($\gamma = 1$), the MSE_{1D} is applied to different time series of the chaotic attractors to measure their degree of irregularity and disorder. It evaluates the probability of finding similar patterns.

Using the Poincaré map method, the bifurcation values are computed from the time series $\mathbf{x}(t)$, against the bifurcation parameter β. The three bifurcation diagrams have an almost identical structure apart from a scale dimensioning on the ordered axis. The maxi, original and mini Chen chaotic attractors depend on the amplitude of the variables $x(t)$, $y(t)$ and $z(t)$, where $x(t)$ is involved in the bifurcation diagrams. The attractors have a higher size at a greater amplitude of bifurcation diagrams. The largest Lyapunov exponent is calculated to analyze the dynamic Chen system for $\mathbf{x}(t)$. It can be observed that the largest Lyapunov exponent values (Figures 7(b), 8(b) and 9(b)) properly reflect the behaviour of the Chen system presented in the bifurcation diagrams (Figures 7(a), 8(a) and 9(a)). Furthermore, these figures show the same bifurcation scenario and the same Lyapunov exponents for the same values of β and independently of γ.

Additionally, MSE_{1D} is sensitive to the signal amplitude changes. A common practice to address this issue is to normalize the signal amplitude. The time series $\mathbf{x}(t)$ is rescaled along the signal amplitude axis with a factor, thus normalising the magnitude of the mini and maxi Chen attractors to the original Chen attractor. The MSE_{1D} is applied to determine their entropy over a scale τ from 1 to 20. The complexity of the Chen system is analyzed by varying the system parameter β from 1 to 7 with a 0.01 step. The results show (Fig. 10) that the mini, original and maxi chaotic attractors have almost the same MSE_{1D} values for all time scales. For the region $\beta \in [5, 7]$, the Chen

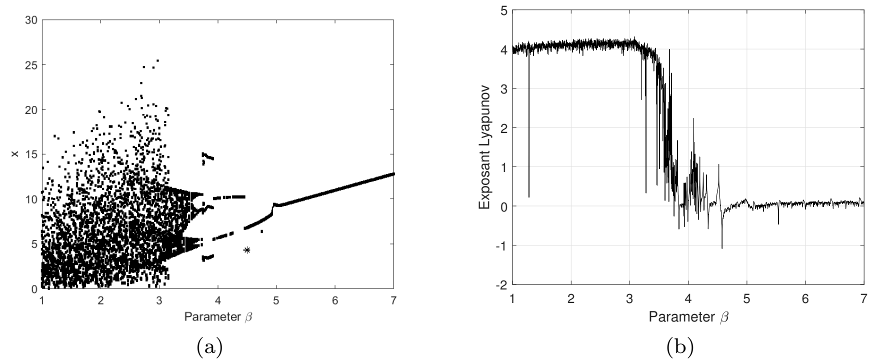

Figure 7: (a) The bifurcation diagram and (b) the largest Lyapunov exponent plotted against the bifurcation parameter β with $\sigma = 35$, $\alpha = 28$ and $\gamma = 0.4$.

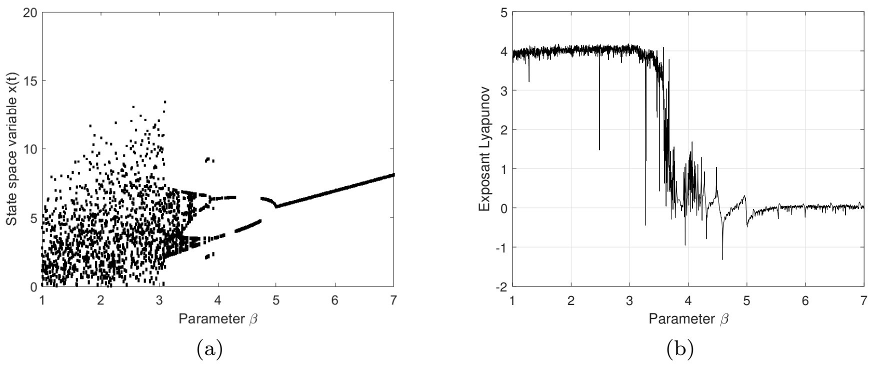

Figure 8: (a) The bifurcation diagram and (b) the largest Lyapunov exponent plotted against the bifurcation parameter β with $\sigma = 35$, $\alpha = 28$ and $\gamma = 1$.

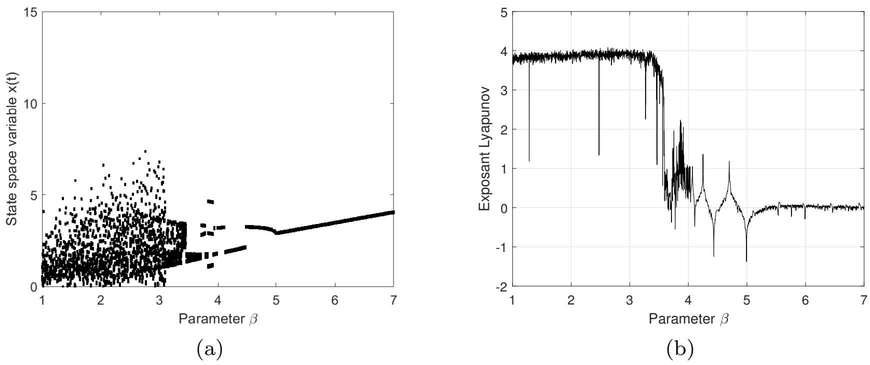

Figure 9: (a) The bifurcation diagram and (b) the largest Lyapunov exponent plotted against the bifurcation parameter β with $\sigma = 35$, $\alpha = 28$ and $\gamma = 4$.

system behaves as a limit cycle attractor, with a simplest behaviour of x. However, when the largest Lyapunov exponent of the system is approximately equal to zero, it corresponds to the oscillations before the first bifurcation point. More specifically, the MSE_{1D} values of the mini, original and maxi periodic attractors are zero (Fig. 10), which indicates a lower complexity. However, the MSE_{1D} surface begins to contain nonzero values after the first bifurcation point. In the range, after the first bifurcation point and before the second bifurcation, the system has an irregular behaviour. After this second bifurcation, the complexity of the oscillations continues to rise. It should be pointed out that for $\beta \in [3.69, 3.8]$, the Chen system has an abundant dynamic behaviour. For this tight interval of β, the original attractor sometimes has the same behaviour as the mini attractor or the maxi attractor or, occasionally, both. For $\beta = 3.73$, Fig. 11 shows the phase portraits of three attractors for $\gamma = 0.4$, 1 and 4. There is a similarity between the two first orbits, but not with the last one. An interesting observation is that the doubling-period bifurcations depend on the parameter γ. Decreasing more $\beta = 3.72$, the periodic orbit of Fig. 11 (a), (b) evolves into the behaviour shown in Fig. 12 (a), (b). Indeed, the Chen system represents the transition from one behaviour to another when the parameter β is slowly varied. Furthermore, the generated mini and maxi attractors are similar to the original attractor, but they have different sizes. The qualitative properties are preserved independently of γ. As shown in Figs. 7, 8 and 9, the Chen system can evolve into the chaotic attractors when $\beta \in [1, 3.69]$. The positive Lyapunov exponents for the mini, original and maxi Chen attractors confirm their chaoticity. Compared with the Lyapunov exponents and bifurcation diagrams, the MSE_{1D} complexities are consistent, which means that complexity can also reflect the chaotic characteristics of the Chen system. MSE_{1D} has small values for the periodic behaviour and increases when the attractor moves from a period to chaos, as in Figure 10. According to the above analysis, the complexity of different attractors has the same level independently of γ and their sizes (the same maximum Lyapunov exponent values, the same MSE_{1D} values). The complexity of the mini ($\gamma = 4$) and maxi ($\gamma = 0.4$) attractors is similar to that of the original attractors ($\gamma = 1$). Moreover, Fig. 13 shows that the complexity decreases with β in the sense of the MSE_{1D} values. To improve the understanding of the Chen attractor behaviour for small values of $\beta < 3$ and for a scale factor $\tau = 1$ (Figure 13), the relative error of MSE_{1D} is calculated. It is very useful to compare attractors of different size to the reference one (the original attractor). This alternative is also used to measure the complexity of attractors that visually look like the original attractor. The accuracy of attractors of different size determines how far this one is from the original attractor. It is often helpful to present numbers as percentages as this gives a sense of proportion. The relative error of MSE_{1D} of the mini and maxi Chen attrators reported to the original Chen attractor is based on the absolute error of the MSE_{1D}. Figure 14 (a) shows the absolute error of the MSE_{1D} of the Chen system with $\gamma = 0.4$ compared to the MSE_{1D} of the original Chen system with $\gamma = 1$. A similar figure (Fig. 14(b)) is obtained from the difference between the MSE_{1D} of the Chen system with $\gamma = 4$ and the MSE_{1D} of the original Chen system with $\gamma = 1$. Figure 14 shows a very small absolute error of 0.005 for the chaotic behaviour and 0 for the periodic behaviour. The mean value of the absolute error of MSE_{1D} is zero for the periodic attractor ($\beta > 4$) and increases to 0.0027, respectively, 0.0023, when the system is in the route to chaos (β <3). Figure 15 (a), (b) shows the relative error of MSE_{1D} for the Chen attractors with $\gamma = 0.4$, $\gamma = 4$ compared to the MSE_{1D} of the Chen attractor with $\gamma = 1$. The MSE_{1D} mean relative error is zero for the periodic attractor ($\beta > 4$) and increases to 6.65 %,

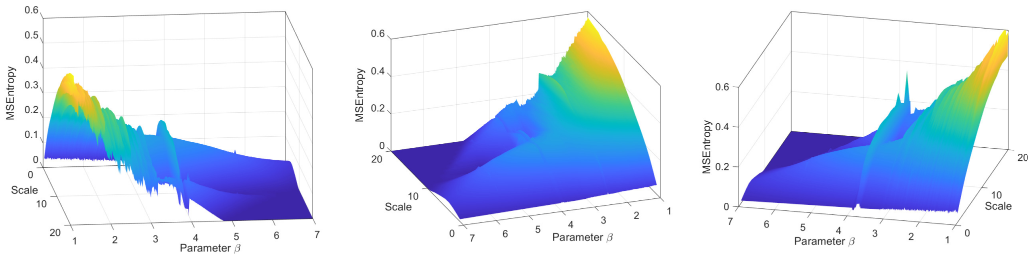

(a) $\gamma = 0.4$ (b) $\gamma = 1$ (c) $\gamma = 4$

Figure 10: MSE_{1D} of $x(t)$ for different scales and for $\sigma = 35$, $\alpha = 28$, $\beta = 3$.

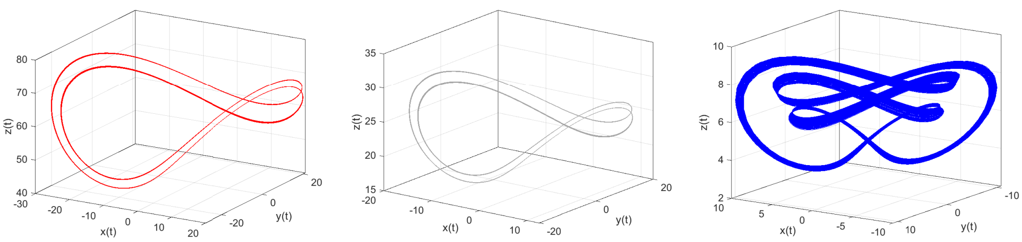

(a) $\gamma = 0.4$ (b) $\gamma = 1$ (c) $\gamma = 4$

Figure 11: The phase portraits of the chaotic attractors for $\sigma = 35$, $\alpha = 28$, $\beta = 3.73$.

respectively, 5.73 %, when the system is in the route to chaos (β <3), as in Figure 15 (a), respectively, (b). In fact, the rise of complexity is significant to MSE_{1D} for $\tau > 1$ and not for $\tau = 1$. Quantitatively, the relative error of MSE_{1D} for the Chen attractors with $\gamma = 0.4$ and $\gamma = 4$ compared to the MSE_{1D} for the original Chen attractor with $\gamma = 1$ is very small, almost insignificant. We can finally conclude that the MSE_{1D} values depict that the complexity of chaotic systems is independent of the size of attractors and matches well with the largest Lyapunov exponent and the bifurcation diagram.

7 Conclusions

In this paper, the dynamic behaviour of the Lorenz system is examined in a previously unexplored region of the parameter γ. The variation of this parameter reveals that the chaotic Lorenz related systems can generate strange attractors of different sizes. The use of bifurcation diagrams and the Lyapunov exponents is proposed to study the global dynamic behaviour of the Chen attractor. Through the theoretical analysis and mathematical simulations, the multiscale entropy MSE_{1D} of different time series under the γ variation parameter is calculated, qualifying the chaotic attractors' irregularity. The complexity of the chaotic sequences tends to be uniform, independent of the γ variation. It is noticeable that all their quantitative properties are preserved for any value of γ. Finally, throught the MSE_{1D}, the complexity of chaotic systems is independent of the size of attractors and matches well with the largest Lyapunov exponents and bifurcation diagrams.

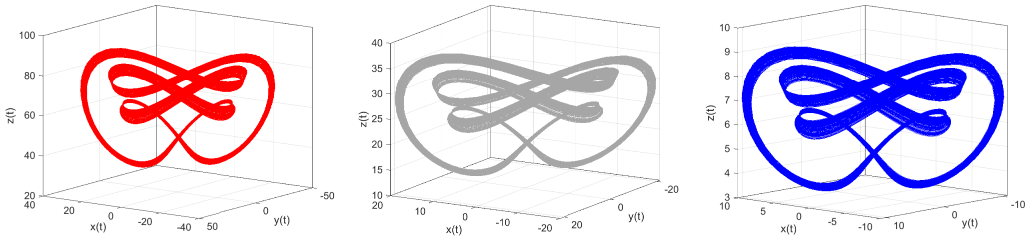

(a) $\gamma = 0.4$ (b) $\gamma = 1$ (c) $\gamma = 4$

Figure 12: The phase portraits of the chaotic attractors for $\sigma = 35$, $\alpha = 28$, $\beta = 3.72$.

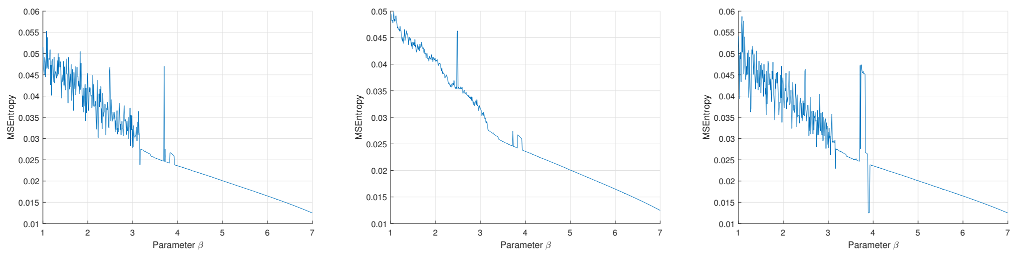

(a) $\gamma = 0.4$ (b) $\gamma = 1$ (c) $\gamma = 4$

Figure 13: MSE_{1D} of $x(t)$ of the Chen attractor for $\tau = 1$, $\sigma = 35$, $\alpha = 28$.

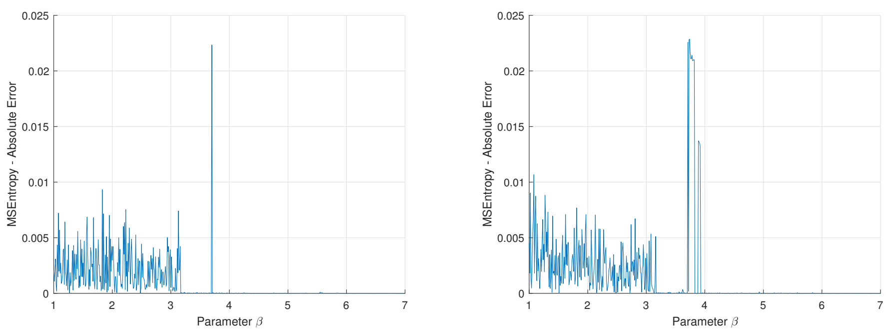

(a) $\gamma = 0.4$ (b) $\gamma = 4$

Figure 14: (a) The absolute error of MSE_{1D} for the Chen attractor with $\gamma = 0.4$ and $\gamma = 4$ compared to the MSE_{1D} with $\gamma = 1$.

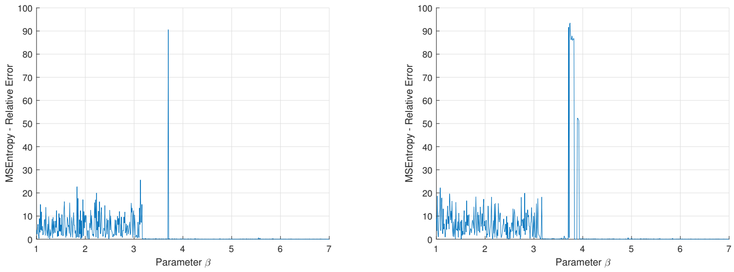

(a) $\gamma = 0.4$ (b) $\gamma = 4$

Figure 15: The relative error of MSE_{1D} for the Chen attractor with $\gamma = 0.4$ and $\gamma = 4$ compared to the MSE_{1D} with $\gamma = 1$.

References

[1] J. Lu, G. Chen and S. Zhang. A hidden chaotic attractor in the classical Lorenz system. *International Journal of Bifurcation and Chaos* **12** (2002) 1001–1015.

[2] J. Lu, G. Chen, S. Zhang and S. Celikovsky. Bridge the gap batween the Lorenz system and the Chen system. *International Journal of Bifurcation and Chaos* **12** (2002) 2917–2926.

[3] R. Barboza. On Lorenz to Chen system. *International Journal of Bifurcation and Chaos* **28** (2018) 1850018.

[4] C. Li and J C. Sprott. Multistability in the Lorenz system: A broken butterfly. *International Journal Bifurcation and Chaos* **24** (2014) 1450131.

[5] S. Jafari and J. Sprott. Simple chaotic flows with a line equilibrium. *Chaos, Soliton and Fractals* **57** (2013) 79–84.

[6] Z. Wei and G. Chen. Dynamical behaviors of a chaotic system with no equilibria. *Phys. Lett. A* **376** (2011) 102–108.

[7] M. Molaie, S. Jafari, J. C. Sprott and S. Golpayegani. Simple chaotic flows with one stable equilibrium. *International Journal Bifurcation and Chaos* **23** (2013) 1350188–1–7.

[8] J. C. Sprott, S. Jafari, V. T. Pham and Z. S. Hosseini. A chaotic system with a single unstable node. *International Journal of Computer Mathematics* **379** (2015) 2030–2036.

[9] C. Morel and R. Vlad. A new technique to generate independent chaotic attractors in the state space of nonlinear dynamics systems. *Nonlinear Dynamics* **59** (2009) 45–60.

[10] G. A. Leonov, N. V. Kuznetsov and T. N. Mokaev. Hidden attractor and homoclinic orbit in Lorenz-like system describing convective fluid motion in rotating cavity. *Commun. Nonlinear Sci. Numerical Simulation* **28** (2015) 166–174.

[11] A. Ouannas. A new synchronization scheme for general 3D quadratic chaotic systems in discrete-time. *Nonlinear Dynamics and Systems Theory* **15** (2015) 163–170.

[12] S. Kaouache, N. E. Hamri, A. S. Hacinliyan, E. Kandiran, B. Deruni and A. C. Keles. Increased Order Generalized Combination Synchronization of Non-Identical Dimensional Fractional-Order Systems by Introducing Different Observable Variable Functions. *Nonlinear Dynamics and Systems Theory* **20** (2020) 107–115.

[13] C. Liu, L. Ding and Q. Ding. Research about the characteristics of chaotic systems based on multi-scale entropy. *Entropy* **21** (2019) 663.

[14] C. Morel and A. Humeau. Multi-scale permutation entropy for two-dimensional patterns. *Pattern Recognition Letters* **150** (2021) 139–146.

Nonlinear Dynamics and Systems Theory, **22** (1) (2022) 82–96

A Mathematical Study of Wuhan Novel Coronavirus Epidemic Model

Sayed Sayari *

Carthage University, Isteub, 2 Rue de l'Artisanat Charguia 2, 2035 Tunis, Tunisia

Received: June 16, 2021; Revised: December 25, 2021

Abstract: In this paper, we introduce a simplified model of the novel coronavirus pandemic (Covid-19), which appeared for the first time at Wuhan city in China. We compute the reproduction number $\mathcal{R}$, an epidemiologic index used to describe whether the disease spreads or ends. We study the model from a mathematical point of view, focusing on the local and global stability of the dynamical system by using Lyapunov functionals. We proof that for $\mathcal{R} < 1$, the disease dies and for $\mathcal{R} > 1$, the disease persists.

Keywords: *COVID-19; coronavirus pandemic; global stability; basic reproduction number; mathematical modeling; Lyapunov function.*

Mathematics Subject Classification (2010): 00A71, 34D23, 35N25, 37B25, 49K40, 60H10, 65C30, 91B70.

1 Introduction

Pandemics are large-scale outbreaks of infectious disease that can cause sudden, widespread morbidity and mortality over a wide geographic area and cause significant economic, social, and political disruption. Throughout history, there have been a lot of pandemics of diseases such as smallpox and tuberculosis. One of the most devastating pandemics was the Black Death, which killed an estimated $75-200$ million people in the 14th century. Other notable pandemics include the 1918 influenza pandemic (Spanish flu), the 2003 severe acute respiratory syndrome (SARS) pandemic, the 2009 influenza pandemic (H1N1), and the pandemic of human immunodeficiency virus/acquired immune deficiency syndrome, current HIV/AIDS. Over the past century, evidence suggests that the likelihood of pandemics has increased because of increased global travel, integration, urbanization and greater exploitation of the natural environment. These trends are likely to continue and intensify around the world with the appearance in 2019-2020

* Corresponding author: mailto:sayari.sayed@gmail.com

of the current coronavirus pandemic. The origin of most diseases occurs through the "zoonotic" transmission of pathogens from animals to humans, on 31 December 2019, the World Health Organization (WHO), China Country Office, was informed of cases of the novel coronavirus (2019-nCoV) detected in Wuhan city. It is reported that the virus might have a bat origin, and the transmission of the virus might be related to the Huanan Seafood Wholesale Market in the same city [2]. Exported internationally via commercial and air travel, the virus reaches several countries around the world. There are now many times more cases outside of China than there were inside of it at the height of the outbreak. There are large outbreaks of the disease in multiple places, including Italy, Spain, France and the United States, which currently has the worst outbreak compared to any country in the world.

Populations, as with individuals, have unique patterns of disease. The science of epidemiology, which straddles biology, mathematical modeling, and dynamical systems, seeks to describe, understand, and utilize these patterns to improve population health. Therefore, several researches are focusing on mathematical modelling of Covid-19 to estimate the transmissibility and dynamic of the transmission of the virus [2]. These researches are focused on calculating the basic reproduction number $\mathcal{R}$.

In this study, we developed and analysed a mathematical model introduced in [2] and references therein, to describe the transmission of the virus from bats to people via the reservoir seafood market. We calculated the basic reproduction number $\mathcal{R}$. We study the basic and global properties of the model. By using Lyapunov functions and LaSalle's invariance principle, we have established the global stability of the equilibria of the model.

This paper is organized as follows. In Section 2, we propose the model and study its basic properties. In Section 3, the local stability of equilibria is established. Section 4 is offered to study the global stability of equilibria. In Section 5, we present some numerical examples to illustrate the obtained results.

2 Mathematical Model and Its Properties

We used a modelling framework similar to that by Chen et al. [2]. The variables of the model are introduced as follows: W denotes the SARS-CoV-2 in the reservoir (the seafood market). The population was divided into five compartments: susceptible individuals (S), exposed individuals (E), symptomatic infected individuals (I), asymptomatic infected individuals (A) and removed individuals (R) including recovered and dead individuals. The model parameters are given as follows: N represents the rate of the recruitment of susceptible (birth rate + rate of people travelling into Wuhan), c is the rate of individuals travelling out from the city. β_w is the transmission rate of the infection of individuals S from a sufficient contact with W, and β is the contagion rate due to the contact with infected people I. $1/\omega$ denotes the incubation period of human infection and $1/\gamma$ denotes the same infectious period of I and A. $1/\varepsilon$ describes the lifetime of the virus in W. The proportion of asymptomatic infection was defined as σ. θ denotes the multiple of the transmissibility of A to that of I (see Figure 1). The population is assumed constant, i.e., the births and natural deaths have the same value, due to the rapid disease spread. We assumed also that the transmissibility rate $\theta \in [0, 1]$.

The diagram (Figure 1) describes the dynamics of the reservoir-people (seafood market) transmission network model, and will be useful in the formulation of model equations. Based on the previous researches [1–4, 7–12, 15, 16] and using some assumptions,

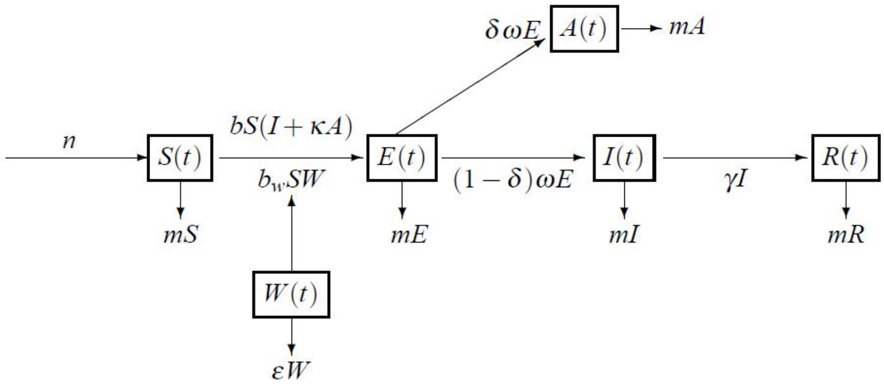

Figure 1: Flow diagram of the reservoir-people transmission network model.

the proposed mathematical model is given as follows:

$$\begin{array}{l}\dot{S} = N - cS - \beta S(I+\theta A) - \beta_w SW,\\ \dot{E} = \beta S(I+\theta A) + \beta_w SW - (\omega + c)E,\\ \dot{I} = (1-\sigma)\omega E - (\gamma + c)I,\\ \dot{A} = \sigma\omega E - (\gamma + c)A,\\ \dot{R} = \gamma(I + A) - cR,\\ \dot{W} = \varepsilon(I + \theta A - W).\end{array} \tag{1}$$

It is subject to the conditions

$$S(0) > 0,\ E(0) > 0,\ I(0) \geq 0,\ A(0) \geq 0,\ R(0) \geq 0. \tag{2}$$

For epidemiological reasons, all model parameters are assumed to be positive. Next, we investigate the basic properties of model (1). Start by giving a result of boundedness and positivity of solutions.

Proposition 2.1 1. *All solutions of the model (1) with initial conditions (2) are bounded and non-negative.*
2. *The region* $\Omega = \{(S, E, I, A, R, W) \in \mathbb{R}^6_+ \ / \ S + E + I + A + R + W \leq \dfrac{N}{\bar{c}}\}$ *is a positively invariant attractor for system (1), where* $\bar{c} = \min(c - \varepsilon, \varepsilon)$.

Proof. 1. The solution is positive due to the fact below. Since $S = 0$, one has $\dot{S} = N > 0$; if $E = 0$, then $\dot{E} = \beta S(I+\theta A)+\beta_w SW > 0$; once $I = 0$, then $\dot{I} = (1-\sigma)\omega E > 0$; if $A = 0$, then $\dot{A} = \sigma\omega E > 0$; if $R = 0$, then $\dot{R} = \gamma(I + A) > 0$; and if $W = 0$, then $\dot{W} = \varepsilon(I + \theta A) > 0$.

The boundedness of solutions of system (1) can be proved by summing up all equations of system (1), and denoting $T = S + E + I + A + R + W - \dfrac{N}{\bar{c}}$, then one obtains the following equation for the totality of individuals:

$$\begin{aligned}\dot{T} &= \dot{S}+\dot{E}+\dot{I}+\dot{A}+\dot{R}+\dot{W}\\ &= N-cS-cE-(c-\varepsilon)I-(c-\varepsilon\theta)A-cR-\varepsilon W\\ &\leq \bar{c}(\frac{N}{\bar{c}}-S-E-I-A-R-W)\\ &= -\bar{c}T.\end{aligned}$$

Then

$$S+E+I+A+R+W \leq \frac{N}{\bar{c}}+\Big(S(0)+E(0)+I(0)+A(0)+R(0)+W(0)-\frac{N}{\bar{c}}\Big)e^{-\bar{c}t}. \quad (3)$$

Then the boundedness of the solution of system (1) holds since all compartments of T are positive.

2. One can easily deduce from equality (3) that the set Ω is a positively invariant attractor for system (1).

3 Stability of the Equilibria of the System

The equilibria are obtained by putting all the equations of the system (1) to zero, as given below.

1. Disease-free equilibrium: $\mathcal{E}^0 = (\frac{N}{c}, 0, 0, 0, 0, 0)$.

2. Endemic or positive equilibrium: $\mathcal{E}^\star = (S^\star, E^\star, I^\star, A^\star, W^\star)$.

To investigate the stability behavior of the equilibria, we need to compute the basic reproduction number $\mathcal{R}$ using the generation matrix method proposed by Diekmann, et al. [5] and elaborated by van den Driessche and Watmough [6] for an ODE compartmental model. Let

$$\dot{x} = F(x) - V(x),$$

where $x = (E, I, A, W)$, $F(x)$ is the matrix of new infection term, and $V(x)$ is the matrix of transfer terms into compartments and out of compartments. In our case, the Jacobian matrices of $F(x)$ and $V(x)$ at $\mathcal{E}^0$ are given by

$$F = \begin{pmatrix} 0 & \frac{\beta N}{c} & \theta\frac{\beta N}{c} & \frac{\beta_w N}{c} \\ 0 & 0 & 0 & 0 \\ 0 & 0 & 0 & 0 \\ 0 & 0 & 0 & 0 \end{pmatrix}, \quad \text{and} \quad V = \begin{pmatrix} \omega+c & 0 & 0 & 0 \\ -(1-\sigma)\omega & \gamma+c & 0 & 0 \\ -\sigma\omega & 0 & \gamma+c & 0 \\ 0 & -\varepsilon & -\varepsilon\theta & \varepsilon \end{pmatrix}.$$

Now,

$$V^{-1} = \begin{pmatrix} \frac{1}{\omega+c} & 0 & 0 & 0 \\ A & \frac{1}{\gamma+c} & 0 & 0 \\ B & 0 & \frac{1}{\gamma+c} & 0 \\ D & E & G & \frac{1}{\varepsilon} \end{pmatrix},$$

where

$$\begin{cases} A &= \dfrac{(1-\sigma)\omega}{(\omega+c)(\gamma+c)}, \\ B &= \dfrac{\sigma\omega}{(\omega+c)(\gamma+c)}, \\ D &= \dfrac{(1-\sigma)\omega+\sigma\omega\theta}{(\omega+c)(\gamma+c)}, \\ E &= \dfrac{1}{\omega+c}, \\ G &= \dfrac{\theta}{\gamma+c}, \end{cases} \tag{4}$$

and then

$$FV^{-1} = \begin{pmatrix} 0 & \dfrac{\beta N}{c} & \theta\dfrac{\beta N}{c} & \beta_w\dfrac{N}{c} \\ 0 & 0 & 0 & 0 \\ 0 & 0 & 0 & 0 \\ 0 & 0 & 0 & 0 \end{pmatrix} \begin{pmatrix} \dfrac{1}{\omega+c} & 0 & 0 & 0 \\ A & \dfrac{1}{\gamma+c} & 0 & 0 \\ B & 0 & \dfrac{1}{\gamma+c} & 0 \\ D & E & G & \dfrac{1}{\varepsilon} \end{pmatrix}$$

$$= \begin{pmatrix} A\dfrac{\beta N}{c} + B\theta\dfrac{\beta N}{c} + D\beta_w\dfrac{N}{c} & \dfrac{\beta N}{c(\omega+c)} + E\beta_w\dfrac{N}{c} & \theta\dfrac{\beta N}{c(\gamma+c)} + G\beta_w\dfrac{N}{c} & \beta_w\dfrac{N}{c\varepsilon} \\ 0 & 0 & 0 & 0 \\ 0 & 0 & 0 & 0 \\ 0 & 0 & 0 & 0 \end{pmatrix}.$$

Then the basic reproduction number for model (1) is given by $\mathcal{R} = \rho(FV^{-1})$, where ρ denotes the spectral radius of the next-generation matrix FV^{-1}. Therefore, the basic reproduction number $\mathcal{R}$ for our model is

$$\mathcal{R} = \frac{N(\beta+\beta_w)\big((1-\sigma)\omega+\sigma\omega\theta\big)}{c(\omega+c)(\gamma+c)} = R_1 + R_2, \tag{5}$$

where $R_1 = \dfrac{N\beta\big((1-\sigma)\omega+\sigma\omega\theta\big)}{c(\omega+c)(\gamma+c)}$ and $R_2 = \dfrac{N\beta_w\big((1-\sigma)\omega+\sigma\omega\theta\big)}{c(\omega+c)(\gamma+c)}$.

Next, the local stability of equilibria was discussed with respect to the basic reproduction number $\mathcal{R}$.

3.1 Analysis of the local stability for $\mathcal{E}^0$

The local stability of the disease-free equilibrium of the system (1) is given in the following theorem.

Theorem 3.1 *The disease-free equilibrium $\mathcal{E}^0$ is locally asymptotically stable when the basic reproduction number $\mathcal{R}$ is less than one and unstable when $\mathcal{R}$ is greater than one.*

Proof. The Jacobian matrix of (1) evaluated at $\mathcal{E}^0 = (\frac{N}{c}, 0, 0, 0, 0, 0)$ is given by

$$J^0 = \begin{pmatrix} -c & 0 & -\frac{\beta N}{c} & -\theta\frac{\beta N}{c} & 0 & -\beta_w\frac{N}{c} \\ 0 & -(\omega+c) & \frac{\beta N}{c} & \theta\frac{\beta N}{c} & 0 & \beta_w\frac{N}{c} \\ 0 & (1-\sigma)\omega & -(\gamma+c) & 0 & 0 & 0 \\ 0 & \sigma\omega & 0 & -(\gamma+c) & 0 & 0 \\ 0 & 0 & \gamma & \gamma & -c & 0 \\ 0 & 0 & \varepsilon & \varepsilon\theta & 0 & -\varepsilon \end{pmatrix}.$$

The characteristic equation of the matrix J^0 is

$$\begin{aligned} P^0(\lambda) =& (\lambda+\gamma+c)(\lambda+c)^2\big((\lambda+\omega+c)(\lambda+\gamma+c)(\lambda+\varepsilon) - (\omega+c)(\gamma+m)R_1\lambda \\ & - \varepsilon(\omega+c)(\gamma+c)\mathcal{R}\big). \end{aligned}$$

Obviously, $-c$ and $-\gamma-c$ are eigenvalues of J^0. To determine the other eigenvalues of J^0, let $p(\lambda) = (\lambda+\gamma+c)(\lambda+c)^2 p_3(\lambda)$, therefore

$$\begin{aligned} P_3(\lambda) =& \lambda^3 + (\omega+c+\gamma+c+\varepsilon)\lambda^2 + \Big(\varepsilon(\omega+c+\gamma+c) + (\omega+c)(\gamma+c)(1-R_1)\Big)\lambda \\ & + \varepsilon(\omega+c)(\gamma+c)(1-\mathcal{R}). \end{aligned}$$

We rewrite $p_3(\lambda)$ as $p_3(\lambda) = \lambda^3 + A_1\lambda^2 + A_2\lambda + A_3$. The Routh-Hurwitz stability criterion ensures that $Re(\lambda) < 0$ under the conditions $A_1,\ A_3 > 0$ and $A_1A_2 - A_3 > 0$ for a monic polynomial of degree 3, then we have

$$\begin{aligned} A_1 =& \omega+c+\gamma+c+\varepsilon > 0, \\ A_2 =& \varepsilon(\omega+c+\gamma+c) + (\omega+c)(\gamma+c)(1-R_1) > 0 \quad \text{for } R_1 < \mathcal{R} < 1, \\ A_3 =& \varepsilon(\omega+c)(\gamma+c)(1-\mathcal{R}) > 0 \quad \text{for } \mathcal{R} < 1. \end{aligned}$$

Now we compute the term $A_1A_2 - A_3$:

$$\begin{aligned} A_1A_2 - A_3 =& (\omega+c+\gamma+c+\varepsilon)\big(\varepsilon(\omega+c+\gamma+c) + (\omega+c)(\gamma+c)(1-R_1)\big) \\ & - \varepsilon(\omega+c)(\gamma+c)(1-\mathcal{R}) \\ =& (\omega+c+\gamma+c)\big(\varepsilon(\omega+c+\gamma+c) + (\omega+c)(\gamma+c)(1-R_1)\big) \\ & + \varepsilon^2(\omega+c+\gamma+c) + \varepsilon(\omega+c)(\gamma+c)(\mathcal{R}-R_1) > 0 \quad \text{for } \mathcal{R} < 1. \end{aligned}$$

This completes the proof.

3.2 Existence and analysis of the local stability for $\mathcal{E}^\star$

In this section, the conditions for the existence of the endemic equilibrium $\mathcal{E}^\star = (S^\star, E^\star, I^\star, A^\star, R^\star, W^\star)$ are investigated and the local stability of the endemic equilibrium $\mathcal{E}^\star$ is discussed. The endemic equilibrium $\mathcal{E}^\star$ is obtained by putting all equations of the system (1) to zero as given below:

$$\begin{cases} N = cS^\star + \beta S^\star(I^\star + \theta A^\star) + \beta_w S^\star W^\star, \\ \beta S^\star(I^\star + \theta A^\star) + \beta_w S^\star W^\star = (\omega+c)E^\star, \\ (1-\sigma)\omega E^\star = (\gamma+c)I^\star, \\ \sigma\omega E^\star = (\gamma+c)A^\star, \\ \gamma(I^\star + A^\star) = cR^\star, \\ I^\star + \theta A^\star = W^\star. \end{cases} \tag{6}$$

Now we get

$$\mathcal{E}^\star = \Big(\frac{(\omega+c)(\gamma+c)}{(\beta+\beta_w)\big((1-\sigma)\omega+\sigma\omega\theta\big)}, \frac{N-cS^\star}{\omega+c}, \frac{(1-\sigma)\omega}{\gamma+c}E^\star, \frac{\sigma\omega}{\gamma+c}E^\star, \frac{1}{c(\gamma+c)}\gamma E^\star, \frac{(1-\sigma)\omega+\sigma\omega\theta}{\gamma+c}E^\star \Big).$$

Using the definition of reproduction number $\mathcal{R}$ in (5), we obtain

$$\begin{cases} S^\star &= \dfrac{N}{c\mathcal{R}}, \\ E^\star &= \dfrac{N}{\omega+c}(1-\frac{1}{\mathcal{R}}), \\ I^\star &= \dfrac{(1-\sigma)\omega N}{(\omega+c)(\gamma+c)}(1-\frac{1}{\mathcal{R}}), \\ A^\star &= \dfrac{\sigma\omega N}{(\omega+c)(\gamma+c)}(1-\frac{1}{\mathcal{R}}), \\ R^\star &= \dfrac{1}{c(\omega+c)(\gamma+c)}(1-\frac{1}{\mathcal{R}}), \\ W^\star &= \dfrac{(1-\sigma)\omega+\sigma\omega\theta}{(\omega+c)(\gamma+c)}N(1-\frac{1}{\mathcal{R}}). \end{cases} \tag{7}$$

Next, we study the local stability of system (1) around the endemic equilibrium $\mathcal{E}^\star$.

Theorem 3.2 *The endemic equilibrium $\mathcal{E}^\star$ exists and is locally asymptotically stable when the basic reproduction number $\mathcal{R}$ is less than one.*

Proof. The matrix J is evaluated at $\mathcal{E}^\star = (S^\star, E^\star, I^\star, A^\star, R^\star, W^\star)$ and is given by

$$J^\star = \begin{pmatrix} -c-\beta(I^\star+\theta A^\star)-\beta_w W^\star & 0 & -\beta S^\star & -\beta\theta S^\star & 0 & -\beta_w S^\star \\ \beta(I^\star+\theta A^\star)+\beta_w W^\star & -\omega-c & \beta S^\star & \beta\theta S^\star & 0 & \beta_w S^\star \\ 0 & (1-\sigma)\omega & -(\gamma+c) & 0 & 0 & 0 \\ 0 & \sigma\omega & 0 & -(\gamma+c) & 0 & 0 \\ 0 & 0 & \gamma & \gamma & -c & 0 \\ 0 & 0 & \varepsilon & \varepsilon\theta & 0 & -\varepsilon \end{pmatrix}.$$

Note that, by using (7), we have $-c-\beta(I^\star+\theta A^\star)-\beta_w W^\star = -c\mathcal{R}$ and $\beta(I^\star+\theta A^\star)+\beta_w W^\star = c(\mathcal{R}-1)$. The characteristic polynomial of the Jacobian matrix $J^\star$ is given by

$$p^\star(\lambda) = (\lambda+c)(\lambda+\gamma+c)\Bigg[(\lambda+c\mathcal{R})(\lambda+\varepsilon)(\lambda+\gamma+c)(\lambda+\omega+c) - (\lambda+c)S^\star\Bigg((1-\sigma)\omega\Big(\varepsilon\beta_w+\beta(\lambda+\varepsilon)\Big)+\sigma\omega\Big(\beta_w\varepsilon\theta+\beta\theta(\lambda+\varepsilon)\Big)\Bigg)\Bigg].$$

Clearly, the two roots of $p^\star$, $\lambda_1 = -c$ and $\lambda_2 = -\gamma-c$ are negative. The remaining roots can be determined by setting $p^\star(\lambda) = (\lambda+c)(\lambda+\gamma+c)p_4(\lambda)$, with $p_4(\lambda) = \lambda^4+B_1\lambda^3+B_2\lambda^2+B_3\lambda+B_4$.

We get

$$\begin{aligned}
p_4(\lambda) =&\lambda^4 + \Big(\omega + c + \gamma + c + \varepsilon + c\mathcal{R}\Big)\lambda^3\\
&+ \Big(\varepsilon c\mathcal{R} + (\omega + c)(\gamma + c) + (\varepsilon + c\mathcal{R})(\omega + c + \gamma + c) - \beta S^\star\big((1-\sigma)\omega + \sigma\omega\theta\big)\Big)\lambda^2\\
&+ \Big(\varepsilon c\mathcal{R}(\omega + c + \gamma + c) + (\varepsilon + c\mathcal{R})(\omega + c)(\gamma + c) - S^\star\big((1-\sigma)\omega + \sigma\omega\theta\big)\times\\
&\big(\beta c + \varepsilon(\beta + \beta_w)\big)\Big)\lambda + \Big(\varepsilon c\mathcal{R}(\omega + c)(\gamma + c) - \varepsilon c S^\star\big((1-\sigma)\omega + \sigma\omega\theta\big)(\beta + \beta_w)\Big).
\end{aligned}$$

Now we show, by a direct calculation, that all coefficients $B_i,\ i = 1, \cdots, 4$, of the polynomial p_4 are nonnegative, more precisely,

$$\begin{aligned}
B_1 =&\omega + c + \gamma + c + \varepsilon + c\mathcal{R} > 0,\\
B_2 =&\varepsilon c\mathcal{R} + (\omega + c)(\gamma + c) + (\varepsilon + c\mathcal{R})(\omega + c + \gamma + c) - \beta S^\star\big((1-\sigma)\omega + \sigma\omega\theta\big)\\
=&\varepsilon c\mathcal{R} + (\omega + c)(\gamma + c) + (\varepsilon + c\mathcal{R})(\omega + c + \gamma + c) - (\omega + c)(\gamma + c)\frac{R_1}{\mathcal{R}}\\
=&\varepsilon c\mathcal{R} + (\varepsilon + c\mathcal{R})(\omega + c + \gamma + c) + (\omega + c)(\gamma + c)(1 - \frac{R_1}{\mathcal{R}}) > 0,\\
B_3 =&\varepsilon c\mathcal{R}(\omega + c + \gamma + c) + (\varepsilon + c\mathcal{R})(\omega + c)(\gamma + c)\\
&- S^\star\big((1-\sigma)\omega + \sigma\omega\theta\big)\big(\beta c + \varepsilon(\beta + \beta_w)\big)\\
=&\varepsilon c\mathcal{R}(\omega + c + \gamma + c) + (\varepsilon + c\mathcal{R})(\omega + c)(\gamma + c) - c(\omega + c)(\gamma + c)\frac{R_1}{\mathcal{R}} - \varepsilon(\omega + c)(\gamma + c)\\
=&\varepsilon c\mathcal{R}(\omega + c + \gamma + c) + c\mathcal{R}(\omega + c)(\gamma + c)(1 - \frac{R_1}{\mathcal{R}^2}) > 0 \quad \text{for } \mathcal{R} > 1,
\end{aligned}$$

and

$$\begin{aligned}
B_4 =&\varepsilon c\mathcal{R}(\omega + c)(\gamma + c) - \varepsilon c S^\star\big((1-\sigma)\omega + \sigma\omega\theta\big)(\beta + \beta_w)\\
=&\varepsilon c\mathcal{R}(\omega + c)(\gamma + c) - \varepsilon c(\omega + c)(\gamma + c)\\
=&\varepsilon c(\omega + c)(\gamma + c)(\mathcal{R} - 1) > 0.
\end{aligned}$$

It follows, by using the Routh-Hurwitz criteria, that all the eigenvalues associated to $J^\star$ have negative real parts iff $B_i > 0,\ i = 1, 3, 4$, and $B_1(B_2B_3 - B_1B_4) - B_3^2 > 0$.

Now, calculating $B := B_2B_3 - B_1B_4$, and after simplifying negative terms, we get

$$\begin{aligned}
B =&\Big(c\mathcal{R}(\omega + c + \gamma + c) + (\omega + c)(\gamma + c)(1 - \frac{R_1}{\mathcal{R}})\Big)\times\\
&\Big(\varepsilon c\mathcal{R}(\omega + c + \gamma + c) + c\mathcal{R}(\omega + c)(\gamma + c)(1 - \frac{R_1}{\mathcal{R}^2})\Big)\\
&+ \varepsilon c(c\mathcal{R} + \omega + c)\Big(\varepsilon\mathcal{R}(\omega + c + \gamma + c) + (\omega + c)(\gamma + c)(1 - \frac{R_1}{\mathcal{R}})\Big)\\
&+ \varepsilon c(\gamma + c)^2\Big(\varepsilon\mathcal{R} + (\omega + c)(1 - \frac{R_1}{\mathcal{R}})\Big) + \varepsilon^2 c(\gamma + c)(\omega + c).
\end{aligned}$$

Let $B' = B_1(B_2B_3 - B_1B_4) - B_3^2 = B_1B - B_3^2$, after simplifying, we obtain

$$\begin{aligned}B' =&(\gamma + c + c\mathcal{R})\Big(c\mathcal{R}(\omega + c) + c\mathcal{R}(\gamma + c) + (\omega + c)(\gamma + c)(1 - \frac{R_1}{\mathcal{R}})\Big)\times\\
&\Big(\varepsilon c\mathcal{R}(\omega + c + \gamma + c) + c\mathcal{R}(\omega + c)(\gamma + c)(1 - \frac{R_1}{\mathcal{R}^2})\Big)\\
&+ (\omega + c)\Big(c\mathcal{R}(\omega + c) + (\omega + c)(\gamma + c)(1 - \frac{R_1}{\mathcal{R}})\Big)\times\\
&\Big(\varepsilon c\mathcal{R}(\omega + c + \gamma + c) + c\mathcal{R}(\omega + c)(\gamma + c)(1 - \frac{R_1}{\mathcal{R}^2})\Big)\\
&+ \varepsilon(\omega + c)(\gamma + c)(1 - \frac{R_1}{\mathcal{R}})\Big(\varepsilon c\mathcal{R}(\omega + c + \gamma + c) + c\mathcal{R}(\omega + c)(\gamma + c)(1 - \frac{R_1}{\mathcal{R}^2})\Big)\\
+ &\varepsilon c(c\mathcal{R} + \omega + c)(\omega + c + \gamma + c + \varepsilon + c\mathcal{R})\Big(\varepsilon\mathcal{R}(\omega + c + \gamma + c) + (\omega + c)(\gamma + c)(1 - \frac{R_1}{\mathcal{R}})\Big)\\
&+ \varepsilon c(\gamma + c)^2(\omega + c + \gamma + c + \varepsilon + c\mathcal{R})\Big(\varepsilon\mathcal{R} + (\omega + c)(1 - \frac{R_1}{\mathcal{R}})\Big)\\
&+ \varepsilon^2 c(\gamma + c)(\omega + c)(\omega + c + \gamma + c + \varepsilon + c\mathcal{R}) + c^2\mathcal{R}^2(\omega + c)^2(\gamma + c)^2(1 - \frac{R_1}{\mathcal{R}^2})\frac{R_1}{\mathcal{R}^2}\\
&+ \varepsilon c^2\mathcal{R}^2(\omega + c + \gamma + c)(\omega + c)(\gamma + c)\frac{R_1}{\mathcal{R}^2}.\end{aligned}$$

Since the compartments $1 - \frac{R_1}{\mathcal{R}}$ and $1 - \frac{R_1}{\mathcal{R}^2}$ are nonnegative for $\mathcal{R} > 1$, we get $B' > 0$. This ends the proof.

4 Global Stability Analysis of Both Equilibria of the System

In what follows, we investigate the global attractivity of both disease-free equilibria $\mathcal{E}^0$ and $\mathcal{E}^\star$.

Lemma 4.1 *The set* $\Omega_2 = \{(S, E, I, A, R, W) \in \mathbb{R}_+^6 \ / \ S + E + I + A + R + W \leq \frac{N}{\bar{c}}; S \leq \frac{N}{c}, W \leq I + \theta A\}$ *is a positively invariant attractor for system (1), where* $\bar{c} = \min(c - \varepsilon, \varepsilon)$.

Proof. It is proved in Proposition 2.1 that Ω_1 is a positive invariant attractor set of all solution of system (1). Now, since $\dot{S}(t) < 0$ for $S(t) > \frac{N}{c}$, one has $\liminf S(t) \leq \frac{N}{c}$. Similarly, since $\dot{W}(t) < 0$ for $W(t) > I(t) + \theta A(t)$, one has $\liminf W(t) \leq I(t) + \theta A(t)$. This completes the proof.

Theorem 4.1 *If $\mathcal{R} \leq 1$, then the disease-free equilibrium $\mathcal{E}^0$ is globally asymptotically stable (GAS). If $\mathcal{R} > 1$, then the disease-free equilibrium $\mathcal{E}^0$ is unstable.*

Proof. Construct the following Lyapunov function $\mathcal{L}(S, E, I, A, R, W)$ as:

$$\mathcal{L} = \omega(1 - \sigma + \sigma\theta)E + (\omega + c)(I + \theta A).$$

Along the trajectory of the solution of system (1), we have

$$\begin{aligned}
\dot{\mathcal{L}} =&\omega(1-\sigma+\sigma\theta)\dot{E}+(\omega+c)(\dot{I}+\theta\dot{A})\\
=&\omega(1-\sigma+\sigma\theta)\Big(\beta S(I+\theta A)+\beta_w SW-(\omega+c)E\Big)\\
&+(\omega+c)\Big((1-\sigma)\omega E-(\gamma+c)I+\sigma\theta\omega E-(\gamma+c)\theta A\Big)\\
=&\omega(1-\sigma+\sigma\theta)\Big(\beta S(I+\theta A)+\beta_w SW-(\omega+c)E\Big)\\
&+(\omega+c)\Big((1-\sigma+\sigma\theta)\omega E-(\gamma+c)I-(\gamma+c)\theta A\Big)\\
=&\omega(1-\sigma+\sigma\theta)\Big(\beta S(I+\theta A)+\beta_w SW\Big)-(\omega+c)(\gamma+c)(I+\theta A)\\
\le&(1-\sigma+\sigma\theta)\frac{\omega N}{c}\Big(\beta(I+\theta A)+\beta_w(I+\theta A)\Big)-(\omega+c)(\gamma+c)(I+\theta A)\\
&\qquad\qquad\qquad\qquad\qquad\qquad(\text{since } S\le\frac{N}{c}, W\le I+\theta A)\\
=&\Big[(1-\sigma+\sigma\theta)\frac{\omega N}{c}(\beta+\beta_w)-(\omega+c)(\gamma+c)\Big](I+\theta A)\\
=&(\omega+c)(\gamma+c)\Big[\frac{(1-\sigma+\sigma\theta)}{(\omega+c)(\gamma+c)}\frac{\omega N}{c}(\beta+\beta_w)-1\Big](I+\theta A)\\
=&(\omega+c)(\gamma+c)(\mathcal{R}-1)(I+\theta A),\ \forall(S,E,I,A,R,W)\in\Omega_2.
\end{aligned}$$

Since all parameters of the model are non-negative, it follows that $\dot{\mathcal{L}}\le 0$ for $\mathcal{R}\le 1$ with $\dot{\mathcal{L}}=0$ only if $I=A=0$. Hence, $\mathcal{L}$ is a Lyapunov function on Ω_2. Further, by Lemma 4.1, Ω_2 is a compact, absorbing subset of $\mathbb{R}^6_+$, and the largest compact invariant set in $\{(S,E,I,A,R,W)\in\Omega_2 : \dot{\mathcal{L}}=0\}$ is the singleton $\{\mathcal{E}^0\}$. Therefore, by Lasalle's invariance principle (see, for instance, [13, Theorem 3.1]), every solution of system (1) with initial conditions in $\mathbb{R}^6_+$ converges to $\mathcal{E}^0$ as $t\to+\infty$.

The global stability of the disease-persistence (endemic) equilibrium $\mathcal{E}^\star$ is given in the following theorem.

Theorem 4.2 *If $\mathcal{R}>1$, then the disease-persistence equilibrium $\mathcal{E}^\star=(S^\star,E^\star,I^\star,A^\star,R^\star,W^\star)$ is GAS. If $\mathcal{R}\le 1$, then the disease-persistence equilibrium $\mathcal{E}^\star$ is unstable.*

Proof. Introduce the following Lyapunov function:

$$\begin{aligned}
\mathcal{H}=&\Big(S-S^\star\ln(\frac{S}{S^\star})\Big)+\Big(E-E^\star\ln(\frac{E}{E^\star})\Big)+\frac{\omega+c}{(1-\sigma)\omega+\sigma\omega\theta}\Big(I+\theta A-(I^\star+\theta A^\star)\times\\
&\ln(\frac{I+\theta A}{I^\star+\theta A^\star})\Big)+\frac{\beta_w S^\star}{\varepsilon}\Big(W-W^\star\ln(\frac{W}{W^\star})\Big).
\end{aligned}$$

The equilibrium $\mathcal{E}^\star$ is the only internal stationary point of system (1). The function $\mathcal{H}(t)$ admits its minimum value $\mathcal{H}_{min}=S^\star+E^\star+\dfrac{\omega+c}{(1-\sigma)\omega+\sigma\omega\theta}(I^\star+\theta A^\star)+\dfrac{\beta_w}{\varepsilon}S^\star W^\star$ when $S=S^\star, E=E^\star, I=I^\star, A=A^\star, W=W^\star$, and $\mathcal{H}(t)\to+\infty$ at the boundary of the positive quadrant. Therefore, $\mathcal{E}^\star$ is the global minimum point, and the function is bounded from below.

Now we compute the derivative of $\mathcal{H}(t)$ along the solutions of system (1) as follows:

$$\begin{aligned}
\dot{\mathcal{H}} =&(1-\frac{S^\star}{S})\dot{S}+(1-\frac{E^\star}{E})\dot{E}+\frac{\omega+c}{(1-\sigma)\omega+\sigma\omega\theta}(1-\frac{I^\star+\theta A^\star}{I+\theta A})(\dot{I}+\theta\dot{A})\\
&+\frac{\beta_w}{\varepsilon}S^\star(1-\frac{W^\star}{W})\dot{W}\\
=&(1-\frac{S^\star}{S})\Big(N-cS-\beta S(I+\theta A)-\beta_w SW\Big)\\
&+(1-\frac{E^\star}{E})\Big(\beta S(I+\theta A)+\beta_w SW-(\omega+c)E\Big)\\
&+\frac{\omega+c}{(1-\sigma)\omega+\sigma\omega\theta}\Big(1-\frac{I^\star+\theta A^\star}{I+\theta A}\Big)\Big(((1-\sigma)\omega+\theta\sigma\omega)E-(\gamma+c)(I+\theta A)\Big)\\
&+\beta_w S^\star(1-\frac{W^\star}{W})(I+\theta A-W)\\
=&(1-\frac{S^\star}{S})\Big(c(S^\star-S)+\beta S^\star(I^\star+\theta A^\star)-\beta S(I+\theta A)+\beta_w S^\star W^\star-\beta_w SW\Big)\\
&+\beta S(I+\theta A)+\beta_w SW-(\omega+c)E-\frac{E^\star}{E}\beta S(I+\theta A)-\frac{E^\star}{E}\beta_w SW+(\omega+c)E^\star\\
&+\Big(1-\frac{I^\star+\theta A^\star}{I+\theta A}\Big)\Big((\omega+c)E-\frac{(\omega+c)(\gamma+c)}{(1-\sigma)\omega+\sigma\omega\theta}(I+\theta A)\Big)\\
&+\beta_w S^\star(I+\theta A)-\beta_w S^\star W-\beta_w S^\star\frac{W^\star}{W}(I+\theta A)+\beta_w S^\star W^\star.
\end{aligned}$$

Using the fact that $(S^\star, E^\star, I^\star, R^\star, W^\star)$ is a solution of system (6), (7) and (5), we get

$$\begin{aligned}
W^\star =&(I^\star+\theta A^\star), N=cS^\star+S^\star(\beta+\beta_w)(I^\star+\theta A^\star),\ (\omega+c)E^\star=\beta S^\star W^\star+\beta_w S^\star W^\star\\
(\omega+c)E =& \frac{E}{E^\star}\beta S^\star W^\star+\frac{E}{E^\star}\beta_w S^\star W^\star \text{ and } \frac{(\omega+c)(\gamma+c)}{(1-\sigma)\omega+\sigma\omega\theta}=S^\star\beta+S^\star\beta_w.
\end{aligned}$$

We obtain

$$\begin{aligned}
\dot{\mathcal{H}} =&-c\frac{(S-S^\star)^2}{S}+\beta S^\star(I^\star+\theta A^\star)-\beta S(I+\theta A)+\beta_w S^\star W^\star-\beta_w SW\\
&-\beta S^\star(I^\star+\theta A^\star)\frac{S^\star}{S}+\beta S^\star(I+\theta A)-\beta_w\frac{(S^\star)^2}{S}W^\star+\beta_w S^\star W+\beta S(I+\theta A)\\
&+\beta_w SW-(\omega+c)E-\frac{E^\star}{E}\beta S(I+\theta A)-\frac{E^\star}{E}\beta_w SW+(\omega+c)E^\star+(\omega+c)E\\
&-S^\star(\beta+\beta_w)(I+\theta A)-\frac{I^\star+\theta A^\star}{I+\theta A}(\omega+c)E+S^\star(\beta+\beta_w)W^\star+\beta_w S^\star(I+\theta A)\\
&-\beta_w S^\star W-\beta_w S^\star\frac{W^\star}{W}(I+\theta A)+\beta_w S^\star W^\star.
\end{aligned}$$

Therefore the expression of $\dot{\mathcal{H}}$ reduces to

$$\begin{aligned}\dot{\mathcal{H}} =& -c\frac{(S-S^\star)^2}{S} + \beta S^\star W^\star + \beta_w S^\star W^\star - \beta S^\star W^\star \frac{S^\star}{S} - \beta_w \frac{(S^\star)^2}{S} W^\star \\ & - \frac{E^\star}{E}\beta S(I+\theta A) - \frac{E^\star}{E}\beta_w SW + \beta S^\star W^\star + \beta_w S^\star W^\star \\ & - \frac{I^\star + \theta A^\star}{I+\theta A}\big(\frac{E}{E^\star}\beta S^\star W^\star + \frac{E}{E^\star}\beta_w S^\star W^\star\big) + S^\star \beta W^\star + S^\star \beta_w W^\star \\ & - \beta_w S^\star \frac{W^\star}{W}(I+\theta A) + \beta_w S^\star W^\star.\end{aligned}$$

More simply,

$$\begin{aligned}\dot{\mathcal{H}} =& -c\frac{(S-S^\star)^2}{S} + \beta S^\star W^\star \left(3 - \frac{S^\star}{S} - \frac{E^\star}{E}\frac{S}{S^\star}\frac{I+\theta A}{I^\star+\theta A^\star} - \frac{I^\star+\theta A^\star}{I+\theta A}\frac{E}{E^\star}\right) \\ & + \beta_w S^\star W^\star \left(4 - \frac{S^\star}{S} - \frac{E^\star}{E}\frac{S}{S^\star}\frac{W}{W^\star} - \frac{I^\star+\theta A^\star}{I+\theta A}\frac{E}{E^\star} - \frac{I+\theta A}{W}\right).\end{aligned}$$

Note that

$$\frac{S^\star}{S}\frac{E^\star}{E}\frac{S}{S^\star}\frac{I+\theta A}{I^\star+\theta A^\star}\frac{I^\star+\theta A^\star}{I+\theta A}\frac{E}{E^\star} = 1,$$

and

$$\frac{S^\star}{S}\frac{E^\star}{E}\frac{S}{S^\star}\frac{W}{W^\star}\frac{I^\star+\theta A^\star}{I+\theta A}\frac{E}{E^\star}\frac{I+\theta A}{W} = 1.$$

We recall also the following inequality:

$$\sqrt[n]{x_1 x_2 x_3 \cdots x_n} \le \frac{x_1 + x_2 + x_3 + \cdots + x_n}{n}, \quad x_1, x_2, x_3, \cdots, x_n \ge 0. \tag{8}$$

Since the geometric mean of nonnegative real numbers is less than the arithmetical one, we obtain the inequalities

$$\begin{aligned} 3 - \frac{S^\star}{S} - \frac{E^\star}{E}\frac{S}{S^\star}\frac{I+\theta A}{I^\star+\theta A^\star} - \frac{I^\star+\theta A^\star}{I+\theta A}\frac{E}{E^\star} \le 0, \\ 4 - \frac{S^\star}{S} - \frac{E^\star}{E}\frac{S}{S^\star}\frac{W}{W^\star} - \frac{I^\star+\theta A^\star}{I+\theta A}\frac{E}{E^\star} - \frac{I+\theta A}{W} \le 0.\end{aligned}$$

Therefore $\dot{\mathcal{H}} \le 0$, and one deduces that $\mathcal{E}^\star = (S^\star, E^\star, I^\star, A^\star, W^\star)$ is stable in the sense of Lyapunov.

Now, to show the asymptotic stability of $\mathcal{E}^\star = (S^\star, E^\star, I^\star, A^\star, W^\star)$, we will use the Lasalle invariance principle cited, for instance, in Theorem 3.1 in [13]. To do this, let us define

$$\begin{aligned} s_2 =& -c\frac{(S-S^\star)^2}{S}, \\ s_3 =& 3 - \frac{S^\star}{S} - \frac{E^\star}{E}\frac{S}{S^\star}\frac{I+\theta A}{I^\star+\theta A^\star} - \frac{I^\star+\theta A^\star}{I+\theta A}\frac{E}{E^\star}, \\ s_4 =& 4 - \frac{S^\star}{S} - \frac{E^\star}{E}\frac{S}{S^\star}\frac{W}{W^\star} - \frac{I^\star+\theta A^\star}{I+\theta A}\frac{E}{E^\star} - \frac{I+\theta A}{W}.\end{aligned}$$

Then one has

$$\dot{\mathcal{H}}(S,E,I,A,W) = 0 \Longleftrightarrow s_2 = s_3 = s_4 = 0.$$

Using the above relations, we obtain the following implications:

$$\begin{aligned}&s_2 = 0 \Longrightarrow S = S^\star,\\&(S = S^\star, s_3 = 0) \Longrightarrow E^\star(I + \theta A) = E(I^\star + \theta A^\star),\\&(S = S^\star, E^\star(I + \theta A) = E(I^\star + \theta A^\star), s_4 = 0) \Longrightarrow E^\star W = EW^\star.\end{aligned}$$

Finally, we obtain

$$\dot{\mathcal{H}}(S, E, I, A, W) = 0 \Longleftrightarrow S = S^\star, E^\star(I + \theta A) = E(I^\star + \theta A^\star), E^\star W = EW^\star. \quad (9)$$

Let $r = \dfrac{E}{E^\star} = \dfrac{I + \theta A}{I^\star + \theta A^\star} = \dfrac{W}{W^\star}$, then $E = rE^\star$, $W = rW^\star$ and $I + \theta A = r(I^\star + \theta A^\star) = rW^\star$.

For $S = S^\star$, the first equation of system (1) gives

$$\dot{S} = \dot{S}^\star = N - cS^\star - \beta S^\star(I + \theta A) - \beta_w S^\star W = 0.$$

Replacing $I + \theta A, W$ in the above equation by their values given by (9) yields

$$N - cS^\star - r\beta S^\star(I^\star + \theta A^\star) - r\beta_w S^\star W^\star = 0.$$

By comparing with the first equation of system (6), we deduce that $r = 1$ and therefore $E = E^\star, W = W^\star$ and $I + \theta A = I^\star + \theta A^\star \ \forall \theta > 0$. Finally,

$$\dot{\mathcal{H}}(S, E, I, A, W) = 0 \Longleftrightarrow (S = S^\star, E = E^\star, I = I^\star, A = A^\star, W = W^\star).$$

Thus $\{\mathcal{E}^\star = (S^\star, E^\star, I^\star, A^\star, W^\star)\}$ is the largest invariant set contained in $\{(S, E, I, A, W)|\dot{\mathcal{H}} = 0\}$. Then the global stability of the equilibrium $\mathcal{E}^\star = (S^\star, E^\star, I^\star, A^\star, W^\star)$ holds according to the Lasalle invariance principle [14].

5 Numerical Examples

The parameters used in the implementation of the model (1) are given by $c = 1$, $\beta = 0.5$, $\beta_w = 0.3$, $\omega = 3$, $\gamma = 5$, $\varepsilon = 0.3$, $\sigma = 0.75$, $\theta = 0.25$.

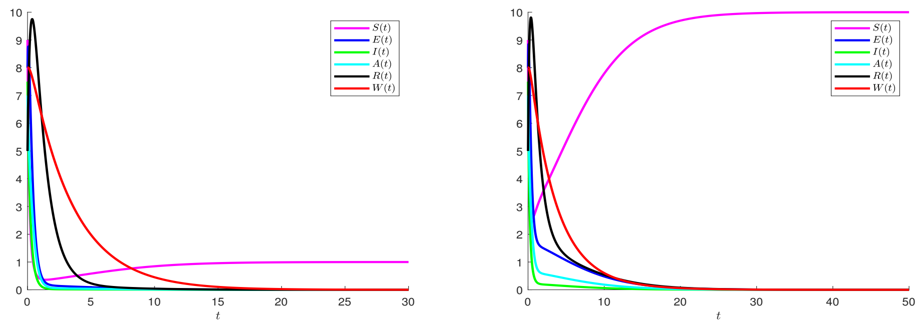

Figure 2: $(S(t), E(t), I(t), A(t), R(t), W(t))$ behaviours for $N = 1$(left), then $\mathcal{R} = 0.044 \leq 1$, and for $N = 10$(right), then $\mathcal{R} = 0.438 \leq 1$.

Four tests were considered. Two of them (Figure 2) confirming the global stability of the disease-free equilibrium $\mathcal{E}^0$ when $\mathcal{R} \leq 1$. We note that the solution of system (1) converges asymptotically to $\mathcal{E}^0$ and only susceptible compartment persists and the other compartments vanish.

The other two tests (Figure 3) confirm the global stability of the disease-persistence equilibrium $\mathcal{E}^\star$ when $\mathcal{R} > 1$. We observe that the solution of system (1) converges asymptotically to $\mathcal{E}^\star$ and all compartments persist.

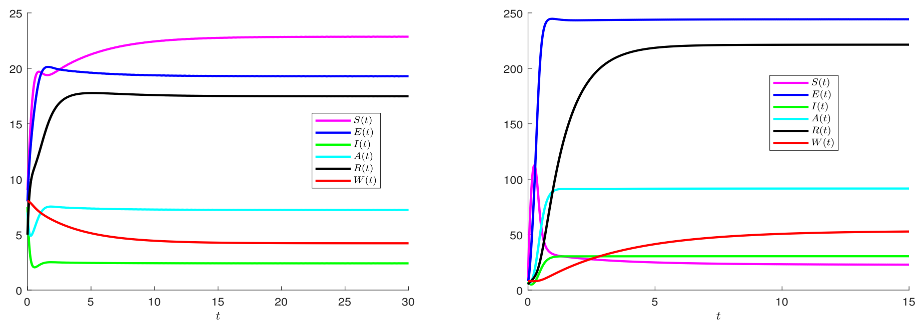

Figure 3: $(S(t), E(t), I(t), A(t), R(t), W(t))$ behaviours for $N = 100$(left), then $\mathcal{R} = 4.375 > 1$, and for $N = 1000$(right), then $\mathcal{R} = 43.75 > 1$.

6 Concluding Remarks

In this paper, we have considered an epidemic model for the Covid-19 coronavirus, in which we have divided the total population into five compartments, namely, susceptible, exposed, symptomatic infected, asymptomatic infected and recovered, and we investigated the dynamical behavior of this model. Here, we have found that

$$\mathcal{R} = \frac{N(\beta + \beta_w)\big((1-\sigma)\omega + \sigma\omega\theta\big)}{c(\omega + c)(\gamma + c)}$$

is the basic reproduction number of system (1), which helps us to determine the dynamical behavior of the system. We showed, for system (1), that the disease-free equilibrium $\mathcal{E}^0$ is globally asymptotically stable when $\mathcal{R} < 1$. However, when $\mathcal{R} > 1$, the endemic equilibrium $\mathcal{E}^\star$ is both locally and globally stable. These results have been verified numerically for some parameters of the model.

Acknowledgment

The author wishes to thank the Editor and the anonymous Reviewers for their helpful feedback to improve the quality of this manuscript.

References

[1] S. Alsahafi and S. Woodcock. Local Analysis for a Mutual Inhibition in Presence of Two Viruses in a Chemostat. *Nonlinear Dynamics and Systems Theory* **21** (4) (2021) 337–359.

[2] T. Chen, J. Rui, Q. Wang, Z. Zhao, J. A. Cui and L. Yin. A mathematical model for simulating the phase-based transmissibility of a novel coronavirus. *Infectious Diseases of Poverty* **9** (24) (2020), 8 pages.

[3] T. Chen, R. K. Leung, Z. Zhou, R. Liu, X. Zhang and L. Zhang. Investigation of key interventions for shigellosis outbreak control in China. *PLoS One* **9** (2014), e95006.

[4] M. H. DarAssi and M. A. Safi. Analysis of an SIRS Epidemic Model for a Disease Geographic Spread. *Nonlinear Dynamics and Systems Theory* **21** (1) (2021) 56–67.

[5] O. Diekmann and J. Heesterbeek. On the definition and the computation of the basic reproduction ratio R_0 in models for infectious diseases in heterogeneous populations. *J. Math. Biol.* **28** (4) (1990) 365–382.

[6] P. Van den Driessche and J. Watmough. Reproduction Numbers and Sub-Threshold Endemic Equilibria for Compartmental Models of Disease Transmission. *Math. Biosci.* **180** (2002) 29–48.

[7] M. El Hajji. Modelling and optimal control for Chikungunya disease. *Theory Biosci.* **140** (1) (2021) 27–44.

[8] M. El Hajji, A. Zaghdani and S. Sayari. Mathematical analysis and optimal control for Chikungunya virus with two routes of infection with nonlinear incidence rate. *Int. J. Biomath.* (2021) 2150088.

[9] M. El Hajji, S. Sayari and A. Zaghdani. Mathematical analysis of an "SIR" epidemic model in a continuous reactor - deterministic and probabilistic approaches. *J. Korean Math. Soc.* **58** (1) (2021) 45–67.

[10] M. El Hajji and S. Sayari. Analysis of a fractional-order "SVEIR" epidemic model with a general nonlinear saturated incidence rate in a continuous reactor. *Asian Research J. Math.* **12** (4) (2019) 1–17.

[11] M. El Hajji. Boundedness and asymptotic stability of nonlinear volterra integro-differential equations using Lyapunov functional. *J. King Saud Univ. Sci.* **31** (4) (2019) 1516–1521.

[12] M. El Hajji, N. Chorfi and M. Jleli. Mathematical model for a membrane bioreactor process. *Electron. J. Diff. Eqns.* **2015** (315) (2015) 1–7.

[13] J.K. Hale. *Ordinary Differential Equations.* John Wiley & Sons, New York, 1969.

[14] J.P. LaSalle. *The Stability of Dynamical Systems.* 25, SIAM, 1976.

[15] S. Sayari and M. El Hajji. How the Fractional-ordre Improve and Extend the Well-Known Competitive Exclusion Principle in the Chemostat Model with n Spacies Competing for a Single Resource?. *Asian Research J. Math.* **12** (3) (2019) 1–12.

[16] A. Zaghdani. Mathematical Study of a Modifed SEIR Model for the Novel SARS-Cov-2 Coronavirus. *Nonlinear Dynamics and Systems Theory* **21** (3) (2021) 326–336.

Nonlinear Dynamics and Systems Theory, **22** (1) (2022) 97–104

Finite Element Solution to the Strongly Reaction-Diffusion System

Muhannad A. Shallal [1], Adham A. Ali [2*] and Ali M. Jasim [1]

[1] *Department of Mathematics, College of Science, University of Kirkuk, Kirkuk, Iraq.*
[2] *Department of Software, College of Computer Science and Information Technology, University of Kirkuk, Kirkuk, Iraq.*

Received: May 19, 2021; Revised: December 9, 2021

Abstract: This research is devoted to demonstrating a numerical solution that adopts the cubic Hermite finite element method for a strongly reaction-diffusion system. L_2 and L_∞ error norms computed at varying time points are employed to draw comparisons between the numerical solutions attained by virtue of the presented technique and both the exact solutions and the analogous numerical ones already available in the literature. Evaluating the accuracy and efficacy of the technique utilized in this study, a perfect agreement with the exact solution is concluded.

Keywords: *finite element method; strongly reaction-diffusion system; cubic Hermite element.*

Mathematics Subject Classification (2010): 74S05, 76M10, 35K57, 70K99.

1 Introduction

The reaction diffusion system occurs in multifarious physical, biological and chemical problems. Numerous numerical techniques such as a cubic B-spline method [1], linearized finite difference scheme based upon the order reduction method [2], exponential cubic B-spline collocation algorithms [3], and trigonometric quintic B-spline collocation method [4] have been used to solve the strongly reaction-diffusion system. On the other hand, global solutions for this system have been addressed in [5]– [9]. The finite element method is one of the most accurate, flexible, and powerful techniques for approximating the solution to a wide range of linear and nonlinear partial differential equations. Examples of its implementation include: the Rosenau-RLW equation by Atouani and Omrani [10], fourth order parabolic equation by Chai et al. [11], biharmonic equation by

* Corresponding author: mailto:adham.ali@uokirkuk.edu.iq

Mu et al. [12], Cahn-Hilliard equation by Wang et al. [13], coupled bulk-surface problems by Burman et al. [14], fracture model in porous media by Capatina et al. [15], Stokes-Darcy coupling by Camano et al. [16], Cahn-Hilliard-Navier-Stokes-Darcy phase field model by Gao et al. [17], and Navier-Stokes/Darcy coupled problem by Discacciati and Oyarza [18], nonlinear nonstandard Volterra integral equations by Khumalo and Dlamini [19], and higher order fractional boundary value problems by Darweesh and Al-Khaled [20]. This paper is organized as follows: In Section 2, the application of the finite element method to the strongly reaction-diffusion system is presented; in Section 3, numerical results are illustrated and discussed. Finally, the paper ends with conclusions in Section 4.

2 Finite Element Solution to the Strongly Reaction-Diffusion System

Consider the strongly reaction-diffusion system as follows:

$$u_t = u_{xx} + (2\pi^2 - 1)u - 2\pi^2 v\,, 0 < x < 1,\ 0 < t < T, \tag{1}$$

$$v_t = u_{xx} + v_{xx} - v\,, 0 < x < 1,\ 0 < t < T \tag{2}$$

with the following boundary and initial conditions:

$$u_x(0,t) = 0\,, u_x(1,t) = 0\,, v_x(0,t) = 0\,, v_x(1,t) = 0\,, 0 < t < T, \tag{3}$$

$$u(x,0) = sin^2\pi x, \quad v(x,0) = cos^2\pi x, \quad 0 < x < 1\,, \tag{4}$$

where $u = u(x,t)$ and $v = v(x,t)$ are two substances of interacting concentrations. The exact solution of the system is [2]

$$u(x,t) = e^{-t} sin^2\pi x, \quad v(x,t) = e^{-t} cos^2\pi x\,.$$

Multiplying equations (1) and (2) by a test function, $w \in W(\Omega)$, where $\Omega = (a,b)$, $a,b \in \Re$, and conducting integration over the finite element (x_e, x_{e+1}) with the length h, we obtain the following equations:

$$\int_{x_e}^{x_{e+1}} (wu_t - wu_{xx} + (1 - 2\pi^2)wu + 2\pi^2 wv)dx = 0, \tag{5}$$

$$\int_{x_e}^{x_{e+1}} (wv_t - wu_{xx} - wv_{xx} + wv)dx = 0\,, \tag{6}$$

which give

$$\int_{x_e}^{x_{e+1}} (wu_t + w_x u_x + (1 - 2\pi^2)wu + 2\pi^2 wv)dx = 0, \tag{7}$$

$$\int_{x_e}^{x_{e+1}} (wv_t + w_x u_x + w_x v_x + wv)dx = 0\,. \tag{8}$$

Owing to the test function w, which satisfies the essential boundary condition, the boundary terms vanish when performing integration by parts. Then the acquired solution that is an approximation to the exact solution can be written as

$$\begin{aligned} u(x,t) &= \sum_{s=1}^{n_e} u_s(t) H_s(x)\,, \\ v(x,t) &= \sum_{s=1}^{n_e} v_s(t) H_s(x)\,, \\ w(x) &= H_i(x)\,, \qquad i = 1, ..., n_e. \end{aligned} \tag{9}$$

Here, $u_s(t)$ and $v_s(t)$, $s = 1, ..., n_e$, are undetermined time dependent quantities and $H_s(x)$ are the interpolation functions. By substituting (9) into (7) and (8), we obtain

$$\sum_{s=1}^{n_e} \int_0^h (H_i H_s \dot{u}_s + H_i' H_s' u_s + (1 - 2\pi^2) H_i H_s u_s + 2\pi^2 H_i H_s v_s) dx = 0, \tag{10}$$

$$\sum_{s=1}^{n_e} \int_0^h (H_i H_s \dot{v}_s + H_i' H_s' u_s + H_i' H_s' v_s + H_i H_s v_s) dx = 0\,, \tag{11}$$

where $\cdot$ denotes the derivative with respect to time. Rewriting the equations (10) and (11) in a matrix form, we get

$$A^e \dot{u}^e + (B^e + (1 - 2\pi^2) A^e) u^e + 2\pi^2 A^e v^e = 0, \tag{12}$$

$$A^e \dot{v}^e + B^e u^e + (B^e + A^e) v^e = 0\,. \tag{13}$$

For the cubic Hermite element, the matrices A^e_{is} and B^e_{is} are given as follows:

$$A^e_{is} = \int_0^h H_i H_s dx = \begin{bmatrix} \frac{13h}{35} & -\frac{11h^2}{210} & \frac{9h}{70} & \frac{13h^2}{420} \\ -\frac{11h^2}{210} & \frac{h^3}{105} & -\frac{13h^2}{420} & -\frac{h^3}{140} \\ \frac{9h}{70} & -\frac{13h^2}{420} & \frac{13h}{35} & \frac{11h^2}{210} \\ \frac{13h^2}{420} & -\frac{h^3}{140} & \frac{11h^2}{210} & \frac{h^3}{105} \end{bmatrix},$$

$$B^e_{is} = \int_0^h H_i' H_s' dx = \begin{bmatrix} \frac{6}{5h} & -\frac{1}{10} & -\frac{6}{5h} & -\frac{1}{10} \\ -\frac{1}{10} & \frac{2h}{15} & \frac{1}{10} & -\frac{h}{30} \\ -\frac{6}{5h} & \frac{1}{10} & \frac{6}{5h} & \frac{1}{10} \\ -\frac{1}{10} & -\frac{h}{30} & \frac{1}{10} & \frac{2h}{15} \end{bmatrix}.$$

The global matrix equation resulted in assembling the element matrices for every included element is formulated by

$$A\dot{u} + (B + (1 - 2\pi^2) A) u + 2\pi^2 A v = 0, \tag{14}$$

$$A\dot{v} + Bu + (B + A) v = 0\,. \tag{15}$$

For the cubic Hermite elements, let $v_{2k-1} = v_x(x_{k-1})$, $u_{2k-1} = u_x(x_{k-1})$, $k = 1, ..., n$, $v_{2k} = v(x_k)$, $u_{2k} = u(x_k)$, $k = 1, ..., n-1$, $v_{2n} = v_x(x_n)$, $u_{2n} = u_x(x_n)$. Afterwards, the formula of the forward finite difference and the Crank-Nicolson scheme are employed to discretize time derivatives $\dot{u}$, $\dot{v}$ and the time dependent quantities $u(t)$, $v(t)$ in equations (14) and (15), respectively:

$$\dot{u} = \frac{u^{j+1} - u^j}{\triangle t}, \dot{v} = \frac{v^{j+1} - v^j}{\triangle t}, u = \frac{u^{j+1} + u^j}{2}, v = \frac{v^{j+1} + v^j}{2}.$$

This leads to

$$\left[\left(1 + \frac{k}{2} - k\pi^2\right) A + \frac{k}{2} B\right] u^{n+1} + k\pi^2 A v^{n+1} = \left[\left(1 - \frac{k}{2} + k\pi^2\right) A - \frac{k}{2} B\right] u^n - k\pi^2 A v^n,$$

$$\left[\left(1 + \frac{k}{2}\right) A + \frac{k}{2} B\right] v^{n+1} + \frac{k}{2} B u^{n+1} = \left[\left(1 - \frac{k}{2}\right) A - \frac{k}{2} B\right] v^n - \frac{k}{2} B u^n,$$

where $k = \triangle t, \{u\} = \{u_x(x_0), u_x(x_1), u_x(x_2), ..., u_x(x_{n-1}), u(x_{n-1}), u_x(x_n)\}^T$, and similarity holds for $\{v\}$.

3 Numerical Results

Aiming at computing a numerical solution for a strongly reaction-diffusion system with the initial conditions (4) and boundary conditions (3), the proposed finite element solution with the cubic Hermite element is applied. Both the L_2 and L_∞ error norms defined by

$$L_2 = \|u^{exact} - u^{num}\|_2 = \sqrt{h \sum_{j=0}^{n} |u_j^{exact} - u_j^{num}|^2},$$

$$L_\infty = \max_j |u_j^{exact} - u_j^{num}|$$

are used as tools to measure the accuracy of the method under consideration. In Table 1 and Table 2, L_2 and L_∞ and error norms at different time levels and different number of partitions have been computed and compared with the errors obtained by [1]. The absolute errors of the proposed numerical solution at some points with $t = 1$ are evaluated and compared with the errors obtained by [1] and [2] and are reported in Tables 3 and 4. It can be seen from Tables 1 and 2 that the error norms obtained from the numerical results reduce with the increasing number of partitions. This indicates that the convergence towards the exact solution increases with the increasing number of partitions for different time levels. It is noted that the convergence towards the exact solution is achieved when $t = 1$ and with different values of x, as shown in Tables 3 and 4. From Tables $1-4$, we observe that our technique has yielded results that are very close to the exact solution. Moreover, in Figs. 1 and 2, the numerical solutions for $u(x,t)$ and $v(x,t)$ have been plotted with the exact solutions at different times. We notice that the plots of those solutions are indistinguishable.

4 Conclusions

A numerical scheme that involves the finite element method with the cubic Hermite element for solving the strongly reaction-diffusion system has been described. The accuracy and performance of the method has been measured using the L_2 and L_∞ error norms. We have illustrated that our numerical results are of higher accuracy than those produced by other methods $[1,2]$. Furthermore, the proposed method shows perfect agreement with the exact solution for different values of time and step size. Here, we point out that the proposed method for dealing with this system is relatively new and more efficient than other methods that were used recently. Therefore, we recommend using this technique to solve different types of partial differential equations.

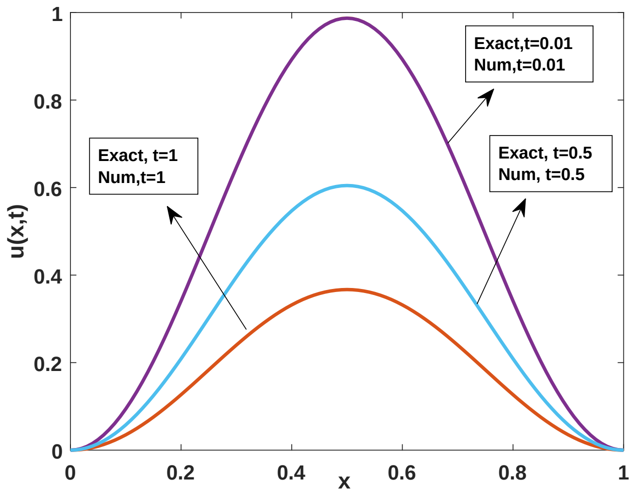

Figure 1: Comparison between numerical and exact solutions for $u(x,t)$ at different time levels .

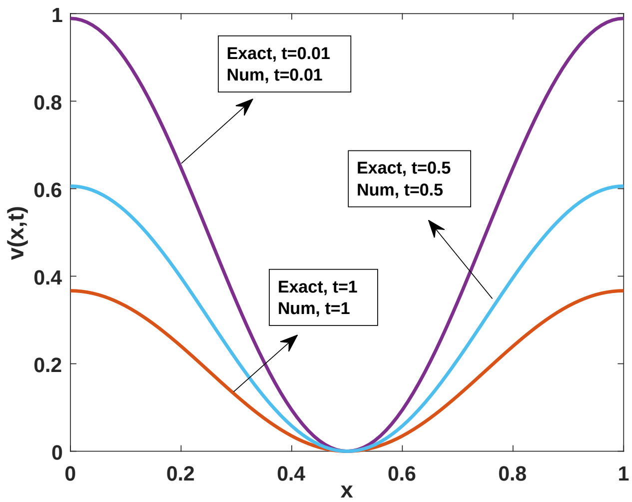

Figure 2: Comparison between numerical and exact solutions for $v(x,t)$ at different time levels .

	T	0.01	0.1	0.5	1
N=100	L_2	3.600E-6	2.731E-5	4.114E-4	5.763E-4
	L_2 [1]	5.90E-05	4.24E-04	1.33E-03	1.60E-03
	L_∞	3.900E-6	3.031E-5	7.233E-4	8.863E-4
	L_∞ [1]	6.95E-05	5.47E-04	2.56E-03	5.06E-03
N=300	L_2	4.231E-7	3.851E-6	3.577E-5	9.224E-5
	L_2 [1]	6.56E-06	4.71E-05	1.48E-04	1.81E-03
	L_∞	4.920E-7	4.371E-6	5.602E-5	8.011E-5
	L_∞ [1]	7.67E-06	6.04E-05	2.83E-04	5.61E-03
N=500	L_2	8.872E-8	6.655E-7	2.143E-6	5.341E-6
	L_2 [1]	2.36E-06	1.69E-05	5.34E-05	8.10E-05
	L_∞	9.774E-8	8.971E-7	9.033E-6	7.558E-6
	L_∞ [1]	2.76E-06	2.17E-05	1.01E-05	2.15E-05

Table 1: Errors at different times and different number of partition for $u(x,t)$ at $\triangle t = 0.001$.

	T	0.01	0.1	0.5	1
N=100	L_2	2.177E-06	2.897E-05	3.015E-04	2.882E-04
	L_2 [1]	1.05E-05	3.25E-04	1.26E-03	1.55E-03
	L_∞	2.683E-06	3.622E-05	5.223E-04	6.531E-04
	L_∞ [1]	1.22E-05	4.14E-04	2.40E-03	4.87E-03
N=300	L_2	1.899E-07	4.411E-06	2.774E-05	2.011E-05
	L_2 [1]	1.16E-06	3.62E-05	1.40E-04	1.74E-04
	L_∞	2.311E-07	5.102E-06	4.111E-05	5.978E-05
	L_∞ [1]	1.36E-06	4.61E-05	2.68E-04	5.45E-04
N=500	L_2	3.443E-08	1.899E-06	7.012E-07	6.767E-07
	L_2 [1]	4.21E-07	1.30E-05	5.07E-05	6.39E-05
	L_∞	3.895E-08	3.773E-06	9.887E-07	8.577E-07
	L_∞ [1]	4.90E-07	1.66E-05	9.65E-05	1.96E-05

Table 2: Errors at different times and different number of partition for $v(x,t)$ at $\triangle t = 0.001$.

n \ x	0.125	0.375	0.625	0.875
16	1.53213E-02	1.69554E-02	1.99778E-02	2.15531E-02
16[1]	3.7790E-02	3.7791E-02	3.7791E-02	3.7790E-02
16[2]	5.5265371E−2	3.1302542E−1	3.1302542E−1	5.5265370E−2
64	6.88663E-04	7.11213E-04	7.88990E-04	8.11892E-04
64[1]	2.7412E-03	2.7476E-03	2.7476E-03	2.7413E-03
64[2]	5.3961404E−2	3.1394376E−1	3.1394376E−1	5.3961404E−2
128	3.01234E-04	3.44501E-04	3.77006E-04	4.11002E-04
128[1]	6.9649E-04	6.8634E-04	6.8638E-04	6.9640E-04
128[2]	5.3896378E−2	3.1398950E−1	3.1398950E−1	5.3896368E−2
256	3.11332E-05	3.76654E-05	3.99815E-05	5.11234E-05
256[1]	1.9977E-04	1.4640E-04	1.4610E-04	2.0048E-04
256[2]	5.3880114E−2	3.1400093E−1	3.1400093E−1	5.3880114E−2
512	6.11889E-06	6.54321E-06	6.78802E-06	7.55001E-06
512[1]	5.1944E-05	4.5862E-05	4.6101E-05	5.2920E-05
512[2]	5.3876051E−2	3.1400379E−1	3.1400379E−1	5.3876051E−2

Table 3: The absolute errors between numerical and exact solution of $u(x,t)$ at $t = 1$.

n \ x	0.125	0.375	0.625	0.875
16	1.60011E-02	1.88555E-02	2.10044E-02	2.51110E-02
16[1]	3.6998E-02	3.6998E-02	3.6998E-02	3.6998E-02
16[2]	3.1290313E−1	5.5387659E−2	5.5387659E−2	3.1290313E−1
64	6.77134E-04	6.89891E-04	7.25778E-04	7.52211E-04
64[1]	2.6762E-03	2.6762E-03	2.6762E-03	2.6762E-03
64[2]	3.1393791E−1	5.3967251E−2	5.3967251E−2	3.1393791E−1
128	3.44899E-04	3.61122E-04	3.98877E-04	4.23321E-04
128[1]	6.7411E-04	6.7406E-04	6.7407E-04	6.7408E-04
128[2]	3.1398804E−1	5.3897831E−2	5.3897831E−2	3.1398804E−1
256	3.32211E-05	3.58876E-05	3.77521E-05	4.01903E-05
256[1]	1.6873E-04	1.6888E-04	1.6877E-04	1.6898E-04
256[2]	3.1400057E−1	5.3880480E−2	5.3880480E−2	3.1400057E−1
512	6.75665E-06	7.10099E-06	7.45565E-06	7.87890E-06
512[1]	4.2123E-05	4.2271E-05	4.2184E-05	4.2334E-05
512[2]	3.1400370E−1	5.3876143E−2	5.3876143E−2	3.1400370E−1

Table 4: The absolute errors between numerical and exact solution of $v(x,t)$ at $t = 1$.

References

[1] M. Abbas, A. A. Majid, Md. AI. Ismail and A. Rashid. Numerical Method Using Cubic B-Spline for a Strongly Coupled Reaction-Diffusion System. *PloS one* **9** (1) (2014) e83265.

[2] H. Y. Cao and Z. S. Zhong. A second-order linearized difference scheme for a strongly coupled reaction-diffusion system. *Numerical Methods for Partial Differential Equations: An International Journal* **24** (1) (2008) 9–23.

[3] O. Ersoy and I. Dag. Numerical solutions of the reaction diffusion system by using exponential cubic B-spline collocation algorithms. *Open Physics* **13** (1) (2015) 414–427.

[4] A. T. Onarcan, N. Adar and Dag. Numerical solutions of reaction-diffusion equation systems with trigonometric quintic B-spline collocation algorithm. *arXiv* (1) (2017).

[5] E. H. Daddiouaissa. Existence of global solutions for a system of reaction-diffusion equations having a triangular matrix. *Electronic Journal of Differential Equations* **2008** (141) (2015) 1–9.

[6] M. Kirane. Global bounds and asymptotics for a system of reaction-diffusion equations. *Journal of Mathematical Analysis and Applications* **138** (2) (1989) 328–342.

[7] L. W. Somathilake and J.M.J.J. Peiris. Global solutions of a strongly coupled reaction-diffusion system with different diffusion coefficients. *Journal of Applied Mathematics* **2005** (1) (2005) 23–36.

[8] C. X. Jiang. Global Bounded Solutions of a Strongly Coupled Reaction–Diffusion System. *Nonlinear Studies* **7** (2) (2000) 22–240.

[9] S. Badraoui. Existence of global solutions for systems of reaction-diffusion equations on unbounded domains. *Electronic Journal of Differential Equations* **2002** (74) (2002) 1–10.

[10] N. Atouani and K. Omrani. Galerkin finite element method for the Rosenau-RLW equation. *Computers and Mathematics with Applications* **66** (3) (2013) 289–303.

[11] S. Chai, Y. Zou, C. Zhou and W. Zhao. Weak Galerkin finite element methods for a fourth order parabolic equation. *Numerical Methods for Partial Differential Equations* **35** (5) (2019) 1745–1755.

[12] L. Mu, J. Wang and X. Ye. Effective implementation of the weak Galerkin finite element methods for the biharmonic equation. *Computers and Mathematics with Applications* **74** (6) (2017) 1215–1222.

[13] J. Wang, Q. Zhai, R. Zhang and S. Zhang. A weak Galerkin finite element scheme for the Cahn-Hilliard equation. *Mathematics of Computation* **88** (315) (2019) 211–235.

[14] E. Burman, P. Hansbo, M. G. Larson and S. Zahedi. Cut finite element methods for coupled bulk–surface problems. *Numerische Mathematik* **133** (2) (2016) 203–231.

[15] D. R. Capatina, H. Luce, H. El-Otmany and N. Barrau. Nitsche's extended finite element method for a fracture model in porous media. *Applicable Analysis* **95** (10) (2016) 2224–2242.

[16] J. Camano, G.N. Gatica, R. Oyarza and R. Ruiz-Baier. New fully-mixed finite element methods for the Stokes–Darcy coupling. *Computer Methods in Applied Mechanics and Engineering* **295** (2015) 362–395.

[17] Y. Gao, X. He, L. Mei and X. Yang. Decoupled, linear, and energy stable finite element method for the Cahn-Hilliard-Navier-Stokes-Darcy phase field model. *SIAM Journal on Scientific Computing* **40** (1)(2018) B110–B137.

[18] M. Discacciati and R. Oyarza. A conforming mixed finite element method for the Navier–Stokes/Darcy coupled problem. *Numerische Mathematik* **135** (2)(2017) 571–606.

[19] M. Khumalo and A. Dlamini. The Finite Element Method for Nonlinear Nonstandard Volterra Integral Equations. *Nonlinear Dynamics and Systems Theory* **20** (2) (2020) 191–202.

[20] A. Darweesh and K. Al-Khaled. Sinc-Galerkin Method for Solving Higher Order Fractional Boundary Value Problems. *Nonlinear Dynamics and Systems Theory* **20** (3) (2020) 267–281.

Nonlinear Dynamics and Systems Theory, **22** (1) (2022) 105–116

Global Stability and Optimal Harvesting of Predator-Prey Model with Holling Response Function of Type II and Harvesting in Free Area of Capture

Syamsuddin Toaha *, Firman and Agustinus Ribal

Department of Mathematics, Faculty of Mathematics and Natural Sciences, Hasanuddin University, Indonesia

Received: May 31, 2021; Revised: December 26, 2021

Abstract: This paper analyzes the dynamical behavior of predator and prey in free and forbidden areas of capture. The dynamics of the populations are expressed in the form of equations system. The predator and prey in the free area are exploited with fixed efforts. The presence of an interior fixed point and its stability is studied. Harvesting efforts as control variables in the model are discussed. The interior fixed point is connected to the problems of maximizing the profit and present value. Local stability of the fixed point is analyzed via linearization and global stability in terms of the Lyapunov function. A critical value of fixed efforts is found, maximizing the profit function and the fixed point remains stable. According to Pontryagin's maximum principle, there exists an optimal path for the harvesting efforts that maximizes the present value of revenues. The predator and prey populations are possibly living together for a certain span of time even though the predator and prey populations are harvested with efforts as control variables. From simulation, the control variables can reduce the predator population and increase the prey population.

Keywords: *predator-prey model; free area of capture; global stability; maximum profit; present value.*

Mathematics Subject Classification (2010): 34Dxx, 49-XX .

* Corresponding author: mailto:syamsuddint@gmail.com

1 Introduction

In various fields, studies on nonlinear dynamics of systems include the behavior and stability of the systems, both local and global stability, for example, see [1], [2], and [3]. The dynamics of population is one of interesting objects of research in the field of mathematical ecology. Interaction between some populations such as predation, competition, and mutualism has ecological consequences. Population as a useful stock also has social and economics consequences. The study of dynamical behavior of population becomes complex and comprehensive because population as a stock should be managed well to protect the population from extinction, besides, the population also gives more benefits for a certain span of time.

Modeling in predator and prey populations involves many factors such as harvesting, tax, migration, diffusion, and stage structure, which have been widely studied by many researchers. Some of them considered the dynamics of one predator with two preys or two predators with one prey in the population behavior. The authors in [4] studied the dynamics of population with a reserve area and imposed tax to control the overexploitation of the populations. In [5], the authors also studied the dynamics of populations in the reserve area with harvesting and considered the problem on maximizing the present value. The behavior of the stage structure of predator and prey model in the two areas of environment with harvesting in the free area of capture was discussed in [6] and a certain condition was obtained to get an optimal value of harvesting.

The effect of selective harvesting in predator and prey populations has been observed in some purposes. Some researchers have examined only the prey being harvested, see for instance [4], [7], and [8]. The studies of predator and prey models when only the predator is harvested, can be seen in [9], [10], [11], and [12]. Some other researchers have studied predator prey models by considering both populations being harvested, the examples can be seen in [10] and [13]. Predator and prey models with exploitation were often associated with the economic point of view including maximum profit and present value problems, some examples can be found in [4], [5], and [13].

In Malili Lake Complex, South Sulawesi, Indonesia, butani fish (Glossogobius matanansis) which lives at the bottom of the lakes and its predator nile tilapia fish (Oreochromis nilotichus) are sources of food for the surrounding community. The dynamics of butani fish as an endemic and its predator must be managed properly to prevent the fish from the extinction. Based on the findings of the researchers above and as a strategy to manage the endemic butani fish and its predator, we consider the dynamical behaviors of both predator and prey populations, where the prey lives in two areas, one of which is a free area of capture and another area is a forbidden area of capture. The economically valuable predator and prey in the free area are exploited with fixed efforts. We study the presence of an interior fixed point and its local and global stability.

2 The Dynamical Behavior of Predator and Prey Populations

We consider predator and prey populations in an environment involving two areas, namely, forbidden and free areas of capture, when no fishing is allowed in the forbidden area. Both areas are considered to have the same conditions. The prey population can move in these areas freely. The prey populations grow in both areas when no predators are assumed to follow the logistic equation. The predator population is assumed to only eat the prey in the free area of capture. The behavior of predator and prey populations are stated in the form of the equations system as follows:

$$\frac{dx}{dt} = rx\left(1-\frac{x}{K}\right)-\tau_1 x+\tau_2 y-\frac{axz}{a+x}, \tag{1}$$

$$\frac{dy}{dt} = sy\left(1-\frac{y}{L}\right)+\tau_1 x-\tau_2 y, \tag{2}$$

$$\frac{dz}{dt} = \frac{\beta\alpha xz}{a+x}-kz. \tag{3}$$

From ecological point of view, we simply consider the model (1)-(3) in $R^3_+ = (x,y,z) \in R^3 \mid x,y,z>0$ or in R^3_+. The variables x and y as the functions of time t denote the population sizes of prey in the free area of capture and in the forbidden area, respectively. The variable z as a function of t denotes the population size of the predator in the free area of capture. The growth rate of populations x and y is denoted by r and s, respectively. Carrying capacity of the environment for populations x and y is denoted by K and L, respectively. The predation rate is denoted by α, and the value of β ($0<\beta<1$) is the predation scale. Parameter τ_1 denotes the movement rate for the prey from the free area to the forbidden area. Parameter τ_2 denotes the movement rate for the prey from the forbidden area to the free area. Parameter k is the mortality rate for the predator in the free area of capture.

The populations are assumed as beneficial stocks, then the predator and the prey populations in the free area of capture are harvested with fixed efforts. The dynamical behavior of predator and prey populations is developed and stated as follows:

$$\frac{dx}{dt} = rx\left(1-\frac{x}{K}\right)-\tau_1 x+\tau_2 y-\frac{axz}{a+x}-q_1E_1x, \tag{4}$$

$$\frac{dy}{dt} = sy\left(1-\frac{y}{L}\right)+\tau_1 x-\tau_2 y, \tag{5}$$

$$\frac{dz}{dt} = \frac{\beta\alpha xz}{a+x}-kz-q_2E_2z. \tag{6}$$

In the model (4)-(6), parameters q_1 and q_2 denote the catchability levels for the prey and predator populations, respectively. The symbols E_1 and E_2 denote the fixed efforts of harvesting satisfying $0 \le E_i \le E_{imax}$ for $i = 1, 2$ and some given value of E_{imax}.

3 Local and Global Stability of Interior Fixed Point

The interior fixed point for model (4)–(6) may exist as long as a certain condition is satisfied. The fixed point of model (4)–(6) is found by equating the equations of the system to zero and solving them. The interior fixed point for the model is $EQ = (x_1, y_1, z_1)$, where
$x_1 = \frac{a(k+q_2E_2)}{\alpha\beta-k-q_2E_2}$, $y_1 = \frac{L(s-\tau_2)+\sqrt{L^2(s-\tau_2)^2+4s\tau_1Lx_1}}{2s}$, and
$z_1 = \frac{\left(rKx_1-rx_1^2-\tau_1Kx_1+\tau_2Ky_1-q_1KE_1x_1\right)(a+x_1)}{K\alpha x_1}$.

From model (4)–(6), we get the Jacobian matrix evaluated at the fixed point $EQ = (x_1, y_1, z_1)$ as

$$J_E = \begin{pmatrix} d_1 & \tau_2 & -d_2 \\ \tau_1 & d_3 & 0 \\ d_4 & 0 & d_5 \end{pmatrix},$$

where $d_1 = r - \frac{2rx_1}{K} - \tau_1 - \frac{\alpha az}{(a+x_1)^2} - q_1E_1$, $d_2 = \frac{\alpha x_1}{a+x_1}$, $d_3 = s - \frac{2sy}{L} - \tau_2$, $d_4 = \frac{\alpha\beta az}{(a+x_1)^2}$, and $d_5 = \frac{\alpha\beta x_1}{a+x_1} - k - q_2E_2$.

The characteristic polynomial corresponds to the Jacobian matrix J_E and is expressed as $f(\lambda) = det(\lambda I - J_E)$, i.e.,

$$f(\lambda) = \lambda^3 + b_2\lambda^2 + b_1\lambda + b_0, \tag{7}$$

where $b_2 = -(d_1 + d_3 + d_5)$, $b_1 = -\tau_1\tau_2 + d_1d_3 + d_1d_5 + d_2d_4 + d_3d_5$, and $b_0 = \tau_1\tau_2d_5 - d_1d_3d_5 - d_2d_3d_4$. From equation (7) and according to the Routh-Hurwitz criteria of stability [14], the interior fixed point $EQ = (x_1, y_1, z_1)$ is locally and asymptotically stable provided the conditions $b_0 > 0, b_2 > 0$, and $b_2b_1 - b_0 > 0$ are satisfied. Global stability of the interior fixed point $EQ = (x_1, y_1, z_1)$ is analyzed using the Lyapunov function. We suppose that the conditions for the presence of the interior fixed point are satisfied. Consider a Lyapunov function

$$V(x,y,z) = \beta\left(x - x_1 - x_1 ln\frac{x}{x_1}\right) + \left(y - y_1 - y_1 ln\frac{y}{y_1}\right) + \left(z - z_1 - z_1 ln\frac{z}{z_1}\right). \tag{8}$$

It is clear that $V(x,y,z)$ is defined and also continuous for all x, y, and $z > 0$. Differentiate the Lyapunov function (8) with respect to t to get

$$\begin{aligned}\frac{dV}{dt} &= \beta\left(\frac{dx}{dt} - \frac{x_1}{x}\frac{dx}{dt}\right) + \left(\frac{dy}{dt} - \frac{y_1}{y}\frac{dy}{dt}\right) + \left(\frac{dz}{dt} - \frac{z_1}{z}\frac{dz}{dt}\right)\\ &= \beta\left(x - x_1\right)\left(r - \frac{rx}{K} - \tau_1 + \tau_2\frac{y}{x} - \frac{\alpha z}{a+x}\right)\\ &+ \left(y - y_1\right)\left(s - \frac{sy}{L} + \tau_1\frac{x}{y} - \tau_2\right) + \left(z - z_1\right)\left(\frac{\alpha\beta x}{a+x} - k\right).\end{aligned} \tag{9}$$

Since $EQ = (x_1, y_1, z_1)$ is an interior fixed point, it follows that $rx_1 - \frac{rx_1^2}{K} - \tau_1x_1 + \tau_2y_1 - \frac{\alpha z_1x_1}{a+x_1} = 0$, $sy_1 - \frac{sy_1^2}{L} + \tau_1x_1 - \tau_2y_1 = 0$, and $\frac{\alpha\beta x_1z_1}{a+x_1} - kz_1 = 0$. Then the equation (9) can be rewritten as

$$\begin{aligned}\frac{dV}{dt} &= \beta\left(x - x_1\right)\left(\left[r - \frac{rx}{K} - \tau_1 + \tau_2\frac{y}{x} - \frac{\alpha z}{a+x}\right] - \left[r - \frac{rx_1}{K} - \tau_1 + \tau_2\frac{y_1}{x_1} - \frac{\alpha z_1}{a+x_1}\right]\right)\\ &+ \left(y - y_1\right)\left(\left[s - \frac{sy}{L} + \tau_1\frac{x}{y} - \tau_2\right] - \left[s - \frac{sy_1}{L} + \tau_1\frac{x_1}{y_1} - \tau_2\right]\right)\\ &+ \left(z - z_1\right)\left(\left[\frac{\alpha\beta x}{a+x} - k\right] - \left[\frac{\alpha\beta x_1}{a+x_1} - k\right]\right)\\ &= -\frac{r\beta}{K}\left(x - x_1\right)^2 - \frac{s}{L}\left(y - y_1\right)^2 + P + Q,\end{aligned} \tag{10}$$

where $P = \left(\beta\tau_2\frac{(x-x_1)}{xx_1} - \tau_1\frac{(y-y_1)}{yy_1}\right)(x_1y - xy_1)$ and $Q = \left(\alpha\beta(xz_1 - zx_1)\frac{(x-x_1)}{(a+x)(a+x_1)}\right)$. If $P \leq 0$ and $Q \leq 0$, then the equation (10) becomes non-positive.

Obviously, the solutions $x(t)$, $y(t)$, and $z(t)$ of model (4)–(6) with the initial conditions $x(0)$, $y(0)$, and $z(0)$ are positive for every time $t \geq 0$. From equations (4)-(5), we have

$$\begin{aligned}\frac{d}{dt}(x+y) &= \frac{dx}{dt} + \frac{dy}{dt} = rx\left(1 - \frac{x}{K}\right) + sy\left(1 - \frac{y}{L}\right) - \frac{\alpha xz}{a+x}\\ &\leq rx\left(1 - \frac{x}{K}\right) + sy\left(1 - \frac{y}{L}\right).\end{aligned} \tag{11}$$

Given any number $\epsilon > 0$ and following the lemma in [15], we get $x(t)+y(t) \leq K+L+\epsilon$ for time t being sufficiently large. This means that the size number of $x(t)+y(t)$ is bounded for every time $t \geq 0$. Further, there exist some points $(x_*, y_*) \in R^2_+$ which satisfy $A(x_*, y_*) = 0$, where $A(x,y) = rx\left(1-\frac{x}{K}\right) + sy\left(1-\frac{y}{L}\right)$. The inequality (11) implies the growth of $x(t)+y(t)$ becomes non-positive. From model (4)-(6), we also know that the populations $x(t)$ and $y(t)$ grow following the logistic equation when there is no interaction and influence from other population. This has the consequence that the populations $x(t)$ and $y(t)$ are bounded and there exist real positive numbers M_1 and M_2 such that $0 < x(t) \leq M_1$ and $0 < y(t) \leq M_2$.

From the three equations of model (4)-(6), we have

$$\begin{aligned}\frac{d}{dt}(x+y+z) &= \frac{dx}{dt}+\frac{dy}{dt}+\frac{dz}{dt} = rx\left(1-\frac{x}{K}\right)+sy\left(1-\frac{y}{L}\right)-\frac{\alpha(1-\beta)xz}{a+x}-kz \\ &\leq rx\left(1-\frac{x}{K}\right)+sy\left(1-\frac{y}{L}\right). \qquad (12)\end{aligned}$$

From the previous analysis, there exist real positive numbers M_3 such that $0 < z(t) \leq M_3$. Since $x(t)$, $y(t)$, and $z(t) \geq 0$ are bounded, and due to inequality (12), there exist M_1, M_2, and $M_3 > 0$ such that $0 < x(t) \leq M_1$, $0 < y(t) \leq M_2$, and $0 < z(t) \leq M_3$. The result of this analysis is summarized in Theorem 3.1.

Theorem 3.1 *Suppose that $EQ = (x_1, y_1, z_1)$ is the only interior fixed point for model (4)-(6). If the conditions $P \leq 0$ and $Q \leq 0$, with $0 < x(t) \leq M_1$, $0 < y(t) \leq M_2$, and $0 < z(t) \leq M_3$ are fulfilled, then the interior fixed point $EQ = (x_1, y_1, z_1)$ is globally and asymptotically stable via the Lyapunov function (8).*

4 Maximum Profit Problems

The interior fixed point EQ of the model (4)-(6) is connected with an economic problem. The predator and prey populations in the free area of capture are assumed as profitable stocks. The populations are then harvested with fixed efforts. The economic activities require operating costs and provide beneficial results. For this purpose, a function of total cost is defined as $TC = cE$, where c states the cost of exploitation and E is the fixed effort of harvesting. A function of total revenue is defined as $TR = pY(E)$, where p denotes the price of profitable stock (N). The result of exploitation is stated as $Y(E,N) = qEN$, where q is the catchability level. Further we also define the profit function as $\pi = TR - TC$. Since the interior fixed point $EQ = (x_1, y_1, z_1)$ leans on the fixed efforts, the profit function also leans on the fixed efforts. Therefore the profit function is stated as $\pi(E) = TR(E) - TC(E)$.

In order to get the fixed point $EQ = (x_1, y_1, z_1)$ lying in the first octant, the condition $\alpha\,\beta - k - q_2E > 0$, i.e. $E < \frac{\alpha\beta-k}{q_2}$ must be satisfied. Under the assumption that the value of effort is non-negative, the values of parameter must satisfy the conditions $\alpha\beta - k > 0$ and $0 \leq E_2 < \frac{\alpha\beta-k}{q_2}$. Besides, we also have to assume that $rkx_1 - rx_1^2 - \tau_1kx_1 + \tau_2ky_1 - q_1KEx_1 > 0$. By taking $E_{1max} = 1$ and $E_{2max} = 1$, the fixed point EQ becomes an interior fixed point when $(E_1,\ E_2) \in D$, where $D = \{(E_1, E_2) : 0 \leq E_2 \leq A,\ 0 \leq E_1 \leq B\}$, $A = min\{1, \frac{\alpha\beta-k}{q_2}, f(0, E_2) = 0\}$, and $B = min\{1, E_{12} = f(E_2)\}$. The function $E_{12} = f(E_2)$ is found from the implicit function $f(E_1, E_2) = rkx_1 - rx_1^2 - \tau_1kx_1 + \tau_2ky_1 - q_1KEx_1 = 0$. Moreover, we assume that $E_1 < E_{12}$. The profit function associated with the fixed point $EQ = (x_1, y_1, z_1)$ is given by $\pi(E_1, E_2) = (p_1 q_1 x_1)E_1 + (p_2 q_2 z_1)E_2 - (c_1 E_1 + c_2 E_2)$.

Example 4.1 Suppose that the hypothetical values of the paramaters of the model are given as $r = 1.5$, $s = 1.5$, $a = 100$, $K = 1000$, $L = 1000$, $\tau_1 = 0.25$, $\tau_2 = 0.25$, $\alpha = 0.5$, $\beta = 0.5$, $k = 0.1$, $q_1 = 1$, $q_2 = 1$, $p_1 = 10$, $p_2 = 12$, $c_1 = 5$, and $c_2 = 6$ with appropriate units. We get the fixed point $EQ = (x_1, y_1, z_1)$, where $x_1 = \frac{100(E_2+1)}{0.15-E_2}$, $y_1 = 416.6667 + 0.3334\sqrt{1562500 + 1500x_1}$, $z_1 = 0.00200\frac{\left(1250x_1 - 1.5x_1^2 + 250y_1 - 1000E_1x_1\right)}{x_1}$. The fixed point becomes an interior fixed point when the conditions $0 \leq E < 0.15$ and $1250x_1 - 1.5x_1^2 + 250y_1 - 1000E_1x_1 > 0$ are satisfied. The positive solutions of $f(E_2) = 0$ are $E_2 = 0.1273$, $E_2 = 0.1500$, and $E_2 = 0.8607$. Therefore, we get $D = \{(E_1, E_2) : 0 \leq E_2 \leq 0.1273,\ 0 \leq E_1 \leq min\{1, f(E_2)\}\}$, where

$$
\begin{aligned}
f(E_2) &= \frac{2.5.10^{-13}}{(3-20E_2)(1+10E_2)}\left[-2.24.10^{14}E_2 - 2.867.10^{14}E_2^2 + 3.255.10^{13}\right. \\
&+ 1.500.10^{10}\sqrt{1.562.10^6 + \frac{1.500 - 10^5(E_2+0.100)}{0.150-E_2}} \\
&- \left(2.000.10^{11}\sqrt{1.562.10^6 - \frac{1.500 - 10^5(E_2+0.100)}{0.150-E_2}}\right)E_2 \\
&+ \left.\left(6.667.10^{11}\sqrt{1.562.10^6 - \frac{1.500 - 10^5(E_2+0.100)}{0.150-E_2}}\right)E_2^2\right]. \qquad (13)
\end{aligned}
$$

The profit function is now written as

$$
\begin{aligned}
\pi(E_1, E_2) &= \left(\frac{1000(E_2+0.1)}{0.15-E_2}\right)E_1 \\
&+ \left(\frac{0.00024E_2}{0.1+E_2}\left(\frac{1.2500.10^5(E_2+0.1)}{-0.15+E_2} + \frac{15000(E+0.1)^2}{(-0.15+E_2)^2}\right.\right. \\
&- 1.0417.10^5 - 83.3333\sqrt{1.5625.10^6 - \frac{1.5.10^5(E_2+0.1)}{-0.15+E_2}} \\
&+ \left.\left.\frac{100000E_1(E_2+0.1)}{(0.15-E_2)}\right)(-0.15+E_2)\left(100 + \frac{100(E_2+0.1)}{0.15-E_2}\right) - 6\right).
\end{aligned}
$$

By observing the critical values of the profit function in the feasible region D and equation (13), a pair of fixed efforts $(E_1^*, E_2^*) = (1,\ 0.10718)$ is found, which maximizes the profit function of $\pi\left(E_1^*, E_2^*\right) = 4833.0425$. The pair of the fixed efforts lies in the curve $f(E_1, E_2) = 0$ which is the boundary of the feasible region D. The critical value of fixed efforts $(E_1^*, E_2^*) = (1,\ 0.10718)$ gives the fixed point $EQ = (483.8687,\ 920.9046,\ 0)$. This condition leads the predator population towards extinction when the fixed point is asymptotically stable.

We consider that there exists a minimum number of predators in the free area of capture, for example, we may assume that the allowed minimum number of the prey population is $z_{1E} = z_{min} = 200$. Then we get a new constrain function $g(E_1, E_2) = 0$, where

$$\begin{aligned} g(E_1,E_2) &= \frac{1}{0.1+E_2}\left(0.00002\left(\frac{125.10^5(E_2+0.1)}{-0.15+E_2}+\frac{15000.(E_2+0.1)^2}{(-0.15+E_2)^2}\right.\right. \\ &- 1.0416.10^5 - 83.3333\sqrt{1.5625.10^6-\frac{1.5.10^5(E_2+0.1)}{-0.15+E_2}} \\ &- \left.\left.\frac{100000E_1(E_2+0.1)}{-0.15+E_2}\right)(E_2-0.15)\left(100-\frac{100(E_2+0.1)}{-0.15+E_2}\right)\right)-200. \end{aligned}$$

The problem now becomes to maximize the profit function (E_1^*, E_2^*) subject to $g(E_1, E_2) = 0$. Solving the equations $\nabla\pi(E_1, E_2) = \mu\nabla g(E_1, E_2) = 0$ and $g(E_1, E_2) = 0$ simultaneously, where μ is the Lagrange multiplication, we get $E_1^* = 0.95507$ and $E_2^* = 0.10249$. By applying the value of the pairs of efforts $(E_1^*, E_2^*) = (0.95507,\ 0.10249)$, we obtain an interior fixed point $EQ = (426.2563,\ 911.2916,\ 200)$. From the Jacobian matrix evaluated at the interior fixed point, we get the eigenvalues $-0.9041,\ -1.5922$, and -0.0075. The maximum profit now becomes $\pi\,(E_1^*, E_2^*) = 4,311.6345$. In this case, if we apply the value of efforts at the level of $E_1^* = 0.95507$ and $E_2^* = 0.10249$, then both populations will live together for a certain span of time even though the populations in the free area of capture are harvested with fixed efforts of harvesting. Besides, the harvested populations also maximize the profit function.

5 Optimal Present Value of Net Revenue

The biological steady state is reached for the equations $\frac{dx}{dt} = 0$, $\frac{dy}{dt} = 0$, and $\frac{dz}{dt} = 0$. The economic steady state is found whenever the total revenue and total cost are at the same level. The profit function for the harvested populations is stated as $\pi(E_1, E_2) = p_1q_1xE_1 + p_2q_2zE_2 - c_1E_1 - c_2E_2$. Our goal is maximizing J as the present value of the net revenue for the problem of infinite horizon which is stated as

$$J = \int_0^\infty e^{-\delta t}\{(p_1q_1x - c_1)E_1(t) + (p_2q_2z - c_2)E_2(t)\}dt. \tag{14}$$

The discount rate of the net revenue is denoted by δ. The present value J subject to the equation (4)–(6) will be maximized using Pontryagin's maximum principle [16]. The control variables $E_1(t)$ and $E_2(t)$ are subject to the condition $0 \le E_i(t) \le E_{imax}$ for $i = 1, 2$. From equation (14), the Hamiltonian function is stated as

$$\begin{aligned} H &= e^{-\delta t}\{(p_1q_1x - c_1)E_1(t) + (p_2q_2z - c_2)E_2(t)\} + \tau_1\{rx\left(1-\frac{x}{K}\right) - \tau_1 x \\ &+ \tau_2 y - \frac{axz}{a+x} - q_1E_1x\} + \lambda_2\{sy\left(1-\frac{y}{L}\right) + \tau_1 x - \tau_2 y\} \\ &+ \lambda_3\{\frac{\beta\alpha xz}{a+x} - kz - q_2E_2z\}, \end{aligned} \tag{15}$$

where the adjoint variables are given by $\lambda_1(t)$, $\lambda_2(t)$, and $\lambda_3(t)$, respectively.

As the necessary conditions, we set $\frac{\partial H}{\partial E_1} = 0$ and $\frac{\partial H}{\partial E_2} = 0$ to get the control variables E_1 and E_2 to be optimal. From equation (15), we have $\frac{\partial H}{\partial E_1} = e^{-\delta t}(p_1q_1x - c_1) - \lambda_1q_1x = 0$ and $\frac{\partial H}{\partial E_2} = e^{-\delta t}(p_2q_2z - c_2) - \lambda_3q_2z = 0$. Then we get $\lambda_1 = \frac{e^{-\delta t}(p_1q_1x - c_1)}{q_1x}$ and $\lambda_3 =$

$\frac{e^{-\delta t}(p_2q_2z-c_2)}{q_2z}$. From equation (15), we also have

$$\begin{aligned}\frac{\partial H}{\partial x} &= e^{-\delta t}p_1q_1E_1 + \lambda_1\left(r - \frac{2r}{K}x - \tau_1 - \frac{\alpha x}{a+x} + \frac{\alpha z}{(a+x)^2} - q_1E_1\right) \\ &\quad + \tau_2\lambda_1 + \lambda_3\left(\frac{\beta\alpha z}{a+x} + \frac{\beta\alpha z}{(a+x)^2}\right), \\ \frac{\partial H}{\partial y} &= \lambda_1\tau_2 + \lambda_2\left(s_2 - \frac{2s}{L}y - \tau_2\right), \\ \frac{\partial H}{\partial z} &= e^{-\delta t}p_2q_2E_2 - \frac{\lambda_1\alpha x}{a+x} + \lambda_3\left(\frac{\beta\alpha x}{a+x} - k - q_2E_2\right).\end{aligned}$$

Following Pontryagin's maximum principle $\dot{\lambda_1} = -\frac{\partial H}{\partial x}$, $\dot{\lambda_2} = -\frac{\partial H}{\partial y}$, $\dot{\lambda_3} = -\frac{\partial H}{\partial z}$, and considering the transversality condition $\lambda_2(t) = 0$ as $t \to \infty$, we get $\lambda_1 = \frac{e^{-\delta t}(p_1q_1x-c_1)}{q_1x}$, $\lambda_2 = \frac{e^{-\delta t}\tau_2(-p_1q_1x+c_1)}{q_1x\left(-\delta+s-\frac{2s}{L}y-\tau_2\right)}$ and $\lambda_3 = \frac{e^{-\delta t}(p_2q_2z-c_2)}{q_2z}$. After substituting $\lambda_1 = \frac{e^{-\delta t}(p_1q_1x-c_1)}{q_1x}$, $\lambda_2 = \frac{e^{-\delta t}\tau_2(-p_1q_1x+c_1)}{q_1x\left(-\delta+s-\frac{2s}{L}y-\tau_2\right)}$ and $\lambda_3 = \frac{e^{-\delta t}(p_2q_2z-c_2)}{q_2z}$ into the equations $\dot{\lambda_1} = -\frac{\partial H}{\partial x}$, $\dot{\lambda_2} = -\frac{\partial H}{\partial y}$, and $\dot{\lambda_3} = -\frac{\partial H}{\partial z}$, we get E_1 and E_2. The optimal paths of E_1 and E_2 still depend on populations x, y, and z, i.e., $E_1 = E_1(x,y,z)$ and $E_2 = E_2(x,y,z)$. By substituting $x = x_1$, $y = y_1$, and $z = z_1$ into the implicit equations $E_1 = E_1(x,y,z)$ and $E_2 = E_2(x,y,z)$, we get the suitable values of control variables E_1 and E_2. The values of E_1, E_2, x_1, y_1, and z_1 give a maximum value of the present value J.

Example 5.1 Suppose that the hypothetical values of the paramaters of the model are given as $r = 1.5$, $s = 1.5$, $a = 100$, $K = 1000$, $L = 1000$, $\tau_1 = 0.25$, $\tau_2 = 0.25$, $\alpha = 0.5$, $\beta = 0.5$, $k = 0.1$, $q_1 = 1$, $q_2 = 1$ in appropriate units. Take $p_1 = 10$, $p_2 = 12$, $c_1 = 5$, $c_2 = 6$, and $\delta = 0.005$ in appropriate units. Further we have the fixed point $EQ = (x_1, y_1, z_1)$, where

$x_1 = \frac{100(E_2+0.1)}{0.15-E_2}$, $y_1 = 416.66667 + 0.33333\sqrt{1,562,500 + 1,500x_1}$, and

$z_1 = \frac{0.00200\left(1,250x_1-1.5x_1^2+250y_1-1000E_1x_1\right)(100+x_1)}{x_1}$.

The adjoint variables are $\lambda_1 = \frac{-e^{-0.005t}(10x_1-5)}{x_1}$, $\lambda_2 = \frac{0.25e^{-0.005t}(5-10x_1)}{(1.245-0.003y_1)x_1}$, and $\lambda_3 = \frac{-e^{-0.005t}(6-12z_1)}{x_1}$.

By solving the equations and then choosing the suitable values of fixed efforts of harvesting, we get $E_1 = 1.13676$ and $E_2 = 0.10278$. Further we get the fixed point $EQ = (429.40138,\ 911.82119,\ 0.01043)$ with the eigenvalues -1.0359, -1.62450, and -3.32935×10^{-7}. Under these conditions, the fixed point EQ is locally and asymptotically stable. The adjoint variables are denoted by $\lambda_1 = 9.988356e^{-0.005t}$, $\lambda_2 = 1.675377e^{-0.005t}$, and $\lambda_3 = -563.471151e^{-0.005t}$. Then we get the maximum value of the present value of the net revenue $J = \int_0^\infty 4,874.957199e^{-0.005t}dt = 9.749914 \times 10^5$.

We now continue the problem of maximizing the present value J of the net revenue for the problem of finite horizon which is stated as

$$J = \int_0^T e^{-\delta t}\{(p_1q_1x - c_1)E_1(t) + (p_2q_2z - c_2)E_2(t)\}dt. \tag{16}$$

The control variables $E_1(t)$ and $E_2(t)$ are subject to the condition $0 \le E_i(t) \le 1$ for

$i = 1, 2$. From equation (16), the Hamiltonian function is stated as

$$\begin{aligned} H &= e^{-\delta t}\{(p_1q_1x - c_1)E_1(t) + (p_2q_2z - c_2)E_2(t)\} + \tau_1\{rx\left(1 - \frac{x}{K}\right) - \tau_1 x \\ &+ \tau_2 y - \frac{axz}{a+x} - q_1E_1x\} + \lambda_2\{sy\left(1 - \frac{y}{t}\right) + \tau_1 x - \tau_2 y\} \\ &+ \lambda_3\{\frac{\beta\alpha xz}{a+x} - kz - q_2E_2z\}, \end{aligned} \tag{17}$$

where $\lambda_1(t)$, $\lambda_2(t)$, and $\lambda_3(t)$ denote the adjoint variables. Again, following Pontryagin's maximum principle, we set $\dot{\lambda_1} = -\frac{\partial H}{\partial x}$, $\dot{\lambda_2} = -\frac{\partial H}{\partial y}$, $\dot{\lambda_3} = -\frac{\partial H}{\partial z}$, with $\lambda_1(T) = \lambda_2(T) = \lambda_3(T) = 0$. Since the equation (17) is linear in E_1 and E_2 with the slope $\frac{\partial H}{\partial E_1} = e^{-\delta t}(p_1q_1x - c_1) - \lambda_1q_1x$ and $\frac{\partial H}{\partial E_2} = e^{-\delta t}(p_2q_2z - c_2) - \lambda_3q_2z$, we define the following to maximize H:

$$E_1^*(t) = \begin{cases} 0, e^{-\lambda t}(p_1q_1x - c_1) - \lambda_1q_1x < 0, \\ 1, e^{-\lambda t}(p_1q_1x - c_1) - \lambda_1q_1x \geq 0 \end{cases}$$

and

$$E_2^*(t) = \begin{cases} 0, e^{-\lambda t}(p_2q_2z - c_2) - \lambda_2q_2z < 0, \\ 1, e^{-\lambda t}(p_2q_2z - c_2) - \lambda_2q_2z \geq 0. \end{cases}$$

Because the Hamiltonian function H is linear in E_1 and E_2, the usual first order condition $\frac{dH}{dE_1} = \frac{dH}{dE_2} = 0$ is inapplicable in our search for $E_1^*(t)$ and $E_2^*(t)$, but here we define $E_1^*(t) = E_2^*(t) = 1$ when $\frac{dH}{dE_1} = \frac{dH}{dE_2} = 0$. The solution for the problem of finite horizon will be given using the forward-backward sweep numerical method to plot the optimal solution of $x^*(t)$, $y^*(t)$, $z^*(t)$, $E_1^*(t)$, and $E_2^*(t)$.

Example 5.2. Suppose that the hypothetical values of the paramaters of the model are given as $r = 1.8$, $a = 200$, $\tau_1 = 0.25$, $\tau_2 = 0.25$, $\beta = 0.15$, $K = 1000$, $\alpha = 0.5$, $s = 1.8$, $L = 1000$, $k = 0.01$, $q_1 = 0.01$, $q_2 = 0.01$ in appropriate units. Take $p_1 = 10$, $p_2 = 12$, $c_1 = 5$, $c_2 = 6$, $\delta = 0.005$, and $T = 200$. Set the initial and terminal conditions $x(0) = 950$, $y(0) = 950$, $z(0) = 600$, and $\lambda_1(T) = \lambda_2(T) = \lambda_3(T) = 0$. The curves of state, costate, and adjoint variables are plotted using a Matlab program as given in Figures 1–4.

Figures 1(a), 1(b) and 2(a) show that when harvesting is not considered in the dynamical behavior of populations, the predator and prey will tend to the stable fixed point. From the previous analysis, we know that a certain condition is found, where the interior fixed point becomes globally and asymptotically stable. Harvesting efforts as control variables influence the dynamical behavior of the populations but the behavior is still similar to the behavior of the population model without harvesting. The dynamical behavior for preys with a control seems to increase with a little oscillation, while the dynamical behavior for predator remains decreasing smoothly.

Harvesting efforts as a control in the model make the predator population decline rapidly compared to the non-harvested one, but the predator population remains sustainable because when the population is very small, then the population will stop being harvested. The reduced predator population due to harvesting makes the effect of predation on the prey in the free area become ineffective. This gives an opportunity for the prey population to grow more rapidly. As a consequence, the prey population in the free and forbidden areas for harvesting grow faster than when there are no harvesting efforts

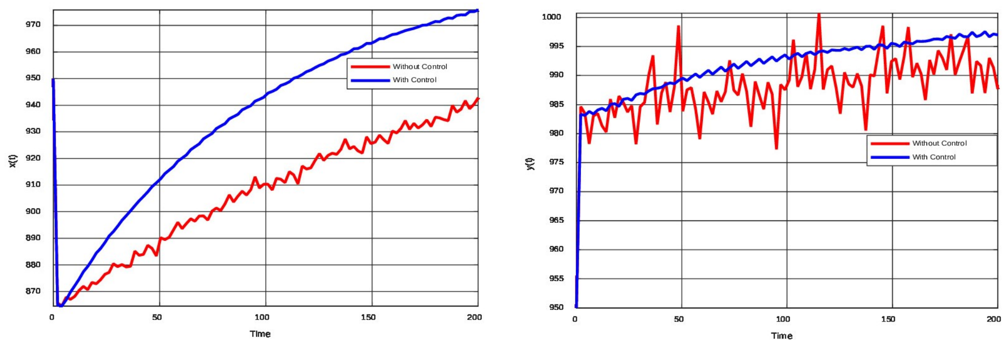

a b

Figure 1: a) plot curve of $x(t)$, b) plot curve of $y(t)$.

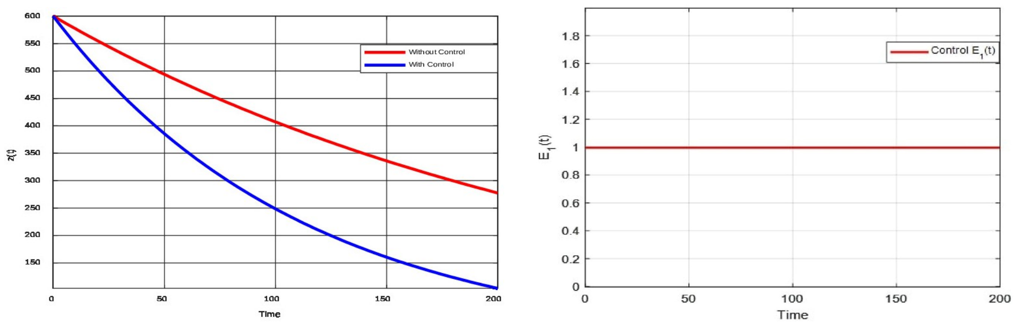

a b

Figure 2: a) plot curve of $z(t)$, b) plot curve of $E_1(t)$.

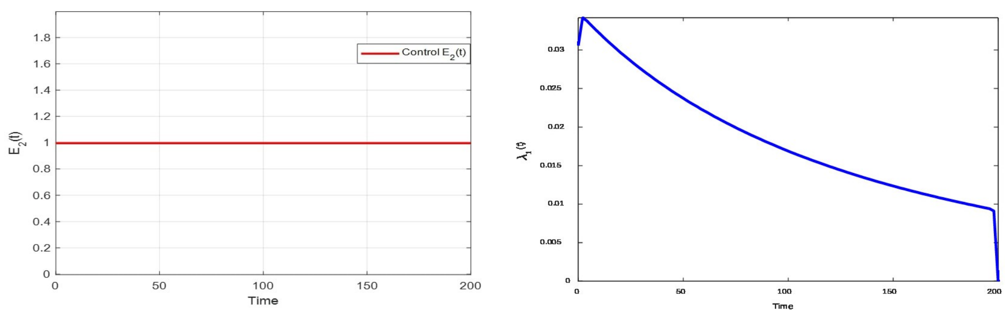

a b

Figure 3: a) plot curve of $E_2(t)$, b) plot curve of $\lambda_1(t)$.

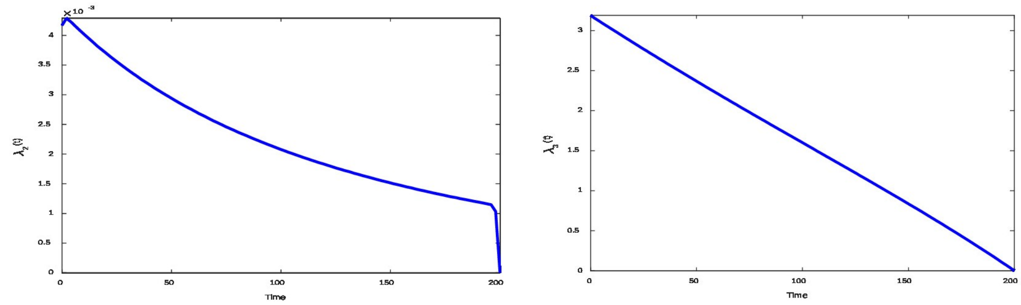

a b

Figure 4: a) plot curve of $\lambda_2(t)$, b) plot curve of $\lambda_3(t)$.

in the model. In this example, the populations are harvested at the maximum level over the time interval $t \in [0, 200]$, see Figures $2(b)$ and $3(a)$. The optimal paths $x^*(t)$, $y^*(t)$, $z^*(t)$, $E_1^*(t)$, and $E_2^*(t)$ maximize the present value J for the problem of finite horizon.

6 Conclusion

The dynamical behavior of preys in the free and forbidden areas of harvesting and predator population with the Holling response function of type II has an interior fixed point when a specific condition is fulfilled. The interior fixed point both for the model with and without harvesting effort was analyzed and it was found that the interior fixed point is locally and globally asymptotically stable. The local stability of the interior fixed point was analyzed via the linearization approach and Routh-Hurwitz stability criteria. The Lyapunov function was constructed under a specific condition to guarantee the global stability of the interior fixed point in the first octant.

In the case of exploitation with the fixed efforts for the predator and the prey populations, there exists an interior fixed point. Under a specific condition, this fixed point becomes globally and asymptotically stable and also gives maximum profit, but the predator population is driven to extinction. By considering that there exists a minimum size of the predator population which is banned to be exploited, we found a pair value of the efforts and the suitable values of parameter to get a globally and asymptotically stable interior fixed point. The stable fixed point also maximizes the profit function for a certain span of time. Both predator and prey populations in the free and forbidden area of capture can be sustainable and also maximize the profit function forever even though the predator and the prey populations in the free area of capture are harvested with fixed efforts of harvesting.

For the problem of maximizing the present value of revenues, there exist extremal paths for harvesting efforts that maximize the present value of net revenues for finite and infinite horizon problems. The harvesting efforts as control variables via simulation show that the harvesting efforts can reduce the predator population and also, at the same time, can reduce the effect of predation on the prey population. The harvesting effect allows the preys to grow rapidly comparing to their growth without harvesting.

Acknowledgment

This research is supported by LPPM Hasanuddin University with the contract number: 915/UN4.22/PT.01.03/2021.

References

[1] L. J. Diblik and D. Khusainov. Stability of an Autonomous System with Quadratic Right-Hand Side in the Critical Case. *Nonlinear Dynamics and Systems Theory* **2** (2) (2002) 145–156.

[2] V.V. Vlasov. Asymptotic Behavior and Stability of the Solutions of Functional Differential Equations in Hilbert Space. *Nonlinear Dynamics and Systems Theory* **2** (2) (2002) 215–232.

[3] Firman, S. Toaha and M. Nur. Asymptotic Stability of Some Class of Affine Nonlinear Control Systems through Partial Feedback Linearization. *Nonlinear Dynamics and Systems Theory* **21** (3) (2021) 238–245.

[4] H. F. Hou, H.M. Jiang and X.Y. Meng. A Dynamic Model for Fishery Resource with Reserve Area and Taxation. *Journal of Applied Mathematics* **2012** (2012) 794719:1–794719:15.

[5] L. Yunfei, R. Yuang and Y. Pei. A Prey-Predator Model with Harvesting for Fishery Resource with Reserve Area. *Applied Mathematical Modelling* **37** (5) (2013) 3048–3062.

[6] M. N. Srinivas, M.A.S. Srinivas, K. Das and N.H. Gazi. Prey-Predator Fishery Model with Stage Structure in Two Patchy Marine Aquatic Environment. *Applied Mathematics* (2) (2011) 1405—1416.

[7] T. K. Kar. A Dynamic Reaction Model of a Prey-Predator System with Stage-Structure for Predator. *Modern Applied Science* **4** (5) (2010) 183—195.

[8] R. P. Gupta, M. Banerje and P. Chandra. Bifurcation Analysis and Control of Leslie–Gower Predator–Prey Model with Michaelis–Menten Type Prey-Harvesting. *Journal Differential Equations and Dynamical Systems* **22** (3) (2012) 339—366.

[9] Y. Qu and J. Wei. Bifurcation Analysis in a Predator-Prey System with Stage Stucture and Harvesting. *Journal of Franklin Institute* **347** (7) (2010) 1096—1113.

[10] K. Chakraborty, M. Chakraborty and T. K. Kar. Optimal Control of Harvest and Bifurcation of Prey-Predator Model with Stage Structure. *Applied Mathematics and Computation* **217** (2011) 8778—8792.

[11] K. Chakraborty, S. Jana and T. K. Kar. Global Dynamics and Bifurcation in a Stage Structured Prey-Predator Fishery Model with Harvesting. *Applied Mathematics and Computation* **218** (5) (2012) 9271—9290.

[12] G. M. V. Laksmi, M. Gunasekaran and S. Vijaya. Bifurcation Analysis of Predator Model with Harvested Predator. *International Journal of Engineering Research and Development* **10** (6), (2014) 42–51.

[13] S. Toaha, J. Kusuma, Khaeruddin and Mawardi. Stability Analysis and Optimal Harvesting Policy of Prey-Predator Model with Stage Structure for Predator. *Applied Mathematical Sciences* **8** (159) (2014) 7923–7934.

[14] L. E. Keshet. *Mathematical Models in Biology.* SIAM, Philadelphia, 2005.

[15] L. Chen and F. Chen. Global Stability of Leslie-Gower Predator-Prey Model with Feedback Controls. *Applied Mathematics Letter* **22** (9) (2009) 1330–1334.

[16] D. Grass, J. P. Caulkins, G. Feichtinger, G. Tragler and D.A. Behrens. *Optimal Control of Nonlinear Processes.* Springer-Verlag, Berlin Heidelberg, 2003.

SCIENDO

Stability: Elements of the Theory and Applications with Examples

328 pp., 2020, ISBN: 978-83-66675-27-8, DOI: 10.2478/9788366675285-fm

A.A. Martynyuk, B. Radziszewski, A. Szadkowski

Kyiv-Warsaw-Southern Pines NC (USA)

Stability is one of the basic concepts used in many of science, technology in everyday life. It expresses the resistance of objects, processes, etc., whose condition may change over time due to various internal or external disturbances. This book sets out the main methods of the modern theory of motion stability, which received significant development in the twentieth century. The presentation covers continuous autonomous and non-autonomous systems of equations of disturbed motion, discrete systems and systems with delay, systems with distributed parameters, as well as stochastic systems and systems with chaotic behavior of trajectories.

Applications and examples illustrate the technique of applying the results presented in solving specific problems in mechanics and physics.

CONTENTS (12 chapters)

Preface, Stability – What Is It, and What Is It For?, Linear Equations with Constant Coefficients, Nonlinear Integral Inequalities in the Stability Theory, Lyapunov Direct Method, Comparison Method and Stability of Motion, Stability Domains, Stability of Manifolds - Selected Subjects, Stability of Difference Equations, Stability in Delay Differential Equations, Stability of Partial Differential Equations, Stochastic Stability, Lyapunov Exponents and Chaotic Systems, References and Index.

This book is intended to familiarize the readers with basic concepts, and classic results of stability theory stated in a way as required by the rigorous rules of contemporary mathematics and, simultaneously, to introduce the learners to broad fields of not only the stability theory but also applications involved. The book is offered as a textbook for the college-level students or as an aid to the PhD students interested in practical problems of the stability theory. The prerequisites are not demanding – the basic knowledge of calculus, complex functions, and linear algebra which are covered in the suitable, elementary courses is required.